1284

BRIDGE GIRDER BUTT WELDS– RESISTANCE TO BRITTLE FRACTURE, FATIGUE AND CORROSION

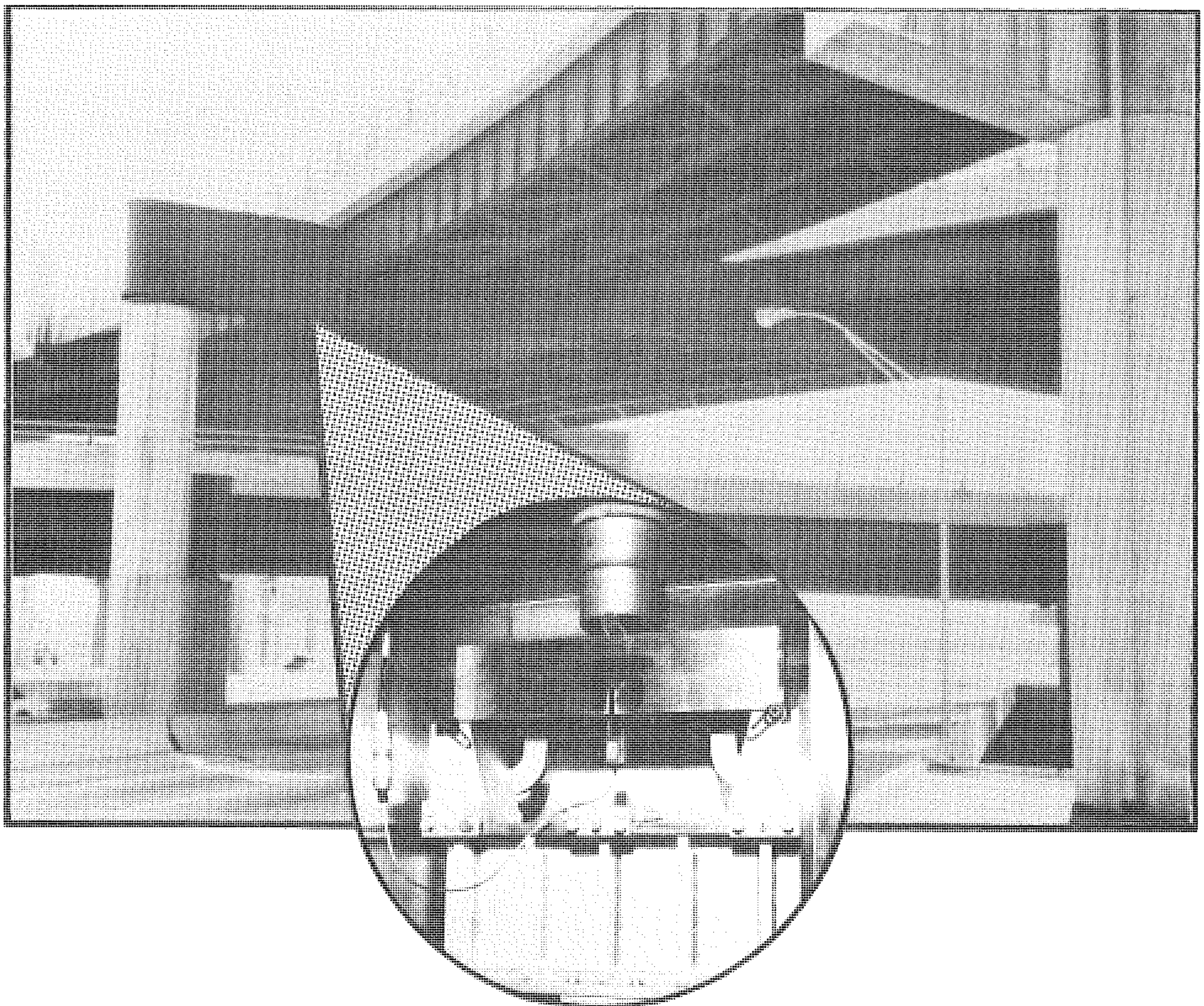

MICHIGAN DEPARTMENT OF TRANSPORTATION
JANUARY 1988

TG 350 C86 1988 mf c. 2
Bridge girder butt welds : resistance to brittle fracture, fatigue, and corrosion

BRIDGE GIRDER BUTT WELDS - RESISTANCE TO BRITTLE FRACTURE, FATIGUE, AND CORROSION

James D. Culp

Final Report on a Highway Planning and Research
Investigation Conducted in Cooperation with the
U. S. Department of Transportation,
Federal Highway Administration

Research Laboratory Section
Materials and Technology Division
Research Project 75 F-144
Research Report No. R-1284

Lansing, January 1988

TABLE OF CONTENTS

ABSTRACT

Welded butt joints, typical of those used in the flange splicing of steel plate girders, were welded by the electroslag, electrogas, and submerged arc welding processes in ASTM A36 and A588 steel plates. A complete series of mechanical and physical tests were conducted on the weldments. Three series of fracture toughness tests were conducted on the weldments and the base plates. The first series utilized the standard Charpy V-notch impact test which was run in accordance with the ASTM Standard Test Method E23, "Standard Methods for Notch Bar Impact Testing of Materials." The second series was the three-point bend specimen fracture toughness test, run in accordance with the ASTM Standard Test Method E399, "Standard Test Method for Plane-Strain Fracture Toughness of Metallic Materials." The third series was a modified E399 type of fracture toughness test designed to circumvent problems encountered in submerged arc weldments where large residual compressive stress zones prevent the growth of a straight fatigue crack front. The two series of fracture tests on the three-point bend specimens were conducted at a test temperature of -30 F (lowest anticipated service temperature for the Michigan region) and a 1-sec. loading rate which is typical of bridge loading rates. These tests reveal that electroslag and electrogas weldments are lower in fracture toughness than submerged arc weldments. In some cases, especially in A588 steel, the electroslag and electrogas weldments exhibited brittle fracture behavior, i.e. valid plane-strain fracture occurred in accordance with the ASTM E399 test method. Some valid plane-strain fractures were also encountered in the A588 base plate. The modified fracture toughness tests illustrate a method for comparing the fracture resistance of weldments which contain residual stress fields that prevent the growth of straight fatigue crack fronts that are necessary in the E399 test method.

SUMMARY CONCLUSIONS

The results of this investigation into the fracture properties of electroslag, electrogas, and submerged arc weldments in ASTM steel types A36 and A588 led to the following conclusions:

1) The weldments produced for this study were of the same general character as reported in a previous research report, "Fracture Toughness and Fatigue Properties of Steel Butt Joints Welded by Submerged Arc and Electroslag Welding Procedures" (1). The same types of nonhomogeneous, coarse-grained weld metal structures were encountered in the electroslag weldments as previously reported. Standard mechanical and physical test results show that all the weldments used in this study were typical of those produced and incorporated in steel highway and railway bridge girders. (Michigan has prohibited the use of the electroslag and electrogas welding processes since June, 1974.)

2) The fracture toughness characteristics of weldments produced in 3-in. thick A36 and A588 steel plates were evaluated using three series of fracture tests. These tests were conducted on weldments made by the electroslag, electrogas, and submerged arc processes as well as on the base plates themselves. The tests do illustrate that both electroslag and electrogas weldments produce lower toughness weldments than the submerged arc process and in some cases a plane-strain or brittle fracture behavior was observed in the electroslag and electrogas weldments. The general conclusions from the three series of fracture tests are as follows:

Series 1 - Charpy V-notch Impact Test

Standard Charpy V-notch impact tests run at a test temperature of 0 F reveal the following trends in the weldments tested:

The submerged arc weldments yielded a very uniform notch toughness throughout the weld nugget and exceeded the required minimum 20 ft-lb in both A36 and A588 base metals.

The notch toughness of the electroslag and electrogas weldments, as measured by the Charpy test, is very nonhomogeneous throughout the weld nugget. The lowest toughness is normally located in the central core of the weld and the electroslag weldments in the A588 steel failed to meet the required minimum 15 ft-lb.

No significant notch toughness problems were noted for the various weldments in the heat-affected zones adjacent to the weld nugget.

Series 2 - Plane-Strain Fracture Toughness Test, K_{IC}

Standard three-point bend specimens, 3-in. in thickness, were tested in accordance with ASTM E399, Standard Test Method for Plane-Strain Fracture Toughness of Metallic Materials, on all the various weldment types and base plates. These tests were run at a test temperature of -30 F (lowest anticipated service temperature) and a 1-sec. loading rate typical of bridge structures. The following trends were noted in the weldments and base plates tested.

None of the submerged arc weldments exhibited plane-strain or brittle fracture behavior. The presence of a large compressive residual stress field in the submerged arc weldments prevented the growth of a straight fatigue crack front as required by the ASTM E399 test method.

Several electroslag and electrogas weldments exhibited valid plane-strain fracture behavior, in most cases in the A588 steel weldments. Thus, the potential for brittle fracture does exist in these types of weldments under actual service conditions.

The full size K_I tests reveal that the electroslag weldments do not exhibit higher toughness in the Zone 2, coarse grained weld metal located off-center in the weld nugget. The Charpy V-notch test did indicate a higher notch toughness in this region (compared to the central core), but this is apparently due to the small size of the Charpy specimen. These full thickness fracture tests reveal a more uniform toughness throughout the weld nugget and illustrate the danger in using small size specimens to evaluate weldment toughness.

The full size K_I tests on the base plates reveal that the lower strength A36 steel exhibited higher fracture toughness than the A588 steel. Several valid K_{IC} test results were achieved on the A588 steel specimens, indicating the possibility of brittle fracture under actual service loading conditions.

Series 3 - Modified Fracture Toughness Tests

Two modified three-point bend fracture tests were conducted to attempt to circumvent the problem of growing a straight fatigue crack front in the submerged arc weldments. These modified tests either limited the fatigue crack growth to maintain a straight crack front or used a straight machined notch to initiate the fracture. Although not recognized as standard test methods these tests revealed several pertinent points.

Valid fracture behavior in a submerged arc weldment is most closely approximated by maintaining a straight crack front, which can be done using a combined fatigue crack and machined notch front.

Submerged arc weldments exhibit a high degree of toughness or fracture resistance when tested in a full-thickness specimen. The compressive residual stress fields that are present enhance the resistance to fracture in that they inhibit the growth of a rapidly propagating crack.

Submerged arc weldments exhibited higher toughness in the modified tests than did the electroslag weldments. This is in agreement with all the other toughness test results.

3) Based on the various fracture toughness tests conducted it is apparent that electroslag and electrogas weldments possess low toughness and have a significant potential for brittle fracture under actual bridge service loading conditions. Hence, the processes should not be used for butt splicing bridge girder members that will be subjected to tension or stress reversals in the finished structure.

4) Although this study did not directly evaluate the fatigue cracking properties of the electroslag and electrogas weldments, it was noted that the weld metals offered very little resistance to the growth of fatigue cracks in the preparation of the K_{IC} fracture toughness specimens. This is a point that should be carefully noted since a rapidly growing fatigue crack could lead to a brittle fracture before being detected by periodic inspection testing required on in-service bridges.

INTRODUCTION

Welded butt joints in flange plates, cover plates, and web plates, ranging from 1/2 to 4 in. thick, are commonly encountered in the fabrication of steel plate girders used in highway and railway bridges. The two predominant welding processes available over the past 15 years for producing these butt welds are the submerged arc process and the electroslag process. Submerged arc welding was introduced with the advent of the welded plate girder and currently is the only process approved for butt welding on bridges fabricated for the Michigan Department of Transportation. From early 1970 to June 1974, the electroslag welding process was approved by the Department and gained a dominant role in the fabrication of steel plate girders. Michigan now has approximately 126 bridges in service with electroslag welded butt joints in the flange plates and in a few beam cover plate butt splices. Some of these structures are constructed of painted ASTM A36 steel and some are constructed of ASTM A588, high strength, low-alloy steel, placed in an unpainted condition.

The use of the electroslag welding process on Michigan bridges was suspended in June 1974. This action was a result of the poor fracture toughness properties and inadequate alloy chemistry of the electroslag weldments as reported in the findings of the Highway Planning and Research Project 72 F-124, "Fracture Toughness and Fatigue Properties of Steel Butt Joints Welded by Submerged Arc and Electroslag Welding Procedures" (1). The research being reported in the present investigation was done subsequent to this first project.

The earlier project provided information that clearly indicated that the electroslag process should not be used for welded tension splices in highway bridges. It did not, however, address the concerns about the serviceability of the existing electroslag welded bridges. Thus, another study was initiated to attempt to quantify information concerning the fracture toughness, fatigue resistance, and corrosion characteristics of electroslag weldments. In this project an attempt also was made to quantify the fracture toughness properties and corrosion characteristics of submerged arc weldments and some typical base metal types. All test weldments were produced in 3-in. thick steel plates which represent the typical maximum thickness used by Michigan in the butt welding processes.

Objectives

A proposal for a research project was submitted to the Federal Highway Administration to perform this work under the Highway Planning and Research (HPR) Program. This proposal was approved and the following objectives as set forth in the proposal, were to be accomplished.

"The primary objective of this project is to evaluate electroslag and submerged arc butt weldments for their fracture toughness, fatigue, and corrosion properties in two grades of steel commonly used in bridge beam construction. The results of such evaluations will allow us to determine: a) what possibility exists for premature fatigue damage, brittle fracture, or excessive corrosion in our electroslag welded structures; b) what action should be taken in the maintenance of our existing structures; and, c) what criteria should be specified in any future use of electroslag welding to preclude fatigue, lack of toughness, and corrosion problems.

This main objective will be achieved by the following specific objectives:

1) To characterize the metallurgical and tensile properties of the submerged arc and electroslag welded butt joints used in this study, which shall be typical of those used in bridge beams.

2) To characterize the fracture toughness properties of the weldments by both Charpy impact testing and linear elastic fracture mechanics measurements of the material property K_{IC} at strain rates typical of bridge loadings. (A possible correlation between the Charpy data and the K_{IC} data will be explored. Such a correlation would allow K_{IC} estimates to be derived from the more easily obtainable Charpy data.)

3) To determine fatigue crack initiation and propagation properties of the weldments by cyclic loading of large section tensile specimens taken from the various metallurgical zones. A "Linear Elastic Fracture Mechanics" approach will be used in the fatigue testing program.

4) To determine the corrosion properties of the weldments when deposited in ASTM A588 steel for use in unpainted exposures. Long term corrosion properties will be assessed by an outdoor exposure of weld specimens and by field evaluation of existing structures.

5) To make appropriate recommendations for any preventive maintenance that is deemed necessary based on the results of these studies.

6) To correlate the toughness and fatigue properties of the weld metals with design requirements to determine the existing factor of safety against failure.

7) If possible, to develop for future specification, acceptance criteria for both electroslag and submerged arc welding that will assure adequate weld metal properties with respect to toughness, fatigue life, and corrosion resistance."

Objective 3 of the proposal, fatigue testing of the weldments, was not carried out. It was discovered early in the laboratory testing that the fatigue characteristics of the butt weldments are very complex. Residual stress fields present in a welded joint and the variations in metallurgical structures within a weldment make fatigue crack initiation and propagation testing extremely difficult using conventional testing methods. Hence, it was decided to defer this phase of the study and to concentrate the research efforts on the fracture toughness testing. A limited number of conclusions concerning fatigue crack initiation are reported from the "fatigue precracking" phase of the fracture toughness testing. These observations will be discussed in that section of the report.

Other work was added to the project that was not part of the original proposal. The following three items were undertaken and the results are reported in the following sections:

1) Electrogas weldments (a flux-cored arc wire version) were made by a manufacturer of electrogas type welding equipment and consumables. These weldments were produced in 3-in. thick A588 steel and were tested for standard mechanical properties and fracture toughness properties along with the proposed project weldments.

2) A modified fracture toughness test was developed and run on full thickness electroslag and submerged arc weldments. The test was a modification of the ASTM E399 test on "Plain-Strain Fracture Toughness of Metallic Materials." This was an attempt to circumvent the problems encountered in applying the standard E399 test to submerged arc weldments where the compressive residual stress fields present in the weld produced gross irregularities in the fatigue precracking front. These results present some interesting alternatives for evaluating weldment fracture resistance when residual stress fields invalidate standard testing techniques.

3) Welded fatigue test samples made of A588 steel were received from Prof. Pedro Albrecht of the University of Maryland, that are part of his on-going investigation of the fatigue behavior of welded details in unpainted exposures of A588 steel. These specimens have been installed under a Michigan bridge for field exposure to a highway environment. At various time intervals they will be removed and tested by Prof. Albrecht for comparison with unexposed, as-welded test specimens, and specimens weathered under "ideal conditions" (2).

The following report is directed at meeting the stated objectives of this project. A brief discussion of the submerged arc, electroslag, and electrogas processes is presented along with the standard physical test data for the weldments produced for this study. This is followed by a detailed presentation of the fracture toughness test methods applied and

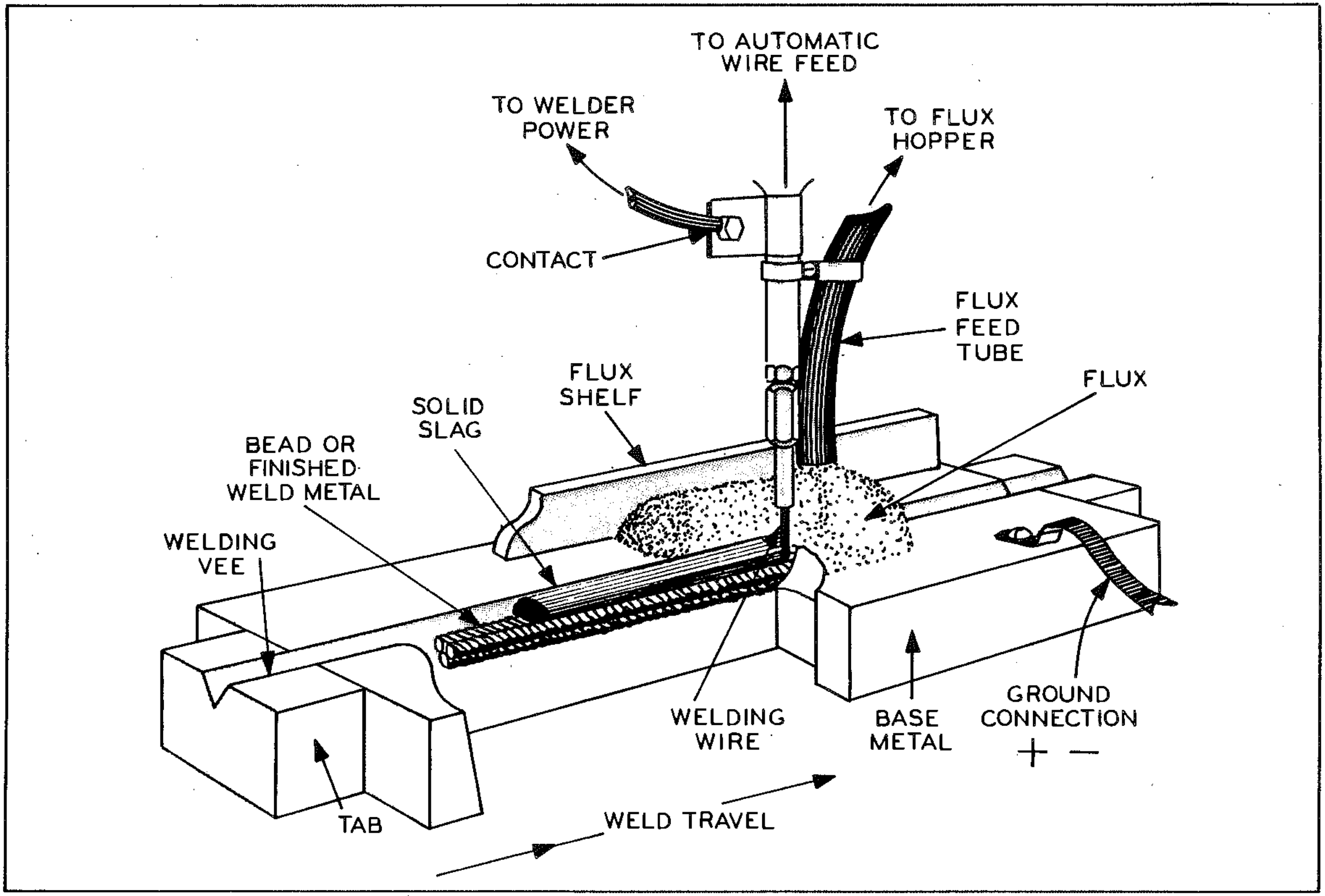

Figure 1. Cutaway view of multiple pass butt welding by the submerged arc welding process.

an analysis of the data obtained on the various submerged arc, electroslag, and electrogas weldments included in the project. Tests conducted on the ASTM A36 and A588 base metals used in the weldments are also included. Then a brief presentation of the corrosion tests initiated on the unpainted, weathering steel (A588) type weldments is included. These corrosion tests are relatively long-term in that they will require a minimum of 8 to 10 years of actual highway environment exposure before they will be "weathered" enough for analysis. When this time arrives, research personnel will carry out the corrosion evaluation and issue a report on the work (not under the HPR Program).

The results and conclusions of this project do meet the objectives of the project proposal as stated, within the application and limitations stated in the report. The details of the report have been made as complete as is practical in consideration of the large variation in the backgrounds of the prospective readers.

DISCUSSION OF RESULTS

Submerged Arc Welding Process

Submerged arc welding (SAW) is defined as ". . . an arc-welding process which produces coalescence of metals by heating them with an arc or arcs between a bare metal electrode or electrodes and the work. The arc and molten metal are shielded by a blanket of granular, fusible material on the work. Pressure is not used and filler metal is obtained from the electrode and sometimes from a supplemental source(s) (welding rod, flux, or metal granules)" (3). As applied to the welding of butt joints, the submerged arc process is a multipass technique. The plates are placed in the flat position and a beveled joint is filled by depositing weld metal in a series of beads (Fig. 1). After each pass the deposited bead is allowed to cool to some prescribed interpass temperature to prevent excessive heat build up in the joint. (Proper control of interpass temperature will optimize the physical properties of the deposited weld metal, especially the Charpy V-notch impact strength.) Each bead must be thoroughly cleaned by chipping and wire brushing before depositing the next bead to ensure good fusion and to eliminate slag inclusions. A small layer of reinforcement is built-up beyond the surface ot the plates being welded which is later ground off to give a smooth, flat contour to the joint surface.

The submerged arc process results in a rather uniformly structured weld joint with a fine grained metal structure as compared to the typical base metal used in bridge construction. One advantage of the multipass

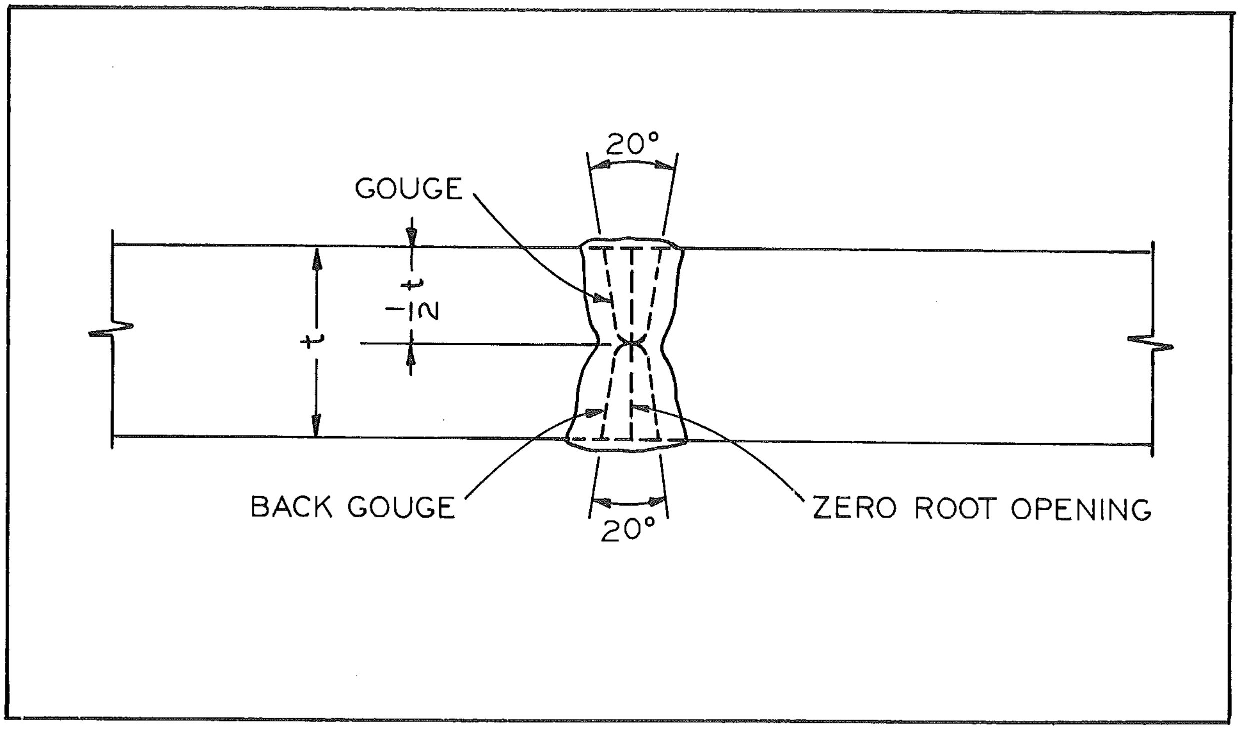

(a) Joint configuration used (AWS designation B-U7-S).

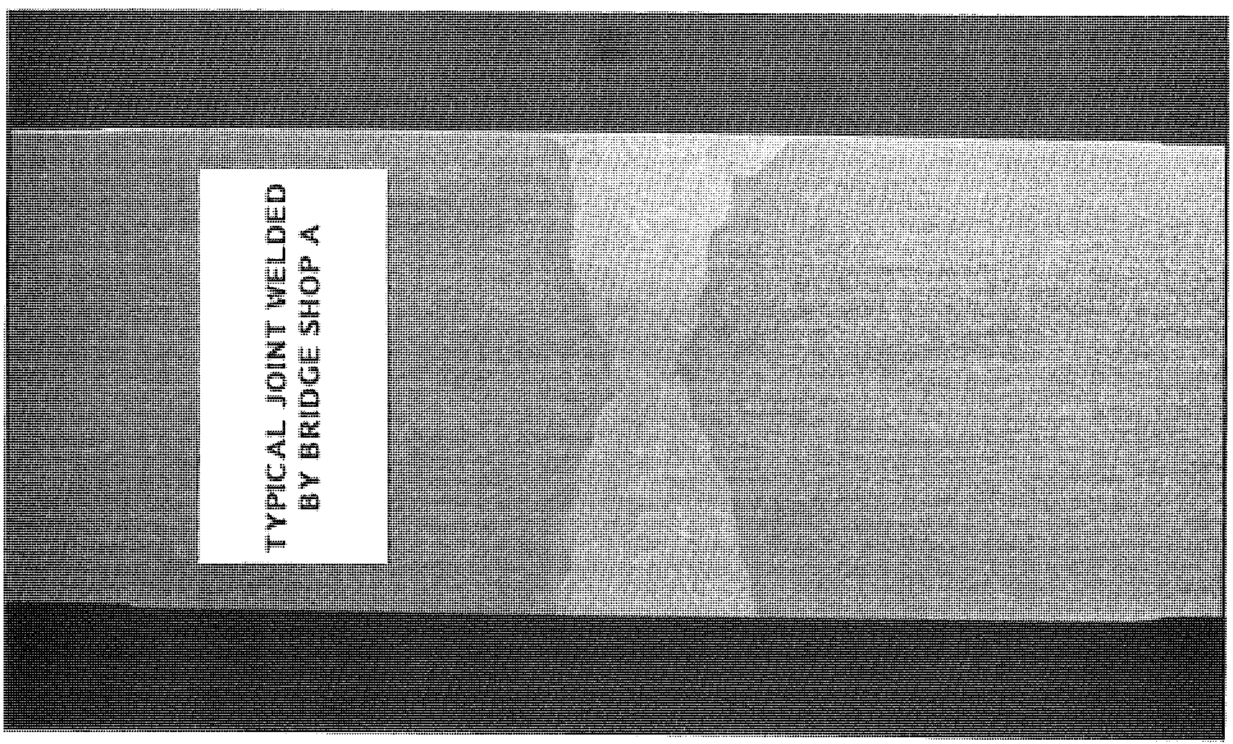

(b) Typical macrostructure of submerged arc welded joint in 3-in thick base plate.

Figure 2. Submerged arc weldments produced by Bridge Shop A.

technique is that the heat generated by the deposition of a weld bead will partially refine the metallurgical structure of the underlying weld metal. Submerged arc butt weldments in flange plates, when properly made, contain no significant nonhomogeneities (i.e., the physical properties are approximately the same at all points in the weld metal) or anisotropies (i.e., directional variations in properties) and only one narrow heat-affected zone (HAZ) in the base metal adjacent to the weld fusion line. In the base metals normally used in highway bridge construction, the HAZ present in a submerged arc weldment will usually have properties superior to those of the unaffected base metal, since the thermal cycle experienced refines the grain structure present in the base metal.

Properly made submerged arc weldments in bridge girder butt joints have good metallurgical, physical, fatigue, and fracture toughness properties and have been proven serviceable for applications involving cyclic and impact loadings through many years of testing and experience (4, 5). The main disadvantages of the submerged arc process as applied to butt jointing plates are the time and labor required to weld a joint and the need for a careful procedure to control the joint distortion that can occur due to shrinkage during the cooling cycle. These disadvantages are not serious, however, and a good welding procedure can minimize the problems. Submerged arc welding is also the process used in the fillet welding of built-up plate girders, e.g., in joining the flange plates to the web or cover plates to flange plates.

Experimental Weldments - Submerged Arc Process

Submerged arc butt weld specimens for this project were made by one of the major bridge fabricators in the midwest. This firm does a significant portion of bridge fabrication for the Michigan Department of Transportation and other midwestern and southern states, and will be referred to as Bridge Shop A. The philosophy applied to the fabrication of these weldments was to produce them in accordance with the same procedure specification that had been qualified by previous tests and was being used in actual girder fabrication. No special precautions or controls were exercised over those that would be rountinely observed in production work. The properties of these weldments are thus typical of those being incorporated into Michigan bridge structures at the time.

The submerged arc weldments produced for the project were made in both ASTM A36 and A588 steel types using 24-in. wide by 3-in. thick plate. The American Welding Society (AWS) welding joint designation used by Bridge Shop A is B-U7-S (6) and is illustrated in Figure 2. The plates welded into the butt joints were cut square and ground to remove all kerf deposits. They were then butted together and secured by welding a runoff block on each end of the joint. The U-groove was then air-carbon-arc gouged in one side to the mid-thickness of the plate joint. After grinding the arc-gouged groove smooth, it was completely filled by depositing a sequence of weld beads. The plates were then turned over and the same procedure followed on the back side, the back gouging being carried into the joint until sound weld metal was reached at the joint mid-thickness. The total number of weld passes to complete the joints in the 3-in. thick plates ranged from 38 to 48. A typical macrostructure of the resulting weldments is shown in Figure 2.

The minimum preheat requirement for welding on the 3-in. thick plate was 225 F in accordance with the AASHTO Welding Specifications (7). The maximum interpass temperature (i.e., temperature not to be exceeded between consecutive weld passes) was kept below 650 F in accordance with the Michigan welding specifications (8). Controlling the interpass temperature is one of the most effective means of limiting weld metal grain size and hence increasing the fracture toughness of weld metal in a butt joint. In butt joints such as those welded here it has been shown that letting the interpass temperature rise to 800 F will seriously decrease the Charpy impact toughness of the deposited weld (1). Table 1 lists the welding variables and types of welding consumables used in the weldments produced for evaluation.

All weldments were nondestructively tested for the presence of defects using both radiographic and ultrasonic techniques. Defects were evaluated in accordance with Michigan's welding specifications (8) and were repaired and retested to ensure acceptability of the completed joint. Upon completion of this nondestructive testing, all weldments listed in Table 1 were typical of actual bridge girder butt welded joints in every respect. The results of the various tests reported in this study are thus considered to be typical of those properties to be found in actual bridge girder butt welded joints.

TABLE 1
WELDING VARIABLES - SUBMERGED ARC WELDMENTS

Weldment Type[1]	Base Metal	Plate Thickness, in.	Weld Length, in.	Electrode-Flux Classification		Current, amps	Voltage/ Polarity, volts	Travel Speed, ipm	Fabricator
				Electrode	Flux				
SAW588-A1,2,3,4	A588	3	24	Raco 815	Lincoln 860	450	34 DCRP[2]	14	Bridge Shop A
SAW588-A5,6,7,8	A588	3	24	Linde WS	Linde 124	525	36 DCRP	19	Bridge Shop A
SAW36-A1,2,3	A36	3	24	Linde 81	Linde 124	550	35 DCRP	19	Bridge Shop A

[1] Identification symbolism:
SAW - Submerged arc weld
588 or 36 - ASTM A588 or A36 Base Metal
A - designates Bridge Shop A
(number suffix denotes weld number)

[2] Direct current reverse polarity (electrode positive)

Mechanical and Physical Properties - Test Results

A complete set of mechanical and physical tests were conducted on a representative weldment from each variation in welding filler metal and base metal listed in Table 1. These tests are routinely required by Michigan specifications (8) and must be conducted on a "production type weldment" before any welding procedure specification is approved for use in fabrication. The following sections report the findings of these tests in characterizing the weldments' chemistry, tensile properties, and Charpy V-notch impact toughness. The metallurgical structures present in the weldments for this project were typical of those reported in detail in the previous study (1).

Weldment Chemistry

Typical chemical compositions of the submerged arc weldment types listed in Table 1 are shown in Table 2. Each weld joint sampled was analyzed for composition on a weld metal sample removed from the surface of the weld and from the interior, widest section of the weld. Base metal and wire compositions are reported for comparison. The ranges of the weld metal chemistries are normal for the types of wire and flux combinations used. Additional discussion of the influence of the various constituents may be found in Ref. 1. Note that the weld metal deposits in A588 steel have a chemistry similar to that specified for the steel. These two electrodes were specially formulated to provide matching chemistry for the A588 types of steel.

Tensile Properties

The tensile properties and side bend test results for the submerged arc weldments are shown in Table 3. The AASHTO Specifications require the use of a welding wire and flux combination that meets the minimum requirements of the F 72-Exxx classification for welding the A588 steel or the F 62-Exxx classification for welding the A36 steel. (The F 72-Exxx classification is also allowed for the welding of A36 steel.) These classifications actually specify an "overmatching" of the minimum tensile requirements of the base metal which is a common specification for weldments. This provides a factor of safety in the weld metal which must function in the presence of residual stresses and microdiscontinuities or flaws. Note that the weld metal deposited in the A36 steel weldment SAW 36-A1 exceeds the maximum tensile stress requirement of the F 72-Exxx classification at the center of the plate (at t/2 which is not a specified test location). The strength values shown are actually an excessive overmatch of the A36 base metal strength and can lead to other problems in the weld metal to base metal interface (fusion line) such as a loss of ductility at the fusion line and cracking due to the build-up of high residual stresses which form during weld cooling. An optimum overmatch of weld metal to base metal strengths would limit the actual yield strength differential to around 10 ksi. No failures were noted in the bend tests or the reduced section tensile tests. All the welding procedures tested would be considered as passing the specified test requirements and could be considered acceptable for use.

TABLE 2
CHEMICAL COMPOSITIONS OF SUBMERGED ARC WELDMENTS

Weldment Type (See Table 1)	Typical Analysis (weight, percent)									Electrode/Flux Classification
	C	Mn	P	S	Si	Ni	Cr	Cu	V	
SAW588-A1										
Weld Metal-Internal	0.08	1.06	0.017	0.024	0.51	0.33	0.48	0.77	0.01	Raco 815/Lincoln 86
Weld Metal-Surface	0.05	1.15	0.016	0.024	0.61	0.32	0.45	0.93	<0.01	
Base Metal-A588	0.13	0.94	0.113	0.014	0.21	0.30	0.49	0.25	0.04	
Wire Analysis	0.08	0.69	0.009	0.021	0.31	0.32	0.50	0.84	—	
SAW588-A5										
Weld Metal-Internal	0.08	0.61	0.011	0.023	0.49	0.47	0.53	0.42	0.01	Linde WS/Linde 124
Weld Metal-Surface	0.06	0.57	0.010	0.025	0.56	0.50	0.52	0.47	<0.01	
Base Metal-A588	0.13	0.94	0.013	0.014	0.21	0.30	0.49	0.25	0.04	
Wire Analysis	0.11	0.46	0.003	0.024	0.31	0.50	0.54	0.44	—	
SAW36-A1										
Weld Metal-Internal	0.09	1.40	0.020	0.023	0.71	—	—	0.10	0.01	Linde 81/Linde 124
Weld Metal-Surface	0.06	1.62	0.029	0.020	0.95	—	—	0.12	0.01	
Base Metal-A36	0.18	1.08	0.010	0.029	0.18	—	—	—	—	
Wire Analysis	0.13	0.84	0.008	0.025	0.25	—	—	0.07	—	

TABLE 3
TENSILE PROPERTIES AND BEND TEST RESULTS FOR SUBMERGED ARC WELDMENTS

Weldment Type (See Table 1)	All Weld Metal Tension Test				Reduced Section Tensile Test		Bend Test (pass or fail)
	Yield Strength, psi	Tensile Strength, psi	Elongation, percent	Reduction of Area, percent	Tensile Strength, psi [3]	Break Location	
SAW588-A1 [1]					81,100	Outside of weld	Pass
Specimen @ t/4	74,500	86,000	28	60			
Specimen @ t/2	77,000	89,500	27	55			
Specimen @ 3t/4	67,300	82,000	30	59			
SAW588-A5 [1]					78,800	Outside of weld	Pass
Specimen @ t/4	71,600	84,100	25	52			
Specimen @ t/2	79,500	91,000	22	48			
Specimen @ 3t/4	65,000	79,000	27	58			
SAW36-A1 [2]					75,500	Outside of weld	Pass
Specimen @ t/4	73,500	88,000	29	51			
Specimen @ t/2	88,000	99,000	23	50			
Specimen @ 3t/4	74,000	90,000	29	55			
[1] Minimum Weld Metal Requirements (A588) (F72-Exxx, AWS5.17) (7)	62,000 min.	72,000-95,000	22 min.				
[2] Minimum Weld Metal Requirements (A36) (F62-Exxx, AWS5.17) (7)	50,000 min.	62,000-80,000	22 min.				

[3] Average of 2 specimens

Electroslag Welding Process

Electroslag welding (ESW) is defined as ". . . a welding process producing coalescence of metals with molten slag which melts the filler metal and the surfaces of the work to be welded. The molten weld pool is shielded by this slag which moves along the full cross-section of the joint as welding progresses. The process is initiated by an arc which heats the slag. The arc is then extinguished and the conductive slag is maintained in a molten condition by its resistance to electric current passing between the electrode and the work. Consumable guide electroslag welding is an electroslag welding variation in which filler metal is supplied by an electrode and its guiding member" (3). Welding by this process is done in the vertical position and joints are usually completed in a single pass for any plate thickness.

The physical setup used in consumable guide electroslag butt welding is shown in Figure 3. This is the variation that was previously used in the fabrication of Michigan bridge girders and studied in this project. As the molten slag pool and weld pool move up to the joint, they are contained by two copper molds or shoes that are clamped on the plate surfaces. These shoes are slightly recessed in the middle to allow weld reinforcement to be built up on the surface. The reinforcement is later ground off flush with the plates. The shoes may be solid copper or hollow for circulating cooling water, called, respectively, the 'solid shoe' and the 'cooled shoe' methods. Both methods have been used on Michigan work and are inlcuded in this study. A sump or starting tab is required at the bottom of the joint to assure that slag depth and fusion are adequate by the time the edges of the plates to be joined are reached. Likewise, runoff tabs are provided at the top edge of the plates to avoid lack of fusion and other flaws that occur at the stopping point of the weld. These starting and runoff tabs are later removed flush with the plate edges by flame cutting and grinding.

The main advantages and disadvantages of the electroslag welding process as applied to bridge girder fabrication are as follows:

Advantages:

1) Since electroslag welding is a single pass procedure with a minimum of joint preparation required, it offers a signficant time savings in butt joint welding of plates from 1 to 8 in. The welding observed in this project showed about a 50 percent savings in welding time as compared to the submerged arc process.

2) Filler metal deposition rates are extremely high in electroslag welding, running from 25 to 45 lb/hr per electrode (9).

3) Since the weld metal pool stays molten for a long period of time and is completely covered with the molten slag pool, the deposited weld metal is generally free of slag inclusions and porosity.

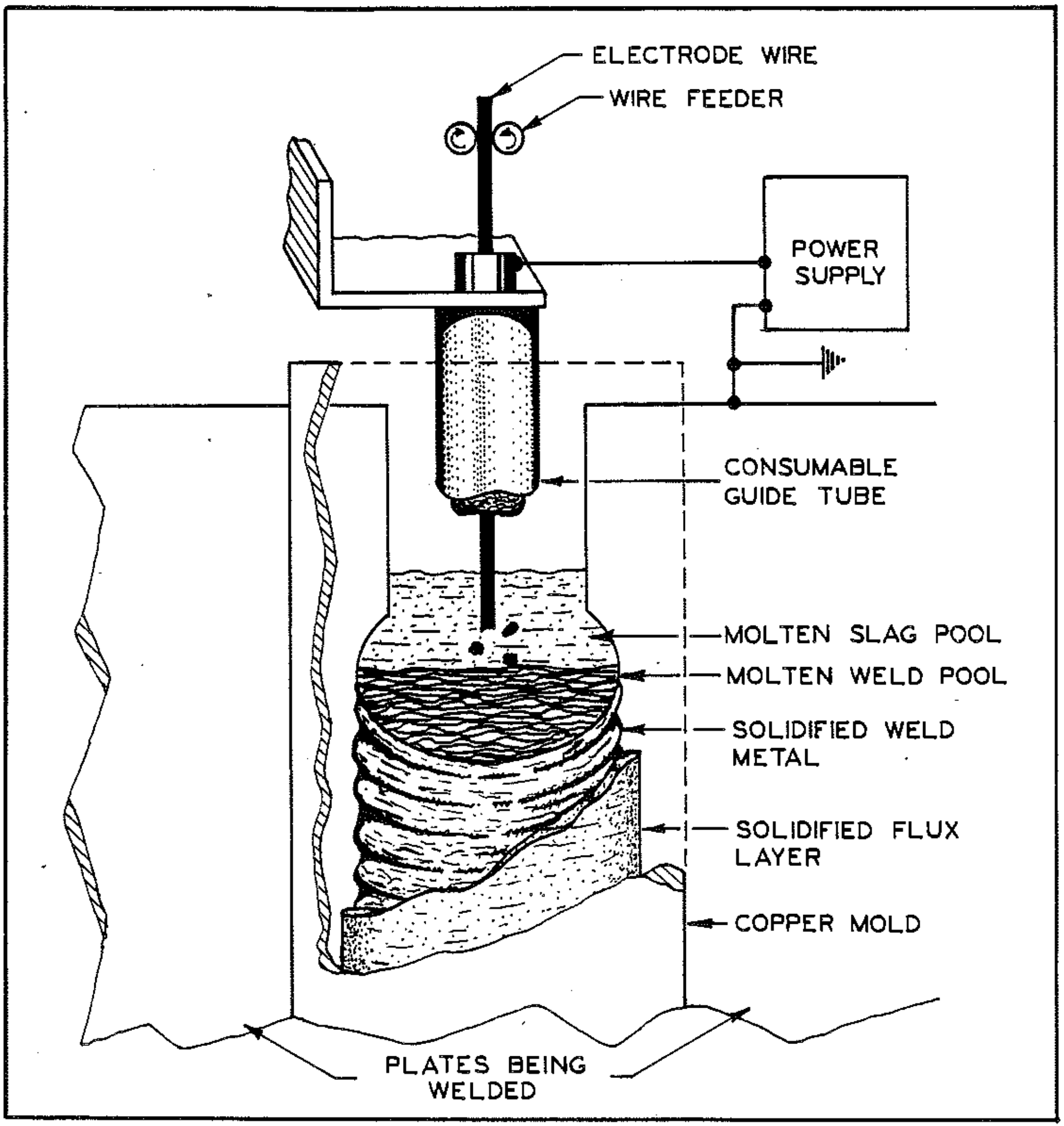

Figure 3. Schematic of consumable guide electroslag welding.

4) The distortion occurring in an electroslag welded joint upon cooling is minimal and can be compensated for in the joint setup.

Disadvantages:

1) The primary disadvantage of the electroslag process is that its very high heat input results in a prolonged thermal cycle with very slow solidification and cooling rates. This thermal cycle results in an anisotropic, nonhomogeneous, large grained weld nugget and extremely large heat-affected zone (Fig. 4). This type of weld metal structure has many

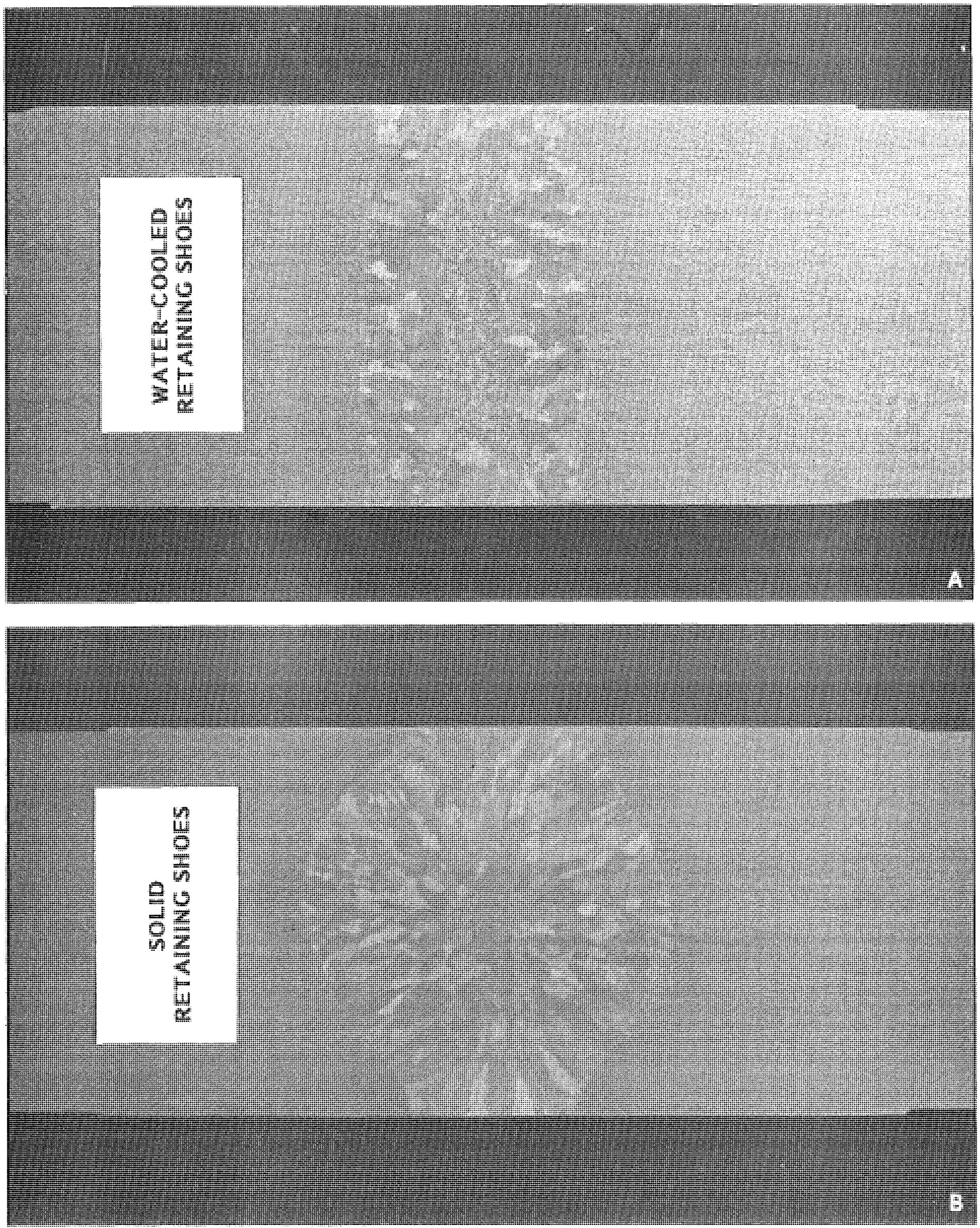

Figure 4. Typical macrostructures of electroslag welded butt joints. (a) welded with "water-cooled shoe" procedure, and (b) welded with non-cooled "solid shoe" procedure.

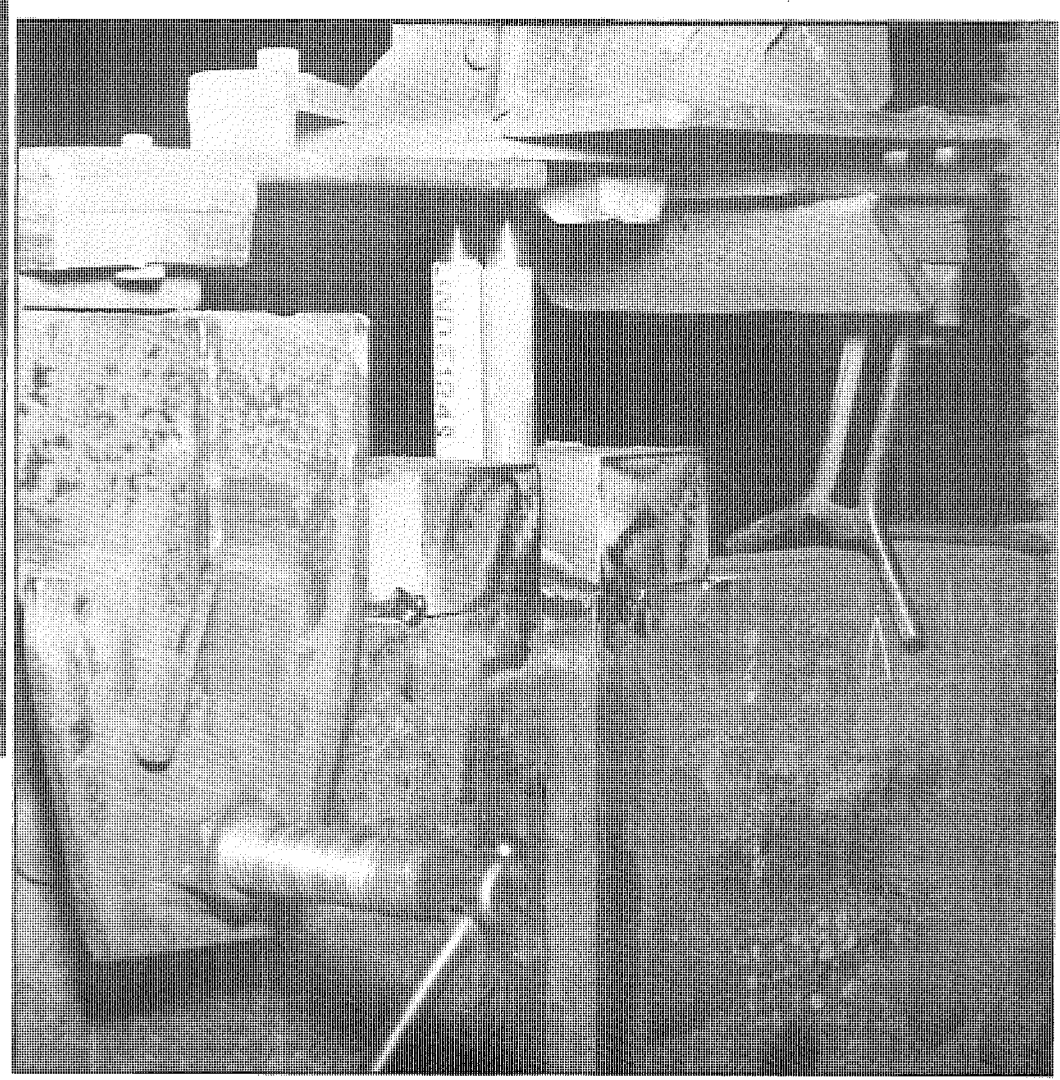

Figure 5. Electroslag welding procedure used by Bridge Shop A with solid retaining shoes (non-cooled). Wire feed coils are located above guide tubes (out of picture).

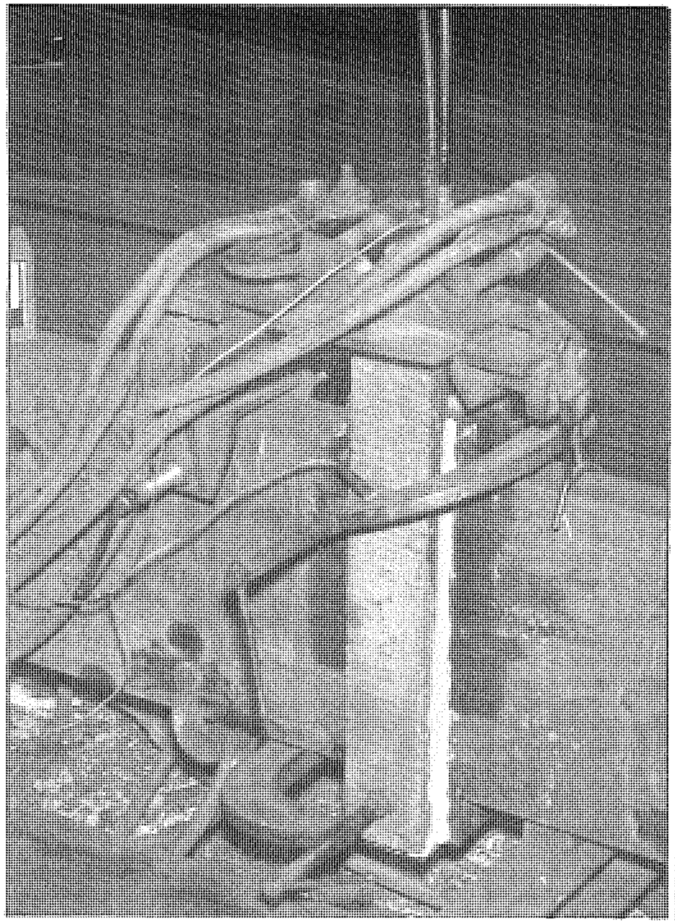

Figure 6. Double guide tube used in 3-in. thick joint by Bridge Shop A (note flux coating on guide tubes).

physical and metallurgical problems and is normally not acceptable for use in the 'as-welded' condition when Charpy V-notch impact requirements are specified (1, 10).

2) If the welding parameters (amperage and voltage) are not carefully controlled the dendritic orientation will shift in the weld metal and a high incidence of centerline cracking can occur (9).

3) Once stopped, an electroslag weld cannot be restarted because of the discontinuities produced at the start-up point. An interrupted weld must be cut out and restarted in a sump.

4) Removal of the weld fixturing, such as the starting sump and run-off tabs, can introduce serious edge defects in actual production work. These defects require meticulous repair and are easily overlooked in inspection (1).

5) The metallurgical structures present in an electroslag weldment in the 'as-welded' condition have been shown to be unreliable for use in fatigue loading applications (1, 11).

6) Field investigations of defective weldments in electroslag welded bridges have revealed problems of variability and uncertainty in the hydrogen cracking susceptability, fracture toughness, defect detection capabilities of current nondestructive testing techniques, and weld repair effectiveness of production type electroslag weldments (12).

Experimental Weldments - Electroslag Process

Electroslag butt welded specimens for this project were produced by two different sources. The first source was Bridge Shop A that produced the submerged arc welded specimens. This major midwest fabricator was a prime user of the electroslag welding process on Michigan plate girder fabrication done between early 1970 and June 1974. They used the consumable guide tube method, with solid copper (non-cooled) retaining shoes. In this method the only cooling supplied to the shoes is the heat loss to the surrounding air. The physical setup of his electroslag welding butt splice technique is shown in Figures 5 and 6. The welding procedure specification followed was the same as that used previously in Michigan bridge girder fabrication. The philosoply applied in so doing was to produce weldments that could be considered as typical of those that were in service in existing bridges. The fabricator also had no ideas or suggestions for improving his technique for electroslag welding, even though previous studies had determined that the resultant weldments would be low in physical properties (1). The weldments were made in both 24-in. wide by 3-in. thick A588 and A36 steel plates. Weldments beyond those originally prepared, were made in 29 in. wide by 2-5/16 in. thick A588 steel plates to test the effects of a special low-alloy wire that was marketed for use in unpainted exposures of A588 (weathering) steel bridges in thicknesses up to 2-1/2 in. The weldment identification descriptions are shown in Table 4 and the welding variables and types

TABLE 4
DESCRIPTION OF ELECTROSLAG AND ELECTROGAS WELDMENTS

Weldment Type[1]	Base Metal	Plate Thickness, in.	Weld Length, in.	Electrode Type[2]	Wire Feed Type[3]	Copper Shoe Type	Fabricator
ESW588-A1,2,3,4	A588	3	24	A	2CT-sta.	Solid	Bridge Shop A
ESW588-A5,6,7,8,9	A588	2-5/16	29	B	1CT-sta.	Solid	Bridge Shop A
ESW588-A11	A588	3	16	A	2CT-sta.	Solid	Bridge Shop A
ESW588-B1,2,3,4	A588	3	24	C	1T-osc.	Water Cooled	Welding Lab B
ESW588-B5,6,7,8	A588	3	24	D	1T-osc.	Water Cooled	Welding Lab B
ESW588-C1	A588	3	16	C	1T-osc.	Water Cooled	Bridge Shop C
EGW588-D1,2	A588	3	16	E	1N-osc.	Water Cooled/Sliding	Welding Lab D
ESW36-A1,2,3,4	A36	3	24	A	2CT-sta.	Solid	Bridge Shop A
ESW36-A5	A36	3	16	A	2CT-sta.	Solid	Bridge Shop A
ESW36-B1,2,3	A36	3	24	C	1T-osc.	Water Cooled	Welding Lab B
ESW36-C1	A36	3	16	A	1T-osc.	Water Cooled	Bridge Shop C

[1] Identification Symbolism:
ESW - Electroslag Welding
EGW - Electrogas Welding
588 or 36 - ASTM A588 or A36 Base Metal
A,B,C,D - designates welding source - Bridge Shop or Laboratory
(number suffix denotes weld number)

[2] A - Flux cored electrode, Linde MC-70
B - Solid electrode, Linde WS (A588 chemistry)
C - Solid electrode, Hobart 25P
D - Solid electrode, Hobart PS 588 (A588 chemistry)
E - Flux cored electrode, Lincoln NR-431

[3] Guide tube (wire feed) types:
2CT-sta. - 2 flux coated tubes (Linde), stationary
1CT-sta. - 1 flux coated tube (Linde), stationary
1T-osc. - 1 uncoated tube (Hobart 48), oscillating
1N-osc. - Single wire feed nozzle, oscillating

TABLE 5
WELDING VARIABLES - ELECTROSLAG AND ELECTROGAS WELDMENTS

Weldment Type	Base Metal	Plate Thickness, in.	Copper Shoe Type[1]	Electrode Feed[2]	Electrode-Flux Classification		Current per Electrode, amps	Voltage/ Polarity, volts	Wire Feed Speed, ipm	Fill Rate, ipm
					Filler Metal	Flux Type				
ESW588-A1	A588	3	S	2CT-sta.	Linde MC-70	Linde 124	550	40 DCRP[3]	—	0.9
ESW588-A6	A588	2-5/16	S	1CT-sta.	Linde WS	Linde 124	550	39 DCRP	—	0.6
ESW588-A11	A588	3	S	2CT-sta.	Linde MC-70	Linde 124	550	36 DCRP	—	0.8
ESW588-B1	A588	3	WC	1T-osc.	Hobart 25P	Hobart PF201	550	40 DCRP	159	0.3
ESW588-B5	A588	3	WC	1T-osc.	Hobart PS588	Hobart PF201	550	40 DCRP	156	0.3
ESW588-C1	A588	3	WC	1T-osc.	Hobart 25P	Hobart PF201	750	42 DCRP	—	0.2
EGW588-D1 (electrogas)	A588	3	WC-Sliding	1N-osc.	Lincoln NR-431	—	800	50 DCRP	515	1.5
ESW36-A1	A36	3	S	2CT-sta.	Linde MC-70	Linde 124	550	40 DCRP	—	0.9
ESW36-A6	A36	3	S	2CT-sta.	Linde MC-70	Linde 124	550	36 DCRP	—	0.8
ESW36-B1	A36	3	WC	1T-osc.	Hobart 25P	Hobart PF201	550	40 DCRP	159	0.3
ESW36-C1	A36	3	WC	1T-osc.	Hobart 25P	Hobart PF201	750	42 DCRP	—	0.2

[1] S - Solid Shoes (non-cooled)
WC - Water cooled shoes

[2] Guide tube or wire feed types:
2CT-sta. - 2 flux coated tubes (Linde), stationary
1CT-sta. - 1 flux coated tube (Linde), stationary
1T-osc. - 1 uncoated tube (Hobart 48), oscillating
1N-osc. - Single wire feed nozzle, oscillating with sliding, water cooled shoes

[3] DCRP - Direct current reverse polarity (electrode positive)

of consumables used are shown in Table 5. A more complete description of the details of the welding technique used may be found in Ref. 1. Weldments ESW588-A11 and ESW36-A5 were left over from this previous project and are included here in the fracture toughness testing phase.

A second source for electroslag butt weld specimens was sought that could use the consumable guide tube method, with water-cooled copper retaining shoes. This variation of electroslag welding had also been used to fabricate Michigan bridges (1) but the fabricator had since gone out of business. Some of his weldments left over from the previous study (1) were included in the fracture toughness testing phase of this study and are designated as being fabricated by Bridge Shop C in Table 2. A welding laboratory (designated Welding Lab B) was contracted to produce the cooled shoe weldments for this project. This laboratory was the same one that had done the developmental testing of the process before it was introduced into the fabricating industry in the United States. In the series of weldments produced by Welding Lab B every effort was put forth to produce the best quality electroslag weldments of which the process was capable. These weldments would thus not be typical of those produced by a fabricator in actual production welding, but were to determine if it was possible to overcome the deficiencies noted in the electroslag weldments in Ref. 1. The physical setup used for welding with the cooled shoe method is shown in Figures 7 through 9. A single uncoated consumable guide tube was used to feed the welding wire into the joint. This guide tube was oscillated back and forth (two seconds dwell, three seconds travel) across the joint during the welding to evenly distribute the heat and deposition of filler metal. The main items that were controlled during welding in addition to those normally included in a written procedure specification were as follows:

1) Consumable guide tubes were cleaned and polished on the outside and reamed clean on the inside to eliminate any chance of hydrocarbon contamination.

2) A double ground system was used on the plate joint to symmetrically distribute the welding current flowing into the weld puddle.

3) The starting sump was preheated to about 300 F before the welding process was started.

4) All flux was stored at 250 F for hours prior to its use and was kept at 250 F until added to the welding joint.

5) The cooling water <u>inlet temperature</u> was controlled to the temperature range of 110 to 120 F. This eliminated the formation of moisture on the copper shoes that can occur with colder water and also affected the rate of cooling.

6) The flux depth over the weld pool was carefully controlled to 1-1/2 to 2 in.

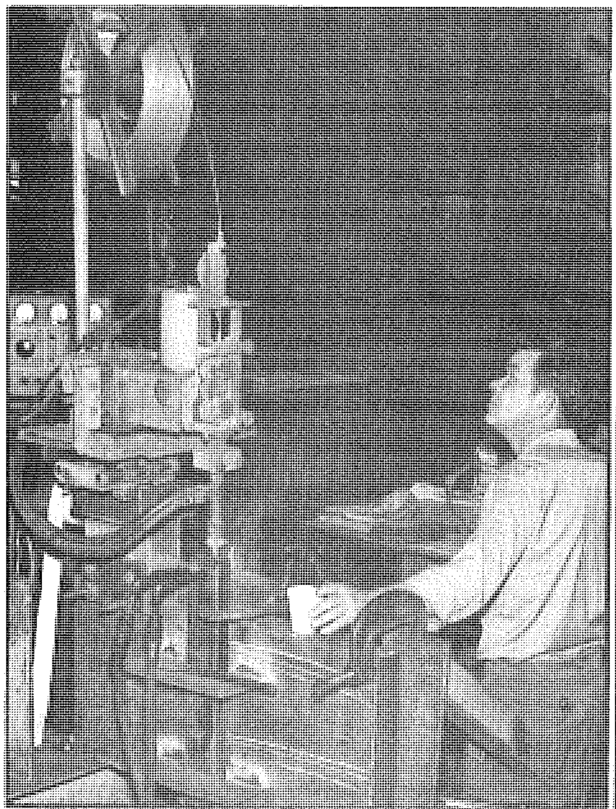

Figure 7. Electroslag welding procedure used by Bridge Shop C with water-cooled retaining shoes.

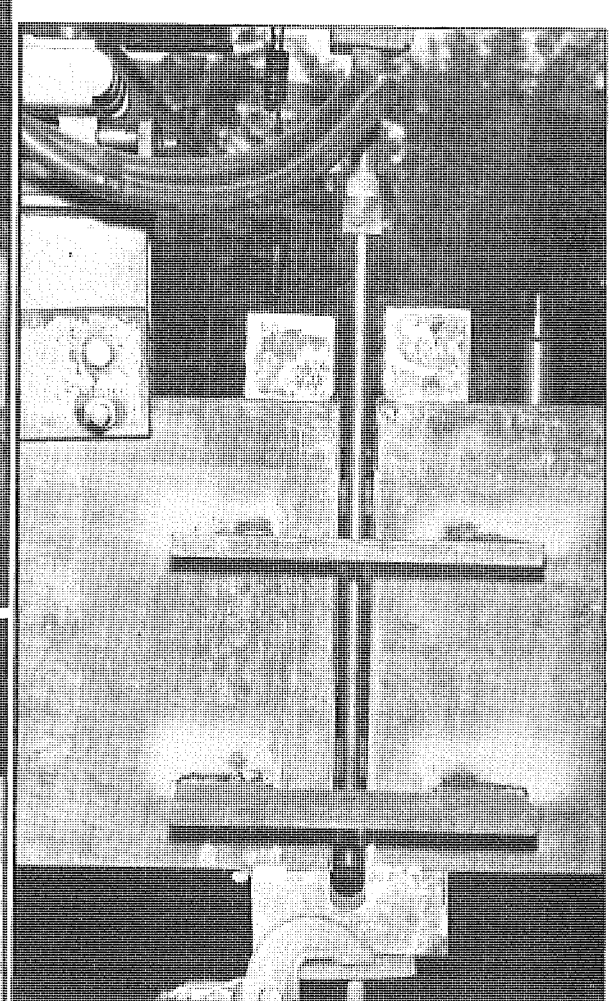

Figure 8. Bridge Shop C electroslag joint preparation showing strong-backs, starting sump, run-off tabs, consumable guide tube, and spacer ring.

Figure 9. Completed electroslag weld with retaining shoes removed, strong-backs, sump and tabs still in place (Bridge Shop C).

7) The restraint on the joint was minimized by using C-clamps to secure the weld fixturing in place.

8) Upon completion of a weld the cooling shoes were left in place with water running for 10 minutes.

Several of the steps (1,4,5,7,8) have a significant influence on the occurrence of hydrogen-induced microcracking that has been identified in electroslag weldments (13). Weldment identification descriptions are shown in Table 4 and the welding variables are listed in Table 5.

Electrogas Welding Process

Electrogas Welding (EGW) is defined as ". . . an arc welding process which produces coalescence of metals by heating them with an arc between a continuous filler metal (consumable) electrode and the work. Molding shoes are used to confine the molten weld metal for vertical position welding. The electrodes may be either flux cored or solid. Shielding gas may or may not be obtained from an externally supplied gas or mixture" (3). Like electroslag, welding with this process is usually done in a vertical position and the joint is completed in a single pass. A complete description of the process is found in Ref. 9.

Electrogas welding was never used on any Michigan bridge fabrication. It was used to a limited extent on girder butt welding for other states. For this reason it was included in this study for comparative purposes. A major industrial welding lab agreed to fabricate the electrogas weldments using a flux-cored arc wire version that required no external shielding gas. The weldments were produced in 24-in. wide by 3-in. thick A588 steel only since this low alloy plate had previously demonstrated the poorest physical properties in electroslag weldments (1). The physical setup for the electrogas welding is shown in Figure 10. The weldment identification and description of welding variables are shown in Tables 4 and 5. Note the high rate of fill or welding speed typical of the self-shielding, flux-cored arc version of electrogas welding (1.5 in. per minute full joint fill for the 3-in. thick plate). A water-cooled, single nozzle wire feed system was employed with the nozzle oscillating back and forth across the joint to evenly distribute the welding heat input. A solid copper shoe was clamped to the back side of the weld joint and a water-cooled sliding shoe covered the joint in the front. The length of the sliding shoe is such that the weld nugget is fully solidified by the time the shoe passed any specific location along the weld.

The advantages and disadvantages of electrogas welding are essentially the same as those listed under electroslag welding. Since the high heat input and thermal cycles of the two processes are similar the weldment metallurgical structures are essentially the same as well. An additional source of defects in the electrogas process arises if the shielding gas is disturbed by air currents or if the flux-cored wire has insufficient fill of its core (9). In the weldments made for this project no problem with

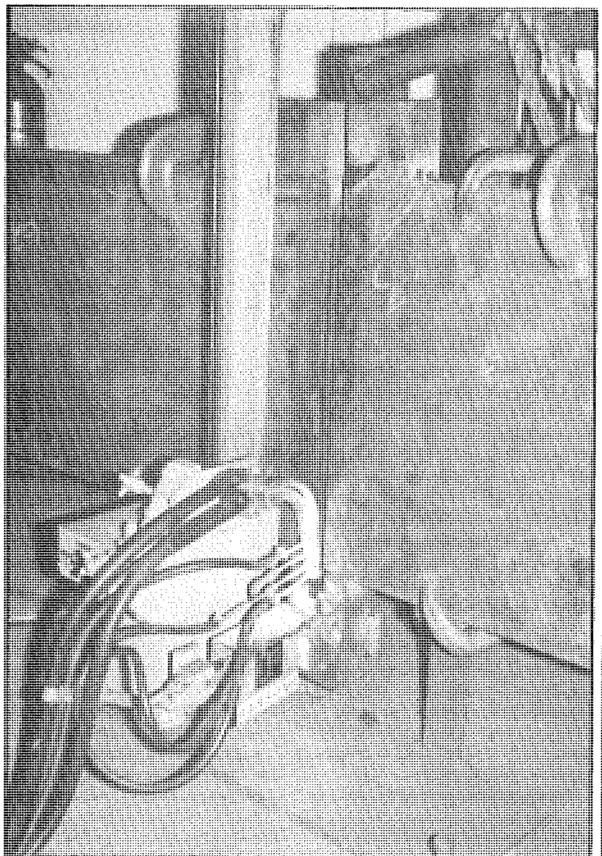

(a) Joint prepared for welding showing moving nozzle feed with sliding, water-cooled shoe on front and solid retaining shoe on back.

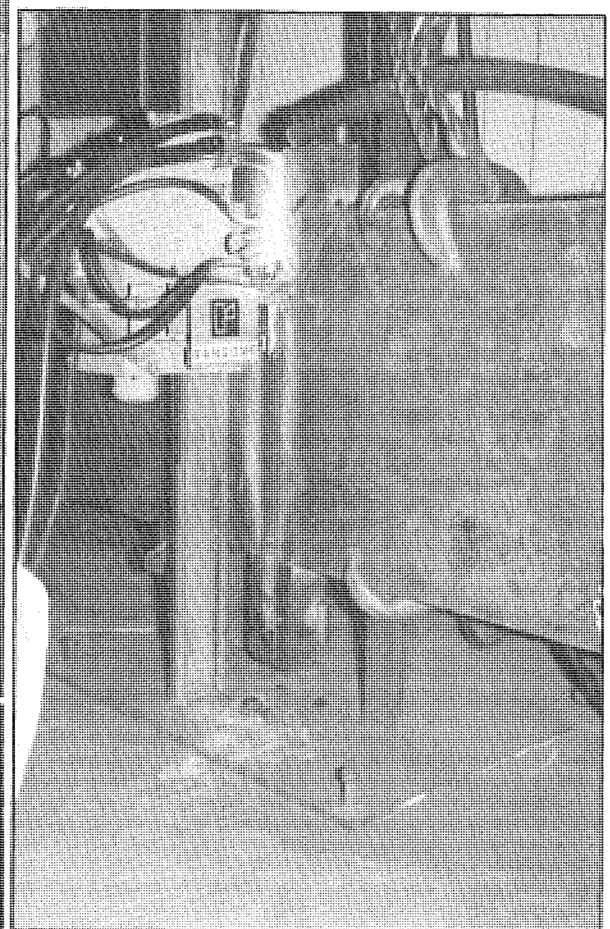

(b) Welding in progress with open arc typical of the flux cored arc process.

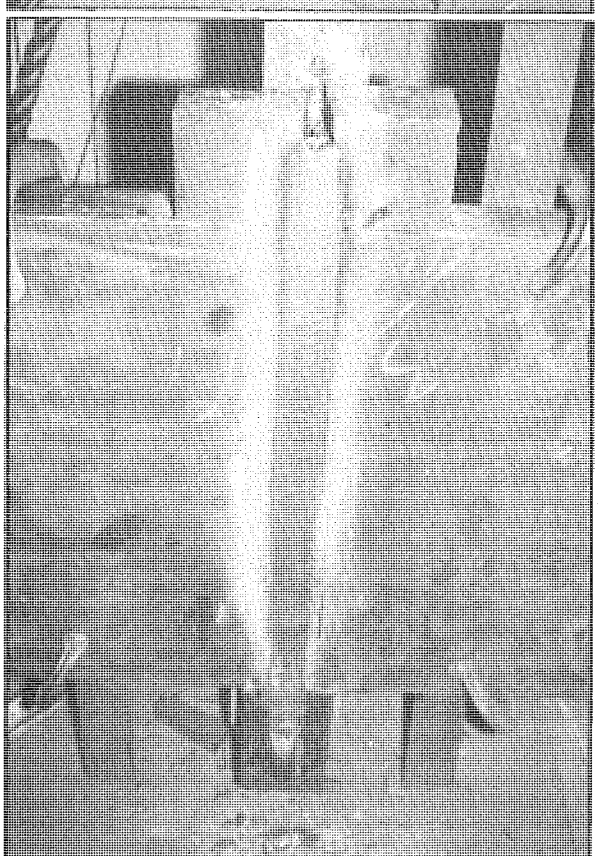

(c) Completed joint welded in a single pass.

Figure 10. Electrogas welding setup used by Welding Lab D.

wire core fill was encountered. The manufacturer of the flux-cored wire used, guarantees the flux core of the wire by a process of 100 percent quality control check for core fill.

Nondestructive Testing of Electroslag and Electrogas Weldments

All weldments were nondestructively tested for the presence of defects using both radiography and ultrasonic techniques. Defects were evaluated in accordance with Michigan's welding specifications (16) and were repaired and retested to ensure the acceptability of the completed joint. It is now well recognized that the welding repair of electroslag (or electrogas) weldments can be very detrimental to the remaining weld metal (12) and should be very carefully controlled. However, during the early years of electroslag welding in the American bridge industry, these effects were not recognized. Hence, most electroslag or electrogas weldments that are currently in service in bridges have an abundance of weld repairs which were thought to be 'cosmetic repairs.' These repairs were done using shielded metal arc, submerged arc, flux-cored arc, and possibly some other processes. In any field investigation or inspection of in-service electroslag or electrogas welded bridges, these repair areas are of the utmost importance to locate and evaluate. In the future, most fatigue cracking and fractures of electroslag or electrogas weldments will most likely be shown to originate at such repair areas. This is mainly due to the overmatching strength of the deposited repair weld metal and the high restraint to shrinkage that surrounds most weld repair zones. The cooled repair weld developes a residual stress field equal to the yield point of the weld metal. The underlying electroslag or electrogas weld metal thus become very susceptable to cold cracking when the repair area cools and shrinks due to its lower strength and its anisotropic, coarse grained structure.

The typical cracking or fissuring that occurs in electroslag or electrogas weld metal can be detected but is usually evaluated as 'acceptable' by existing nondestructive testing codes. This is mainly due to the fact that the existing welding codes (6, 7, 14, 15) were developed with radiography and ultrasonic criteria based on a relatively homogeneous and fine-grained base metal and weld metal. The electroslag weld metal structure is very coarse-grained and anisotropic which presents some unique differences that were never accounted for in the codes. The most significant characteristics of the electroslag or electrogas weld metal as affects nondestructive testing are the orientation of the cracking when it occurs along the network of prior austenite grain boundaries, and the increased attenuation and scattering of ultrasonic waves as they travel through the coarse-grained structure. This makes defects appear to be smaller than they are. Thus, many defects were put into service because they were 'masked' when evaluated by the existing codes.

Recognizing this possibility and considering the low fatigue strength and low toughness properties of electroslag weld metal (1), and the susceptability to grain boundary cracking, it should be expected that in the

TABLE 6
CHEMICAL COMPOSITIONS OF ELECTROSLAG AND ELECTROGAS WELDMENTS IN A588 STEEL

Weldment Type (See Table 4)	Typical Analysis (weight, percent)										Electrode/Flux Classification
	C	Mn	P	S	Si	Ni	Cr	Cu	V	Mo	
ESW588-A1											
Zone 1 Weld Metal	0.12	1.24	0.012	0.015	0.33	0.19	0.30	0.15	0.02		Linde MC-70/Linde 12
Zone 2 Weld Metal	0.12	1.24	0.011	0.018	0.32	0.18	0.29	0.14	0.02		
Base Metal-A588	0.13	0.94	0.013	0.014	0.21	0.30	0.49	0.25	0.04		
ESW588-A6											
Zone 1 Weld Metal	0.13	0.79	0.011	0.024	0.34	0.33	0.51	0.38	0.02		Linde WS/Linde 12
Zone 2 Weld Metal	0.15	0.79	0.010	0.023	0.33	0.32	0.51	0.38	0.02		
Base Metal-A588	0.16	1.17	0.015	0.029	0.24	—	0.55	0.27	0.06		
Wire Analysis	0.11	0.46	0.003	0.024	0.31	0.50	0.54	0.44	—		
ESW588-B1											
Zone 1 Weld Metal	0.12	1.07	0.017	0.021	0.35	0.16	0.21	0.10	0.015		Hobart 25P/ Hobart PF201
Zone 2 Weld Metal	0.15	1.08	0.015	0.026	0.38	0.15	0.20	0.10	0.016		
Base Metal-A588	0.18	0.99	0.010	0.018	0.22	0.32	0.50	0.22	0.042		
Wire Analyses (typ.)	0.076	1.24	0.016	0.016	0.57	—	—	0.007	0.003		
ESW588-B6											
Zone 1 Weld Metal	0.20	1.14	0.013	0.023	0.43	0.55	0.51	0.35	0.027		Hobart PS588/ Hobart PF201
Zone 2 Weld Metal	0.16	1.10	0.012	0.020	0.39	0.54	0.51	0.35	0.026		
Base Metal-A588	0.19	0.97	0.011	0.018	0.22	0.32	0.51	0.22	0.040		
Wire Deposit Analysis (typ.)	0.055	0.92	0.012	0.015	0.25	0.83	0.53	0.45	0.004		
EGW588-D1											
Zone 1 Weld Metal	0.12	1.23	0.006	0.020	0.14	0.11	0.16	0.13	0.03	—	Lincoln NR-431
Zone 2 Weld Metal	0.11	1.29	0.006	0.020	0.15	0.11	0.16	0.13	0.03	—	
Base Metal-A588	0.19	1.19	0.005	0.023	0.22	0.17	0.60	0.34	0.05	—	
Wire Deposit (typ.)	0.086	1.33	0.005	0.017	0.12	0.03	0.02	0.10	0.03	0.21	

TABLE 7
CHEMICAL COMPOSITIONS OF ELECTROSLAG AND ELECTROGAS WELDMENTS IN A36 STEEL

Weldment Type (See Table 4)	Typical Analysis (weight, percent)									Electrode-Flux Classification
	C	Mn	P	S	Si	Ni	Cr	Cu	V	
ESW36-A1										
Zone 1 Weld Metal	0.15	1.29	0.012	0.026	0.30	0.03	0.03	0.02	<0.01	Linde MC-70/Linde 124
Zone 2 Weld Metal	0.15	1.27	0.012	0.027	0.30	0.03	0.03	0.02	<0.01	
Base Metal - A36	0.18	1.08	0.010	0.029	0.18	—	—	—	—	
ESW36-B1										
Zone 1 Weld Metal	0.13	1.04	0.016	0.025	0.33	—	—	0.014	0.005	Hobart 25P/Hobart PF201
Zone 2 Weld Metal	0.14	1.05	0.015	0.023	0.33	—	—	0.014	0.005	
Base Metal - A36	0.25	1.08	0.008	0.041	0.20	—	—	0.027	0.005	
Wire Analysis (typ.)	0.076	1.24	0.016	0.016	0.57	—	—	0.007	0.003	

years to come, the development of cracked bridge members with in-service electroslag or electrogas weldments will be quite common. Certainly this requires that any structure with fracture-critical electroslag or electrogas weldments be carefully inspected and monitored to preclude a catastrophic failure. In such instances, the prudent thing to do would be to bolt-splice steel plates over the suspect weld joints due to the remaining uncertainties in nondestructive testing and the probability of defects growing to a critical size between inspection periods. On a fracture critical structure there is generally no question of "Will the weld joints require repair splicing?" but only "When?" Thus, the safest and most cost effective decision would appear to be to splice the joints immediately and eliminate the need for an on-going inspection program and the risk of the interim uncertainties.

The weldments produced for this study did contain most of the common defects that are typical of the electroslag and electrogas processes (1, 12). These were prepared in the same manner as was used in the bridge industry in building bridge girders and retested for acceptance in accordance with the standard welding codes; hence, the weldments are as nearly representative of in-service bridge joints as possible.

Mechanical and Physical Properties - Test Results

Mechanical and physical tests were conducted on a representative weldment from each variation in welding wire and flux combination and process variation as shown in Tables 4 and 5. These tests are required by the Michigan Department of Transportation's Welding Specifications, although when the electroslag process gained initial acceptance on Michigan bridges they were not adequately enforced. It was the strict enforcement of these 'procedure qualification tests' that led to the exclusion of the electroslag welding process for weldments subject to tension or stress reversals on Michigan bridges. Additionally, the Michigan specification was rewritten in recognition of the fact that the central zone of the electroslag weld nugget could contain the lowest strength and lowest toughness (1). Hence, all the distinct weld metal zones were subject to tests, not just the t/4 location as required by the AWS Structural Welding Code (6). The following sections report the findings of these typical 'Michigan procedure qualification tests.' Although all the specified requirements for tensile properties and Charpy V-notch impact toughness are not met, the weldments are representative of those tested previously (1) and of those currently in service in bridges.

Weld Metal Chemistry

Typical chemical compositions of samples of 'all weld metal' taken from the two zones of weld metal in the electroslag and electrogas weldments are shown in Tables 6 and 7. Zone 1 represents the central core of the weld nugget and is composed of long, thin columnar crystals that are aligned in the direction of welding. Zone 2 represents the coarse, columnar crystals that lie around the periphery of the weld nugget and

TABLE 8
TENSILE PROPERTIES AND BEND TEST RESULTS FOR ELECTROSLAG AND ELECTROGAS WELDMENTS (A588 STEEL)

Weldment Type (See Table 4)	All Weld Metal Tension Test				Reduced Section Tensile Test		Bend Test (pass or fail)
	Yield Strength, psi	Tensile Strength, psi	Elongation, percent	Reduction of Area, percent	Tensile Strength, psi[3]	Break Location	
<u>ESW588-A1</u>[1]					79,600	Outside of weld	pass
Zone 1 Weld Metal	53,000	79,000	18	30			
Zone 2 Weld Metal	58,200(3)[2]	81,800	25	48			
<u>ESW588-A6</u>[1]	Zone 1				79,930	Inside of weld	fail
Zone 1 Weld Metal	(not present)						
Zone 2 Weld Metal	54,100(3)	78,400	25	56			
<u>ESW588-B1</u>[1]					76,500	Inside of weld	pass
Zone 1 Weld Metal	48,500	73,200	30	68			
Zone 2 Weld Metal	49,100(3)	74,000	26	66			
<u>ESW588-B6</u>[1]	Zone 1				83,400	Outside of weld	fail
Zone 1 Weld Metal	(not present)						
Zone 2 Weld Metal	62,700(4)	89,600	25	55			
<u>EGW588-D1</u>[1]					89,000	Inside of weld	pass
t/4 Locations	63,900(2)	83,600	28	65			
t/2 Location	64,200	83,400	27	64			
[1] Minimum Weld Metal Requirements (A588)	50,000 min.	70,000 min.	21 min.	—			

[2] Numbers in parenthesis are number of specimens tested (when greater than one) to give the average values shown

[3] Average of two specimens

TABLE 9
TENSILE PROPERTIES AND BEND TEST RESULTS FOR ELECTROSLAG WELDMENTS (A36 STEEL)

Weldment Type (See Table 4)	All Weld Metal Tension Test				Reduced Section Tensile Test		Bend Test (pass or fail)
	Yield Strength, psi	Tensile Strength, psi	Elongation, percent	Reduction of Area, percent	Tensile Strength, psi[3]	Break Location	
<u>ESW36-A1</u>[1]					71,200	Inside of weld	fail
Zone 1 Weld Metal	40,000(2)[2]	70,300	33	62			
Zone 2 Weld Metal	41,200	71,000	27	36			
<u>ESW36-B1</u>[1]					69,200	Inside of weld	pass
Zone 1 Weld Metal	38,300	66,700	31	59			
Zone 2 Weld Metal	42,000(3)	68,600	32	67			
[1] Minimum Weld Metal Requirements (A36)	36,000 min.	60,000 min.	24	—			

[2] Numbers in parenthesis are number of specimens tested (when greater than one) to give the average values shown

[3] Average of two specimens

grow inclined to the direction of welding (see Ref. 1 for a complete description of the weld metal zones). The compositions reported are typical of those previously tested and discussed (1) and are typical of electroslag and electrogas weldments in bridges. Note that the weldments ESW588-A6 and ESW588-B5 were produced using wires that had been designed to match the average chemical compositions of the various grades of ASTM A588 steel. Thus, they have a much higher content of nickel, chromium and copper than the other 'plain carbon' types of wires.

Tensile Properties

The tensile properties and side bend test results for the various electroslag and electrogas weldment types are shown in Tables 8 and 9. The test requirements specified by the American Welding Society (14) and the American Association of State Highway and Transportation Officials (15) called for essentially a 'matching of minimum base metal properties' for the deposited electroslag and electrogas weld metal. Note that this is in contrast with the 10 ksi 'overmatching' requirement that traditionally has been specified for submerged arc weld metal. The only rationale behind the lower strength requirement for the electroslag and electrogas weldments seems to be that it was the best that the processes could produce repeatedly and engineers thought that it 'was good enough.' Unfortunately, they failed to heed the warning signs that were evident in the tensile test that the coarse grained weld metal had some serious nonhomogeneous and anisotropic characteristics that were responsible for its low strength achievement (1). This oversight eventually led to some of the problems that were inherent in electroslag and electrogas weldments as put into service in bridge structures.

Note in Table 8 that the all weld metal yield strength of weldment ESW588-B1 did not meet the minimum yield requirement. This was reported earlier in Ref. 1 where it was noted that in the high-strength, low-alloy A588 steel the electroslag welding process produces low tensile properties. Also note that the Zone 1 weld metal, which is composed of long, thin crystals oriented along the longitudinal axis on the center of the weld nugget, constitutes the lowest strength position of the weldment. This also constitutes the region of lowest toughness as measured by the Charpy V-notch impact test. The Michigan specifications required the testing of procedure qualification weldments at this critical location as well as at the t/4 locations (16). The specifications issued by the American Welding Society (14) and the American Association of State Highway and Transportation Officials (15) still do not recognize this in their testing requirements. This information is not new as it was reported by Paton (17) in his textbook on electroslag welding that was translated into English (from Russian) and published by the American Welding Society in 1962. Also note that several of the reduced section tensile specimens exhibited breaks 'inside the weld,' which is an indicator that the weld metal is actually an 'undermatch' compared to the base metal strength. This is true since although 50,000 psi and 70,000 psi are the minimum yield and tensile strengths required of A588 steel, the actual strengths are usually 5,000 to 10,000 psi higher. Hence, the electroslag weld metal becomes the weakest link in the butt joint. Also note the lack of ductility typical of electroslag weld metal as exhibited in the bend test failures. See Ref. 1 for further discussions on the tensile properties of electroslag weldments as affected by the coarse, nonhomogeneous grain structures.

Fracture Toughness Testing

The rapidly developing field of 'fracture mechanics' is thoroughly understood by only a relatively small esoteric group of engineers, college professors, and mathematicians who have had occasion to study and work in the field. The concepts of fracture mechanics are only recently being introduced to structural engineering curriculums at this country's colleges and universities, and then largely in graduate school programs. The principles applied are not necessarily complex and difficult to understand but only new and somewhat foreign to the uninitiated structural engineer. Fracture mechanics analyses have revolutionized the field of structural engineering as applied to bridges and buildings in that it presents an accurate viewpoint of 'real life conditions' that exist in steel structures. Many of the results of fracture mechanics analyses have been adopted into code books (6, 7) in the form of material toughness requirements or the limitation of live-load stress ranges on welded details. This was generally done without the understanding or input of the average structural engineer, i.e., the fracture mechanics aspects of the bridge design were done for him by others. Although this approach was effective in achieving a 'quantum jump' for the bridge industry into effective fracture control, the time has come for all structural engineers to gain an understanding of the field of fracture mechanics and begin to make their own design decisions. With this goal in view, a brief description of the principles and applications of the field as pertains to steel bridge analysis is presented to aid in understanding the relevance of the fracture toughness testing presented in the following section. For a complete understanding of the field the interested reader should study Refs. 18 and 19.

The traditional viewpoint of structural engineering analysis assumes that steel is a homogeneous (i.e., mechanical properties are the same at all points within the material) and isotropic (i.e., mechanical properties are the same in all directions at each point) material. The traditional elastic design analysis proceeds to evaluate the distribution of loads on a structure through its various members and connections. This distribution of loads and bending moments, evaluated in terms of stress, gives the rational basis on which steel members may be sized. A typical bridge girder, for instance, is proportioned to keep the actual stresses induced by the bending moment and by the axial and shear loads below a certain percentage of the steel's minimum yield point. These stresses are termed 'the allowable stresses' and are dictated by the various codes which govern the design and construction of a bridge (6, 7). If a designer is asked to calculate the ultimate or failure load of his structure, he simply begins to increase the applied loading until the yield stresses are exceeded at various locations and the critically stressed portions of a structure reach the ultimate tensile strength, which occurs after some plastic or permanent deformation has occurred in the structure. There are several plasticity theories that can predict the actual failure point of the overstressed component, but they all actually view the material as 'tearing apart' or 'rupturing' because its ultimate tensile (or shear) strength was exceeded.

This design philosophy has worked well over the years for statically loaded structures that were constructed with low and medium strength steels fabricated in many cases by riveting, and not subjected to extreme numbers of cycles of high live loading. With the advent of high strength steels and welded fabrication, however, several realities of nature that had been previously ignored became very relevant and caused the engineering community to re-evaluate its design approach. This became especially true in structures that were subject to moving loads (such as bridges) where the rate of loading and repetition of loading (fatigue) became influential on the response of the structural materials. The factors that have been ignored in the traditional elastic design analysis of engineering structures are the following:

1) Presence of flaws and defects in steel and weldments

In real life there is no such thing as a steel component that is homogeneous, isotropic, and free of flaws and defects. All engineering materials contain variations in physical properties and defects or discontinuities. The relevant question is how large are such discontinuities and how are they oriented and distributed within the material and with respect to the applied stresses. Defects that had been innocuous in low strength steel members suddenly became very active in welded high strength steel members that were subject to repeated live loads. Fracture mechanics analysis provides a method of accounting for such defects within a structural component and actually designing against the failure that they can cause. This philosophy, known as 'damage tolerant design,' or 'leak before bursting,' has been applied to the design of aircraft structures and pressure vessels, respectively, for many years.

2) Stress concentrations, and residual stress fields in welded steel structures

Traditional engineering design analysis did include some basic allowances for the stress concentrations (or stress raisers) that occur at abrupt changes in a section, etc. However, the understanding of the true stress condition at all locations in a welded plate girder, such as at various connection points, and the presence of residual stresses, and three-dimensional stresses were seriously lacking. Hence, many regions of a welded girder that were assumed to be conservatively designed, such as the ends of welded cover plates or gusset plate attachments to girder webs and flanges, were overstressed in fatigue loading and led to premature cracking of bridge members. These conditions were further complicated by the presence of residual stress fields that occur in the vicinity of weldments. These residual stresses develop as deposited weld metal cools and shrinks and typically reach a magnitude equal to the yield strength of the respective weld metal or base metal. Added to the residual stresses are the restraint stresses developed by the three-dimensional effects in thick plates. The thicker a flange plate is, the more the three-dimensional restraint affects the fatigue life of a welded attachment and the actual fracture toughness of the base plate. Through fracture mechanics analysis and full-scale laboratory testing, the behavior of these details are now understood (18) and a welded structure can be designed to preclude premature fatigue or fracture failures.

3) Rate-of-loading and temperature effects

The fracture strength of all steels is dependent upon the rate at which the loading is applied and the temperature of the steel at the time of loading. In the traditional design approach to bridge structures the analysis was based on static conditions and an 'impact factor' was applied to the resulting stresses to try to account for the dynamic effects in a bridge. Although this approach worked for the large part, there are cases where such analysis proved inadequate. A further hedge against the effects of dynamic loading was to specify material toughness requirements on the steel based on the Charpy V-notch impact test. Again, this was an effective screening device to eliminate the extremely low toughness heats of steel, but often proved inadequate in critical applications. The effects of temperature on the fracture strength of a steel member were only indirectly considered through the Charpy impact test requirements. A fracture mechanics approach to design accounts for the true rate-of-loading on a steel component and the lowest anticipated service temperature to which the structure will be exposed.

Fracture Mechanics Design - An Overview

The field of fracture mechanics as applied to the analysis of steel bridge structures involves the concept of 'damage tolerant design' carried over from other industries (such as aircraft and pressure vessel design). In these other fields of engineering it has long been recognized that the effects of defects, stress concentrations, residual stress fields in weldments, temperature, and rate-of-loading could not be ignored in a rational design. In brief, the following initial design assumptions are recognized and dealt with in a fracture mechanics design analysis:

1) Initial flaws/defects exist in all structure components

This assumption is basic to the fracture mechanics analysis and is directly supported by real life service experience. Any welded steel bridge member contains initial flaws, defects, or discontinuities that are built into the structure either in the steel manufacturing process or in the welding and fabrication of the member. Criteria are established for the acceptable size of these initial flaws. Nondestructive testing techniques using magnetic particle inspection, radiography, and ultrasonic testing are rigorously applied to ensure that any defects exceeding the specified limits are repaired before the member is put into service. The initial flaws that remain are either analyzed for their affect on the steel members fatigue and fracture behavior or laboratory tests are conducted to predict such behavior. At present, most of the typical details in a welded steel bridge have been evaluated and rated based on full-scale laboratory fatigue and fracture tests (18, 19).

2) Welded joints and connections in steel bridge members contain residual stress fields and stress concentration regions

This assumption is the most complex to evaluate analytically but the fatigue and fracture behavior of most typical details have been discovered through full-scale laboratory tests (18, 19). These results agree very well with in-service case studies of fatigue and fracture failures that are occurring in the bridge field. This knowledge can now be applied to avoid such failures in new designs and to retrofit existing structures before such failures can occur.

3) The service life of a bridge component is based on its total fatigue life in addition to its ultimate strength

Once a member has been proportioned in the traditional design manner to carry the applied loads without exceeding a specified percentage of its yield strength (typically 0.50 to 0.60 σ_y) the magnitude of stress (assuming no overloads occur) no longer dictates the service life of the member. The controlling factor becomes the fatigue live loading cycle in terms of the applied stress range. This applied fatigue stress range will determine a finite life for all the various regions of a steel bridge member, based on the types of welded details encountered and the initial flaw sizes that are accepted by nondestructive testing. A combination of theoretical analysis and laboratory testing can be applied to determine a conservative fatigue life (in terms of cycles of applied live load) for each type of detail encountered (18). Design against failure then becomes a matter of either proportioning the member to further reduce the applied stress range or reducing the number of anticipated cycles of applied load below the fatigue life of the detail. Tables of most typical details are currently displayed in the code books (6, 7) which allow the designer to preclude premature fatigue failure in a bridge member. Any detail that is not found in such references should be avoided or very carefully evaluated before use. (Such nonstandard cases often arise in the rehabilitation and welding of existing steel structures.)

4) A material property, called 'fracture toughness' controls the behavior of a loaded steel member in the regions surrounding flaws and defects

The traditional method of engineering analysis of a structure utilizes material properties of a steel such as the yield strength, tensile strength, ductility (as measured by elongation), and thermal properties. Fracture mechanics utilizes another material property, called the 'material fracture toughness,' which is quite distinct from the other properties. It is actually a measure of the steel's ability to resist or prevent rapid, unstable crack propagation from occurring in the vicinity of a sharp crack or defect present in a loaded member. Stated another way, fracture toughness is a measure of the material's ability to deform plastically in the presence of a sharp notch or flaw. The fracture toughness of a steel is dependent on the microstructure of the steel, the state of stress, the rate-of-loading, the material temperature, and other environmental factors. This property can be measured experimentally on a given material and then used for design analysis to prevent unstable crack growth or fracture of a steel member by controlling the applied stress field, limiting the fatigue stress range, and controlling other variables in the vicinity of anticipated cracks or defects.

What actually occurs in steel bridge members is that the steel making, welding, and fabrication processes build small initial flaws or discontinuities into a girder that either are undetected or judged as acceptable by the nondestructive testing criteria, as mentioned above in point 1. In the regions of a welded girder where these small initial defects experience the highest live load stress range, mentioned in points 2 and 3, these defects experience a finite fatigue life that can be viewed as two parts. The first portion of the fatigue life is called the initiation phase and usually consumes more than 75 percent of the total fatigue life of the member (19). During this phase, the defects or microdiscontinuities grow from a dormant defect into a sharp-tipped, active fatigue crack. The second and terminal part of the fatigue life then beings, which is the crack propagation life. The fatigue crack that has developed from an intial defect begins to grow in size until it reaches a critical size at which the structural component fails upon one more application of live loading. It is the material property of fracture toughness that determines how large the critical crack size can become before fracture occurs. A damage tolerant design philosophy is based on the premise that given enough fracture toughness in a material, a structure can operate in the presence of such growing flaws or damage without suffering a fracture or failure. It then becomes the role of periodic inspections, using nondestructive testing, done on the structural components to detect, quantify, and repair any propagating fatigue cracks before they reach the critical size and cause a fracture. This is what happens in reality and constitutes the safest approach to building and maintaining a structure. Many case studies have been generated over the past 10 years that illustrate the consequences of failing to recognize these realities of nature (18). It is obvious in this approach to the design of a structure that periodic inspections to detect fatigue cracks that have initiated and repair them before they reach their critical size are of the utmost importance. When this inspection program is lacking, the structures experience unexpected cracking and failures as has been the recent experience in steel bridges.

5) Development of a 'fracture control plan'

The previous assumptions that are considered in a fracture mechanics analysis are incomplete unless a comprehensive overview occurs with the objective being to prevent fracture of a structure during its entire service life. Such an overview is termed a 'fracture control plan' and should be developed and specified by the engineer acting in responsible charge on behalf of the owner. A fracture control plan must include as a minimum all of the following phases of designing, constructing, maintaining, and operating a bridge structure:

1) Planning decisions (type of structure)
2) Design and specification writing
3) Fabrication/quality control/quality assurance
4) Construction/quality control/quality assurance
5) Inspection program - in service
6) Maintenance and repair
7) Monitoring of traffic loading and overloads

To date, the Federally funded highway system has made significant strides towards implementing the concepts of damage tolerant design with respect to steps 1 through 4. There are pressing needs in the areas of 5) Inspection programs, and 6) Maintenance and repair techniques. Most state highway departments face budget constraints too severe to enable them to advance to the technological level needed to inspect bridges for the presence of fatigue cracks. This inspection requires the application of nondestructive testing techniques such as dye-penetrant testing, magnetic particle testing, radiography, and ultrasonic testing. Until such programs are recognized as essential, and properly funded, our best hedge against disruptive bridge failures is through the use of redundant designs where no one member is 'fracture critical' to the structure. Thus, when a member is fractured due to the development of a critical crack, the load is redistributed to adjacent members and the bridge continues to function until the member can be repaired. Indeed, this is the case in the majority of documented bridge failures in this country (18). In the case of a fracture critical bridge, there is no safety net to rely on and the development of a crack to its critical size will lead to the collapse of the structure. In these instances the engineering community has no choice but to insist on a meaningful and rigorous inspection program as part of an ongoing fracture control plan, throughout the service life of the structure.

The Federal Highway Administration under the U. S. Department of Transportation, has issued a model "Fracture Control Plan" to be applied to new fracture critical transportation bridge structures (20). This plan gives extensive detail on the current state of knowledge pertaining to the design, fabrication, and construction of a structure. However, it does not give much direction concerning the inspection and maintenance of the structure throughout its service life. These areas are yet to be formulated by the bridge engineering community. Understanding the importance of the detection and repair of growing cracks certainly underscores the importance of the maintenance phase of a fracture control plan. Similar fracture control plans have been issued by the American Association of State Highway and Transportation Officials (21) and by the American

Railway Engineering Association (22) to be specified for fracture critical steel bridge members. **Both of these plans are also lacking in the in-service inspection and maintenance requirements.**

The objective of this research project was to evaluate the material property of fracture toughness (Item 4 above) of various types of steel butt weldments. The sections that follow describe the various types of tests conducted to measure toughness and report the results of these tests. This work is unique in that, to date, only a limited amount of published data exist that characterize the fracture toughness of the types of weld metal, that are used to weld-splice steel girders, especially in thicker plates. This lack of data limits the ability of engineers to properly evaluate the significance of flaws in bridge structures, which can lead to either being overconservative and repairing harmless discontinuities or being nonconservative and allowing a critical flaw to exist in a bridge under service loading. Fracture toughness data also are very valuable in allowing the welding engineer to select the most reliable welding process for the application, based on the assurance of having adequate toughness in the resulting weldment. Knowledge of the metallurgical structure of a weldment is also important in understanding its inspectability for the presence of subcritical flaws and growing fatigue cracks.

Charpy V-Notch Impact Testing

Fracture toughness has been defined as a material property of a steel that measures its ability to resist or prevent rapid, unstable crack propagation from occurring in the vicinity of a sharp crack or defect present in a loaded member. Such rapid fractures or crack growth are termed brittle fracture and are usually characterized by a very flat, crystalline appearing cleavage surface that is oriented normal to the principal applied stress field. A true brittle fracture shows no sign of ductility on the fracture surface, such as 45° shear lips, surface dimpling or tearing, or shear ridges. Stated another way, fracture toughness may be considered as the ability of a material to resist such brittle fracture behavior in the presence of a sharp notch or crack and to deform plastically at the crack tip, hence redistributing the concentrated stresses in such a manner as to prevent a fracture initiation. Thus, a material with a high fracture toughness will exhibit a very ductile fracture behavior with all the signs of plastic tearing present on a fractured surface. Tough materials do fracture if the loading is high enough but exhibit a very different mode of failure than brittle materials.

The Charpy V-notch impact test is a type of test that belongs to a group referred to as 'notch-toughness tests.' Although it is not a direct, quantitative measure of the material property of fracture toughness, it has proven to be an effective screening test since it will normally rate materials in their proper order of comparative toughness. Hence, the Charpy test has long been used in the steel industry as such a screening test in the development of alloys, in steel manufacturing, and as a fabrication (welding) quality control test. The Charpy V-notch impact test has often been correlated with successful service experience and in some cases has demonstrated a reliable empirical correlation with more sophisticated tests that measure fracture toughness directly (19). The current codes that pertain to steel manufacturing and to welded fabrication all specify a minimum required fracture toughness as estimated by an equivalent Charpy V-notch impact value with the test conducted at a prescribed temperature (6, 7, 21, 22).

The Charpy V-notch test is governed by standard test method E23, Standard Methods for Notch Bar Impact Testing of Metallic Materials, a specification of the American Society for Testing and Materials (23). For a complete discussion of the historical origin of the Charpy test and its correlation with service experience and other fracture toughness tests the reader is referred to Ref. 19. Suffice it to say here that the Charpy impact test is currently the most widely used test in this country for estimating the property of fracture toughness in both steel manufacturing and in welded fabrication. The present exceptions being the use of more sophisticated test methods for very high strength steels that are welded and used at low temperatures, such as oil drilling platforms in the North Sea regions and in critical pressure vessel applications.

Charpy V-notch impact tests were conducted in this study to evaluate the relative toughness of the various zones of the submerged arc and electroslag weldments. Extensive testing was performed in the previous research project (1) that characterized the weldments as to their toughness variation with temperature, and the effects of the nonhomogeneous and anisotropic metallurgical structure on the Charpy impact toughness. In the present study only the standard sets of five specimens were tested from each zone of the respective butt weldments as required by the welding specifications (6, 8). This was done for comparison of the weldments notch toughness to the code requirements, and to previous results on the same weldment types (1). The data are presented in graphical form in Figures 11 through 15 which show in outline the various metallurgical regions of the weldments. All specimens were machined as longitudinal Charpy tests, which means that the long axis of the Charpy specimen was oriented along the direction of principal tensile stress (which is transverse to the weld) as would be applied to a typical welded splice. This forces the crack in the Charpy test specimen to run along the longitudinal axis of the weld (i.e., perpendicular to the applied stress) the same direction that a crack would propagate in a loaded bridge member with respect to the butt weld. Note that by doing this we are recognizing that the material property of fracture toughness is very directionally dependent. A designer must be very careful to always specify the required material toughness at the orientation that is perpendicular to the principal applied tensile stress. If a component of a structure is to be subject to biaxial or triaxial stress, then material toughness must be specified and tested in two or three directions, respectively, under the appropriate conditions of biaxial or triaxial constraint. Service failures have occurred in all fields of structural engineering where either this principle was overlooked or the fabricator inadvertently oriented the rolled steel product

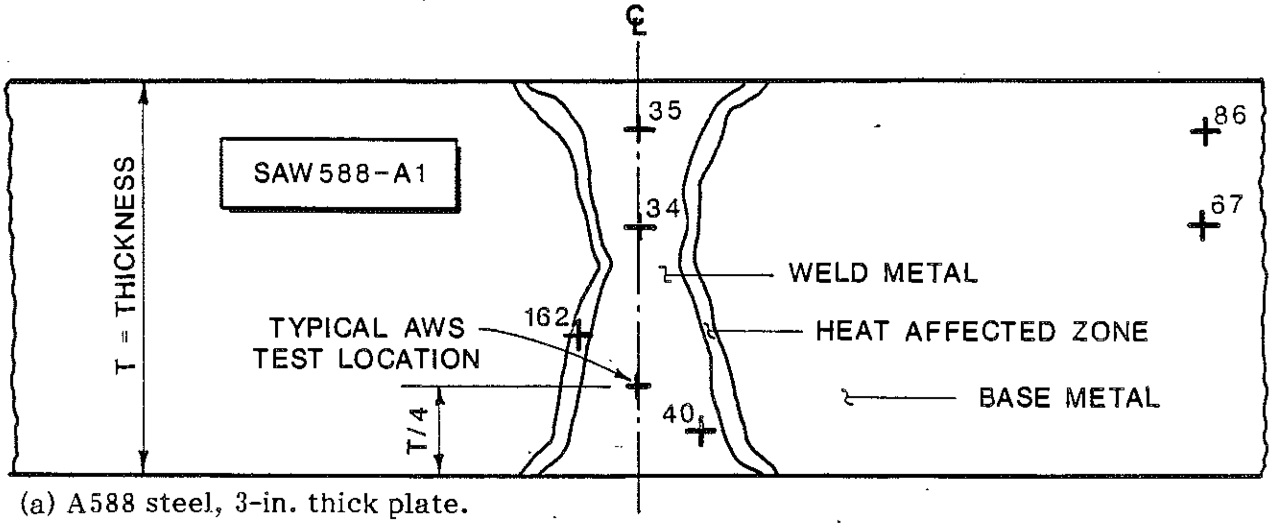

(a) A588 steel, 3-in. thick plate.

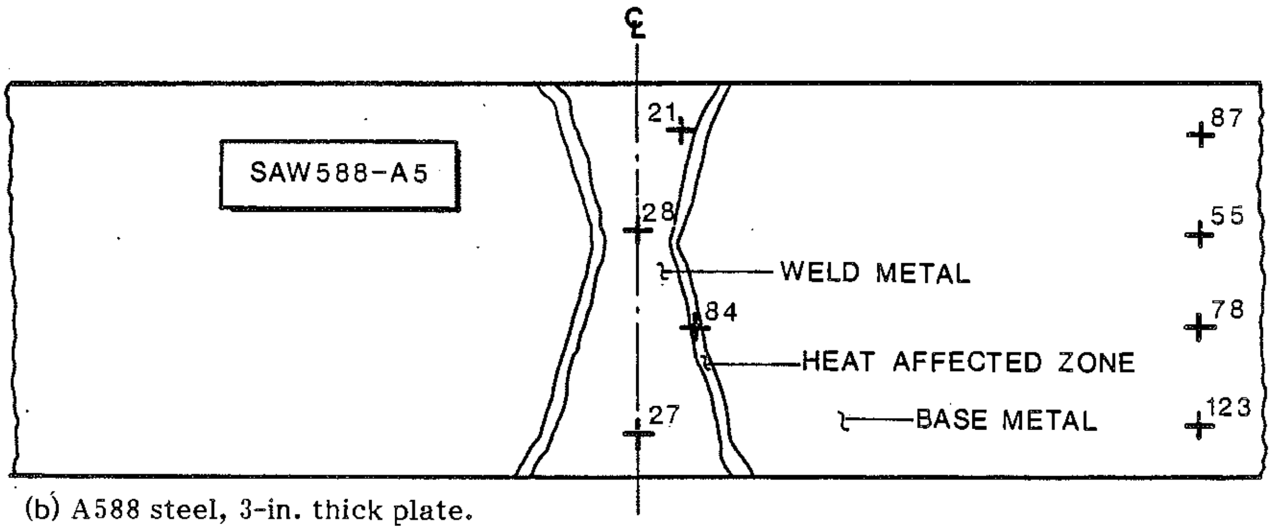

(b) A588 steel, 3-in. thick plate.

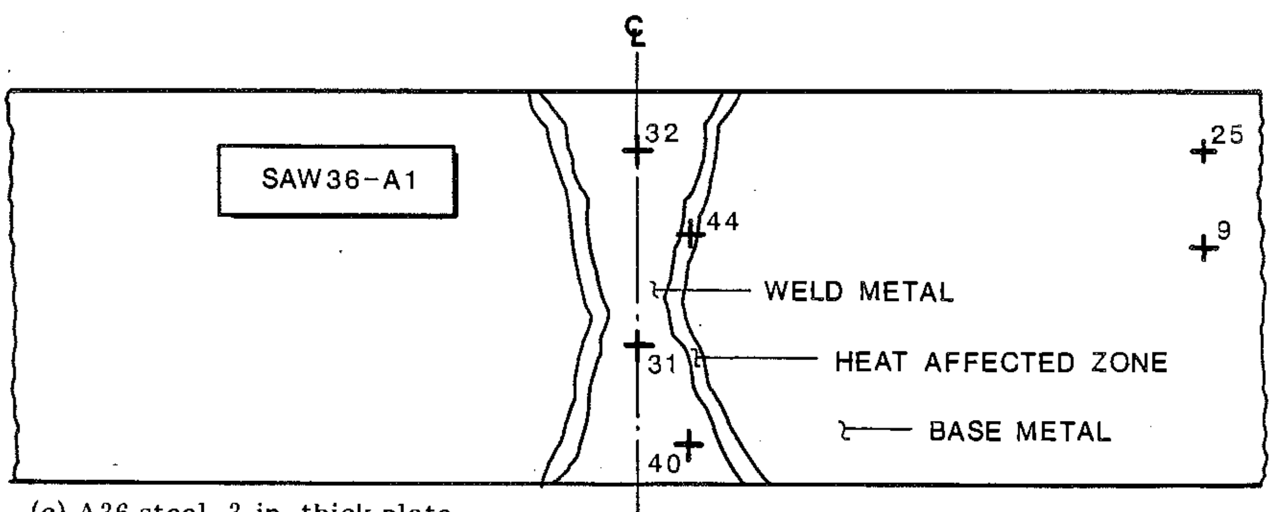

(c) A36 steel, 3-in. thick plate.

Figure 11. Charpy V-notch impact toughness (ft-lb) of submerged arc weldments made by Bridge Shop A. All tests conducted at 0 F. Each value shown represents an average of 5 specimens taken from the location shown.

incorrectly with respect to the direction of rolling. Due to the nonhomogeneous and anisotropic results of the steel making process, a piece of steel can have very good tensile and toughness properties in the direction of rolling and greatly reduced properties in the directions normal to the direction of rolling.

The Michigan specification (8) calls for mandatory Charpy V-notch impact testing of all welding processes and procedures used to butt splice bridge members. There is no recognition given to a proposed welding procedure as being 'prequalified' as is noted in the AWS Code (6). It has been our experience over the past 15 years that even though a written welding procedure may have been tested and proven acceptable many times, this does not mean that just anybody can follow the procedure and produce a satisfactory weldment. (Using a tried and true recipe is no guarantee that everybody can bake the cake!) Consequently, every fabricator must qualify by test each welding procedure to be used prior to fabrication. This philosophy is now being adopted by code writing bodies in the various fracture control plans specified for fracture critical, non-redundant steel members (21, 22). However, routine fabrications for redundant structures are still often welded under the concept of a 'prequalified welding procedure.' This philosophy is risky because you never know for certain what properties the welds being produced will possess. Hence, there is a reliance on the structure's redundancy to prevent a structural collapse in the case of a weld fracture. The problem with this approach is that when such fractures occur they are hard to discover and can be very costly to repair, whereas the cost of prequalification testing of welding procedures is relatively low and is an effective means of precluding inferior weldments being produced (providing that the quality control is sufficient to ensure that the procedures are followed in production).

Discussion of Charpy Test Results

In Figure 11 we see that all the submerged arc welding procedures exceeded the minimum impact requirement of 20 ft-lb at 0 F required by specification (8). Note that the toughness values are very uniform throughout the weld metal region which indicates a relatively homogeneous weld deposit. This is possible in the submerged arc process if a good procedure is used since the weld region is built up using 40 to 50 passes (for the 3-in. thick joint) and each pass is deposited identically to the others if the preheat and maximum interpass temperatures are controlled. Michigan specifications require that the interpass temperature, i.e., the weld region temperature achieved between weld passes, be kept below a maximum of 650 F. If this is not done the weld metal toughness near the surface of the plates can be seriously degraded as was shown in the previous study (1). The specified 'average test location' required by the AWS Code (6, 14) is shown in Figure 11a. This 1/4 thickness location is to be placed on the centerline of the weld. No guidance is given as to which side to take the Charpy specimens from. In the case of a non-symmetrical weld procedure, such as the commonly used AWS joint B-U3c-5, where the majority of the weld metal is deposited from one side, the Charpy test should always be located at 1/4t from that surface.

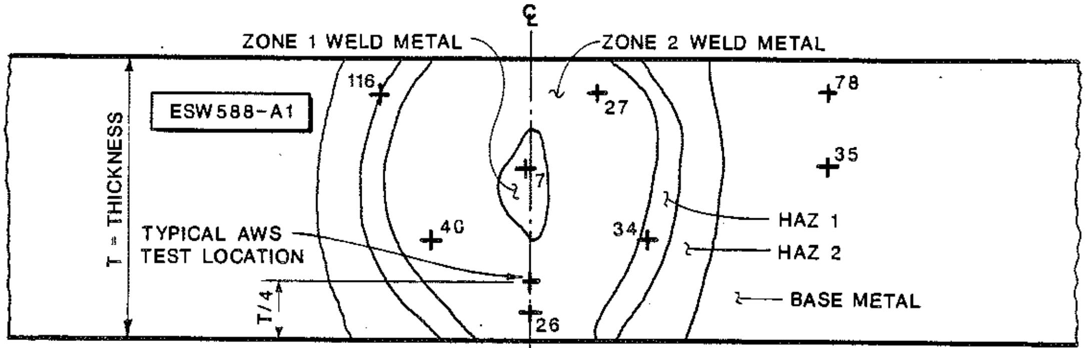

(a) A588 steel, 3-in. thick plate.

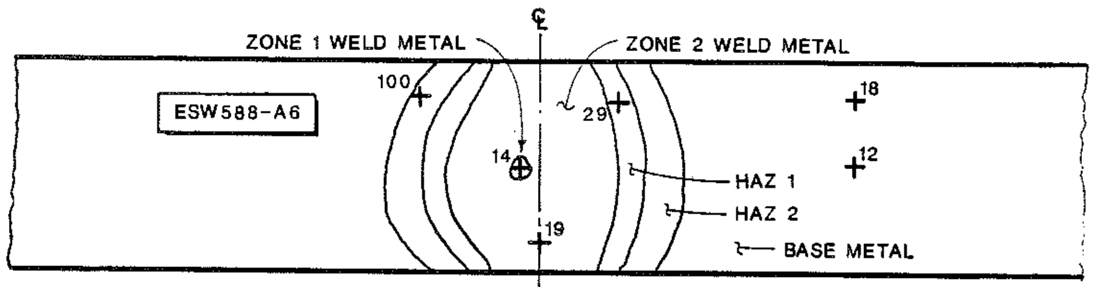

(b) A588 steel, 2-5/16-in. thick plate.

Figure 12. Charpy V-notch impact toughness (ft-lb) of electroslag weldments made by Bridge Shop A using the solid (non-cooled) shoe method. All tests conducted at 0 F. Each value shown represents an average of 5 specimens taken from the location shown.

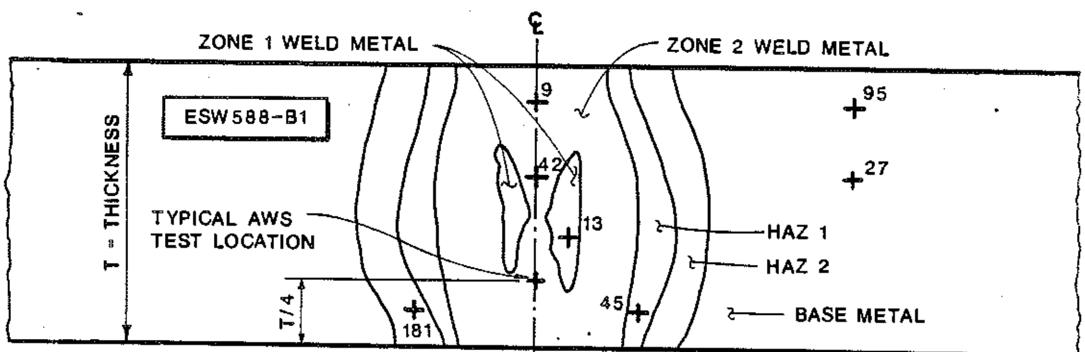

(a) A588 steel, 3-in. thick plate.

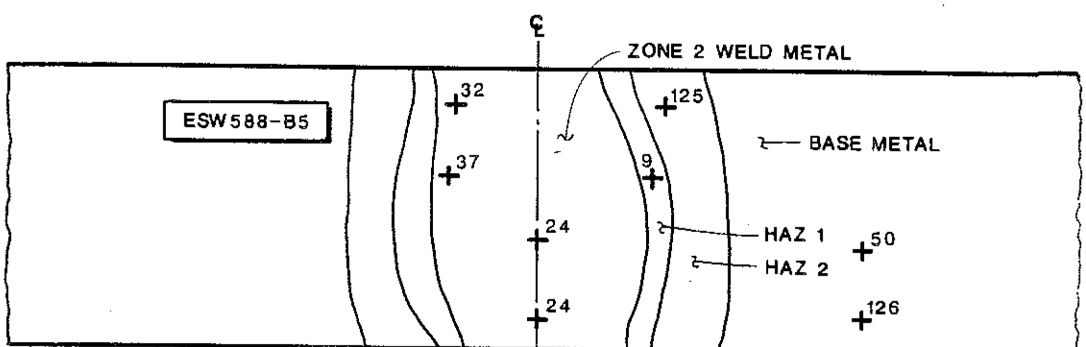

(b) A588 steel, 3-in. thick plate.

Figure 13. Charpy V-notch impact toughness (ft-lb) of electroslag weldments made by Welding Lab B using the water-cooled shoe method. All tests conducted at 0 F. Each value shown represents an average of 5 specimens taken from the location shown.

This is because the lowest toughness will generally occur in the heaviest portion of the weld metal nugget. Problems can also arise in the area of the weld root, which occurs at the 1/2t location in the joints in Figure 11. This is true because of the high dilution of weld metal with the base metal in the narrow root area. The prudent thing to do in a critical joint procedure (such as a fracture critical joint) is to **test the Charpy impact strength of both 1/4t locations and the weld root location as well.** This is the only way to ensure that the deposited weld metal uniformly exceeds the minimum impact toughness required. Note that the submerged arc process produces only one narrow heat affected zone (HAZ) in which the original grain structure of the base metal is usually refined or normalized. Thus, the Charpy impact toughness of the typical HAZ in a submerged arc weldment will be higher than the toughness of the original base plate. The impact toughness shown for the base plate is very good in these examples, which were tested at 0 F, considering that the AASHTO minimum toughness requirement for this material in a 3-in. thickness is 20 ft-lb when tested at +40 F. (The origin of this requirement will be discussed in the next section on plane-strain fracture toughness testing.)

Figures 12 thru 14 present the Charpy test results on the various types of electroslag weldments and Figure 15 the electrogas weldment. The various weld zones are shown in the schematic views of the weld cross-sectional drawings which were produced from etched sections of the actual weldments tested. The Zone 1 weld metal (when present) which occurs in the central core of the weld nugget is composed of long, thin crystals that are oriented almost in line with the longitudinal axis of the weld. The Zone 2 weld metal appears around the periphery of the weld nugget and is composed of coarse prior austinite grains with relatively fine secondary transformation products with the grains. The grains are normally oriented at an acute angle with the longitudinal axis of the weld. The first heat affected zone (HAZ 1) is a region where the original grain structure of the base metal has been coarsened by the high heat input of the electroslag process. The second heat affected zone (HAZ 2) is the region where a grain refinement or normalizing occurs similar to that of the HAZ in a submerged arc weldment. For a complete illustration and discussion of these weldment zones see Ref. 1 and 17.

The AWS code requirement for Charpy V-notch impact strength of electroslag weld metal is 15 ft-lb at 0 F. Note that this requirement is lower than that specified for submerged arc weld metal, i.e., 20 ft-lb at 0 F. The only rationale for this lower requirement appears to be that the electroslag process never could reliably produce an impact strength equivalent to the submerged arc process (1). Therefore, the toughness limit had to be lowered to allow its use. At the time that this was done, however, the code writing bodies considered 15 ft-lb at 0 F to be adequate toughness for the application of the process to bridge welding. Note also that the typical AWS specified Charpy test location is again on the weld centerline at the 1/4 thickness point, as illustrated in the figures. This is a serious deficiency in the code for electroslag weldments, due to the non-homogeneous nature of the weld nugget and the appearance of radically different weld metal zones. Note that the Zone 1 weld metal always

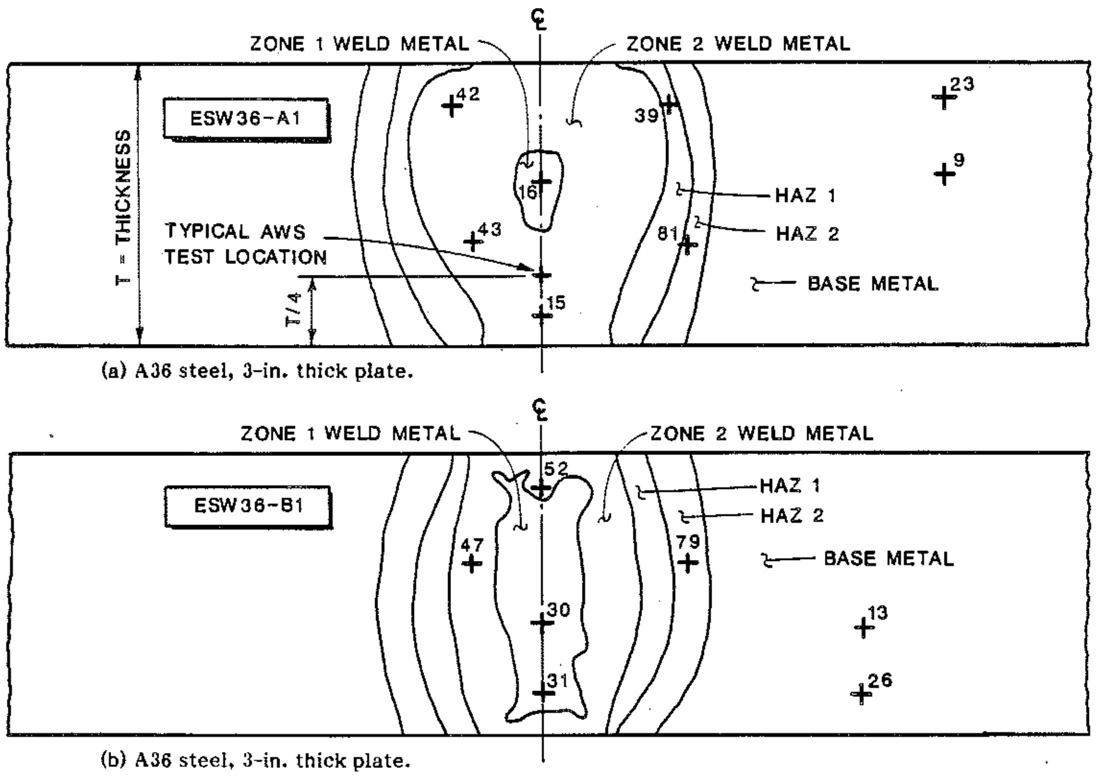

Figure 14. Charpy V-notch toughness (ft-lb) of electroslag weldments made by solid (non-cooled) shoe method (a) and the water-cooled shoe method (b). All tests conducted at 0 F. Each value shown represents an average of 5 specimens taken from the location shown.

represents the lowest toughness region of the weld, and in the A588 alloy steel does not meet the 15 ft-lb minimum test requirement. This weld metal zone cannot be located by a geometric specification but only by etching the cross-section to reveal its presence. Note in Figure 13a that the Zone 1 weld metal actually occurs on either side of the weld centerline. The Charpy impact toughness of the Zone 2 weld metal is seen to be relatively high in most of the weldments. This is mostly due to the orientation of the coarse crystals that comprise Zone 2 which lie at an acute angle to the transverse direction of the Charpy crack propagation. As shown in the previous study (1) the same Zone 2 weld metal suffers a drastic reduction in Charpy toughness when the specimen is rotated to send the crack along the direction of the coarse grain boundaries. Note that sometimes the HAZ 1 is equal to or better than the impact strength of the base metal and sometimes (Figure 13b) it is less than the base metal toughness. The effect of the grain coarsening of HAZ 1 seems to be dependent on the original base metal toughness. When the original toughness is moderate, the HAZ 1 toughness is either equivalent or improved. When the original toughness is very high, the HAZ 1 toughness is lower. The HAZ 2 toughness is always much higher than the original base metal due to the normalizing effect that it contains. For a more complete discussion on the Charpy impact results of the weld zones as relates to the metallurgical structures see Ref. 1.

The electrogas weldment in Figure 15 reveals a similar type of weld zone definition and relative toughness as the electroslag weldments. Metallurgically, the grain structures within these zones appear practically identical, although the chemistry is slightly different due to the use of a flux-cored wire rather than a running flux. The welding speed is much greater in the electrogas process tested and the heat cycle at any given point along the weld is shorter. Hence, it is observed that the various weld metal zones are narrower than those in the electroslag process. This may also offer the beneficial effect of lowering the amount of base metal dilution in the weld nugget (which can run as high as 60 percent in electroslag welding). The same low toughness of Zone 1 weld metal versus the high toughness of Zone 2 weld metal exists in the electrogas deposit.

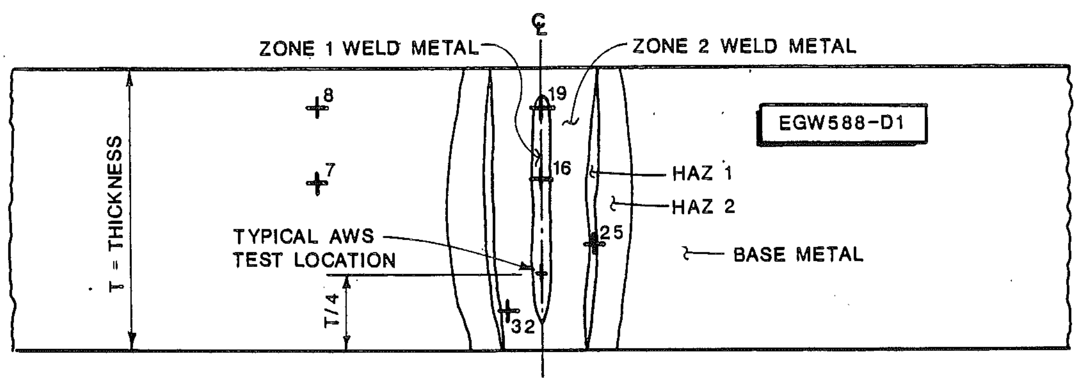

Figure 15. Charpy V-notch impact toughness (ft-lb) of electrogas weldment in 3-in. thick A588 steel. All tests conducted at 0 F. Each value shown represents an average of 5 specimens taken from the location shown.

Plane-Strain Fracture Toughness Testing - K_{IC}

One of the main shortcomings of the Charpy V-notch impact test is that the specimen size (0.394 by 0.394 by 2.165-in.) is often too small to evaluate the full plate or full weldment fracture toughness. This concern is especially valid when the size of the grain structure of the metal being tested is of the same order of magnitude as the test specimen, which is true in the case of electroslag and electrogas weldments. If the Charpy specimen's notch is aligned with a single prior austinite grain boundary, the resulting impact toughness would be comparatively low. If the specimen is shifted slightly so the notch crosses the same boundary, rather than following it, the measured toughness would be considerably higher. Thus, the results of the test become dependent upon specimen orientation. This indeed undermines the reliability of the test results as pertaining

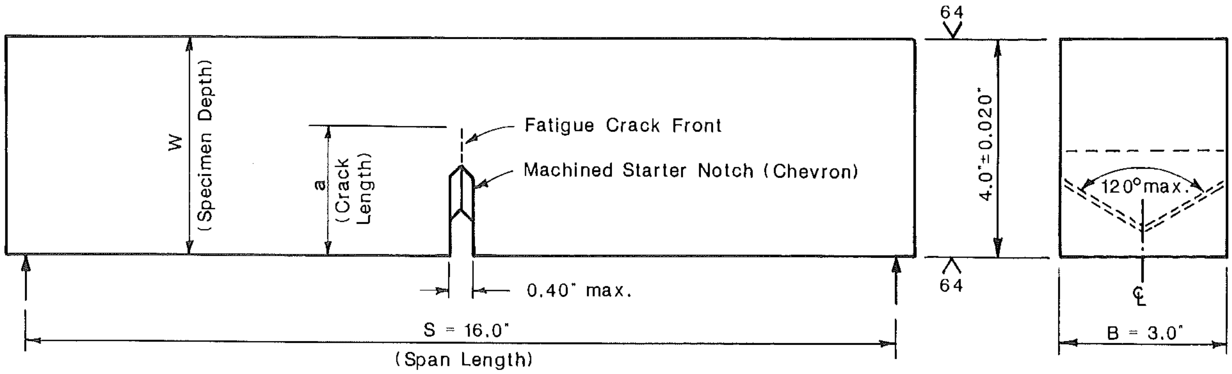

$K_Q = \left(\frac{P_Q S}{B W^{3/2}}\right) f(a/w)$ f(a/w) = relationship based on the ratio of (a/w)

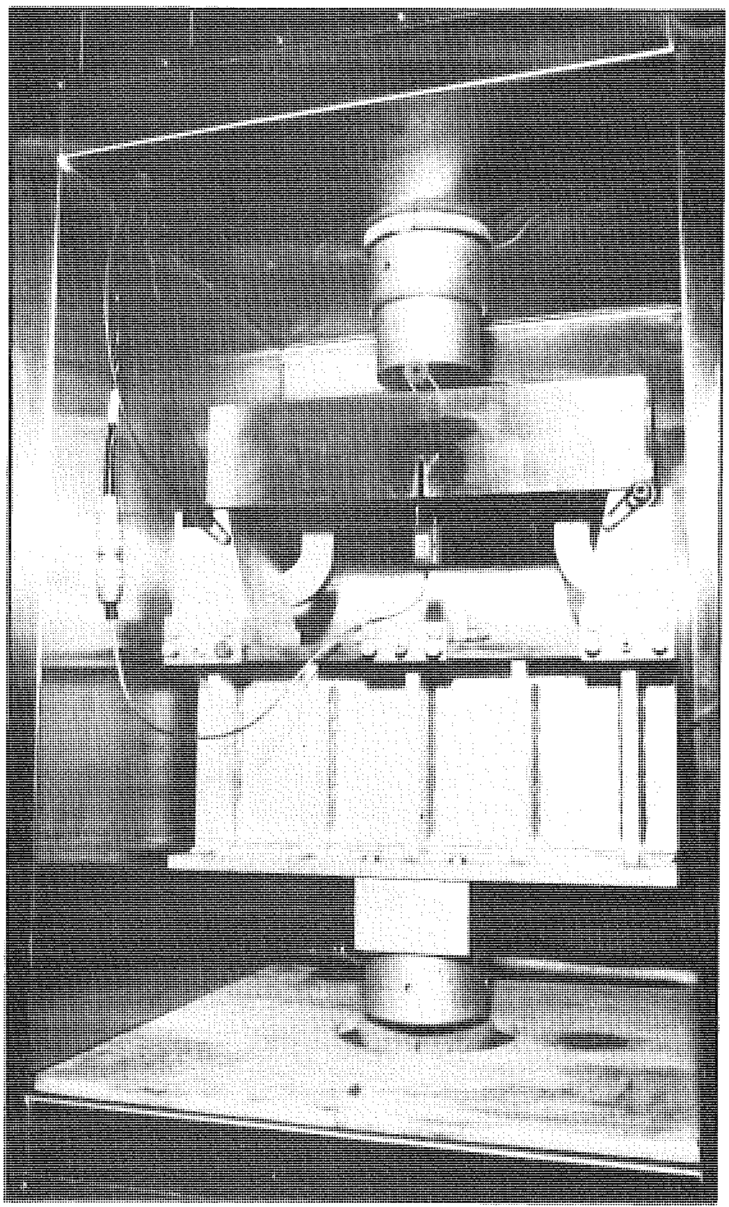

(a) K_{IC} specimen for the opening mode of crack propagation, i.e., tensile stresses applied normal to the crack plane.

(b) Actual specimen setup.

Figure 16. Plane-strain fracture toughness specimen (ASTM E399) using the three-point bend test. Test conducted in an environmental cooling chamber.

to a rational design against fracture in a full scale weldment. To circumvent this problem the same weldment types were tested with a very sophisticated fracture toughness test which uses a specimen sized to the full thickness of the welded butt joint.

The test method used is described in ASTM E399, Standard Test Method for Plane-Strain Fracture Toughness of Metallic Materials (23). The type of specimen used was the three-point bend specimen as shown in Figure 16. In this test the specimen thickness, t, was made equal to the actual thickness of the weldment plates being tested (2-5/16 and 3 in.). All other specimen dimensions were proportioned to this thickness based on the ratios specified in the E399 test method. This test method involves the fracturing of a steel beam specimen that has a fatigue precrack developed to a prescribed initial length. This fatigue crack is grown to size by repetitive loading applied to the specimen with a machined starter-notch placed in the area where cracking is desired. The fatigue loading is carefully controlled within the cyclic range specified by the test method. The fracture test is conducted with a precooled specimen enclosed in an environmental chamber to precisely control the steel temperature at the moment of fracture. The rate of loading was controlled by use of a 220,000-lb capacity electrohydraulic, closed-loop test system. The test data were recorded by an autographic plot of applied load versus the crack-opening-displacement across the fatigue cracked notch. From this load-displacement plot, data are obtained that allow the calculation of the material property, K_{IC}, called the plane-strain fracture toughness for the opening mode of fracture as defined by the ASTM E399 test method. If the specimen used is of sufficient thickness to exhibit a true, elastic brittle fracture then the test is considered 'valid' which means that the specified conditions of plane-strain existed in the test (i.e., the fracture was brittle). When this is true, the value of K_{IC} is believed to represent a lower limiting value of the material's fracture toughness. This value may then be used to estimate the relationship between failure stress and maximum defect size for a given material in-service if the same plane-strain conditions are experienced. Simply stated, the conditions of plane-strain exist whenever a material experiences severe tritensile constraint (i.e., constraint in three directions) near the tip of a sharp crack and the crack-tip plastic region is small in comparison with the total crack size and specimen dimensions. Under these conditions the fracture that occurs is referred to as a brittle fracture. Plane-strain behavior is dependent on both the yield strength of the steel and the thickness of the specimen. It had been previously discovered that the type of electroslag weldments used in bridge steels approached this condition at about 3-in. plate thickness (11). It was on this basis that the 3-in. thickness was chosen for this study. Electroslag weldments in this thickness and above do exist in bridge structures throughout the country. When the conditions of plane-strain are not met as specified in the E399 test method, then the fracture that occurs is viewed as a combination of elastic (brittle) and plastic (ductile) behavior. The test results are still useful in estimating the potential fracture resistance of the material, but the measured K_I value is not the lower bound value and does not represent an invariant material property.

New test methods are being developed to evaluate elastic-plastic fracture behavior (19).

Several features of the plane-strain K_{IC} test need to be discussed for those unfamiliar with the subject in order to understand the relevance of the test data. These features are discussed in the following four points:

1. Analytical solution

The three-point bend specimen used has prescribed geometric proportions and crack size. The fracture of the specimen is termed 'opening made' since the applied stresses act to open the crack as it propagates. The exact, analytical solution for the stress condition at the crack tip exists as a function of the ratio (a/w) of crack length, a, to depth, w. The crack must be a sharp-tipped fatigue crack as the apparent fracture toughness is sensitive to crack tip acuity. A blunt-tipped crack or machined notch would yield a higher fracture load and ductile type fracture. The solution relates the stress intensity factor, K_Q, to the applied load and other geometric variables (23). Hence, when the specimen size is such that true plane-strain conditions exist (i.e., the fracture is brittle in nature) the calculation of the K_Q value yields K_{IC}, the lower bound toughness which is considered to be a material property.

2. Thickness effects

The conditions of plane-strain occur when a given steel plate is thick enough that the strain or deformation in the thickness direction (normal to the applied stress) in the vicinity of a crack is nearly zero. This resistance to straining normal to the applied stress field increases with plate thickness and with the yield strength of the steel. Plane-strain simply means that all strain is confined to a plane, namely the plane of the applied stress. The other term applied to this condition is tritensile constraint. What this actually means is that a condition exists at a point where either stress or high constraint is applied in each of the three spatial directions or planes. When these conditions occur a steel indeed exhibits its lowest resistance to fracture and the fracture that occurs is normally termed 'brittle fracture.'

It is a physical fact that as a given steel is produced in increasingly thicker plates, its fracture toughness behavior decreases until the minimum, represented by K_{IC}, is achieved. This thickness effect on the fracture toughness is illustrated in Figure 17 which is a schematic of the relationship between plate (specimen) thickness and the opening-mode fracture toughness, K_I. It can be seen how the material fracture toughness approaches the minimum value of K_{IC} as a limit when the plate or specimen thickness reaches a critical dimension, B_C. Above this thickness the fracture behavior of the material will be brittle, below it will be either ductile or a combination of ductile and brittle.

Such testing, therefore, gives not only a means of estimating the relationship between crack size and applied stress at fracture but also the

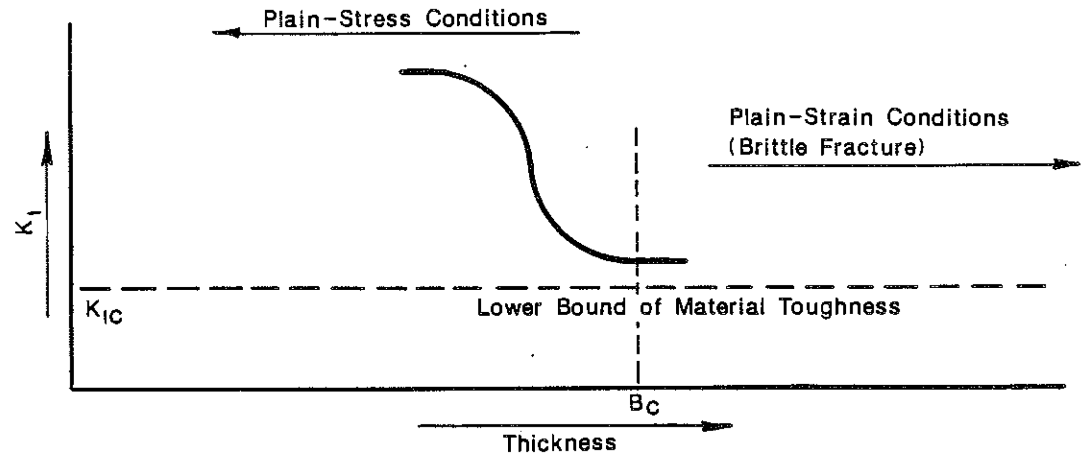

Figure 17. Schematic relationship between specimen thickness and the fracture toughness, K_I.

minimum thickness where true brittle conditions can exist. This becomes a valuable design guide in attempting to proportion steel bridge members to stay below this critical plate thickness. This is in fact the origin of the current proposed design criteria of keeping steel bridge girder flange plates below 2-1/2-in. thick. When this cannot be done, especially in a fracture critical member, then very stringent toughness and flaw inspection criteria must be specified because the conditions of brittle fracture can develop in the thicker plates. Hence, the allowable critical crack size must be made very large, which is accomplished by a high toughness requirement. In addition, the periodic inspection process must be very reliable to detect growing cracks before they approach this critical size. A similar effect is seen on the fracture toughness as the plate thickness is held constant and the yield strength is increased. The possibility of brittle fracture increases as the yield strength of the plate (or the weldment) increases. High strength steels are more fracture-sensitive to defects than low strength steels.

It should also be noted here that the steel in thin rolled plates (less than 1-1/2 in.) is inherently higher in fracture toughness than the steel in thicker plates. This is due to the various metallurgical changes that occur in the steel making and plate rolling processes. Thus, thick steel plates have both the effects of plane-strain and the inherent lower toughness of the steel making process. The metallurgical effects can be somewhat eliminated by heat treating the thick plates after rolling.

3. Temperature effect

The material property of fracture toughness is also dependent on the steel temperature at the time of fracture. As the temperature decreases, the fracture toughness will decrease. Therefore, any meaningful assessment of a steel component's potential to fracture in the presence of a flaw must be conducted at the lowest temperature that the component will be exposed to in service. This is referred to as the 'Lowest Anticipated Service Temperature' (LAST) and the AASHTO and AREA Specifications (22, 24) now give these temperatures for the various geographical regions of the United States. Michigan lies in the region referred to as Zone 2, where the LAST is -30 F. All K_{IC} tests in this project were conducted with the steel fracture specimen at a test temperature of -30 F (tolerance of +0 F, -3 F). This was accomplished by precooling the specimen in a special freezer to a uniform temperature as measured by thermocouples on the surface of the specimen and inserted in a small hole drilled to mid-thickness near one end of the specimen. During removal of the specimen from the freezer and the fixturing for the test, a slight increase in surface temperature would occur, so the specimen was recooled in an environmental chamber using CO_2 gas until the -30 F was again uniformily achieved. The test was then initiated, which takes only one to three seconds to failure.

4. Rate-of-loading effects

In most steels the material fracture toughness is also dependent on the rate at which the loading is applied. Hence, a flawed component may resist fracture under a static or slow application of load but fracture suddenly under the same load when applied rapidly. The effects of loading rate can be separated into three main categories, namely, slow or static, fast or dynamic (impact), and intermediate rates. Building structures are normally designed for statically applied live loads (except for wind and earthquake loadings). Dynamic or impact analyses are done on structures that are loaded instantaneously (i.e., load applied in less than 0.1 second). Most bridge components are loaded at a rate that falls in the intermediate time range. This intermediate bridge loading rate is most easily expressed as one to three seconds from time of no load to full application of load on the member. This has been estimated by strain rates determined from strain gages attached to bridge members. This is the loading rate criterion applied to the K_{IC} test conducted in this study. This rate has been previously used by other investigators to evaluate the toughness of bridge steels and weldments typical of welded bridge girders (11, 19). Although this loading rate designation has not as yet been incorporated in the ASTM standard test method, it is generally agreed upon and used amongst investigators doing fracture toughness testing on bridge steels and is also the basis for setting the AASHTO bridge steel toughness requirements (25, 26).

The schematic plot in Figure 18 shows the relationships between fracture toughness, K_{IC}, loading rate, and temperature. First note how the fracture toughness at any particular loading rate varies as a function of temperature, increasing as the temperature increases. Then note that an increase in loading rate has the effect of shifting and stretching the K_{IC} vs. Temperature curve to the right. Thus a given level of fracture toughness, K_o, occurs at the low temperature of T_1 for a statically loaded specimen. When the loading rate is increased, this same level of toughness is present only at higher temperatures, T_2 for intermediate loading

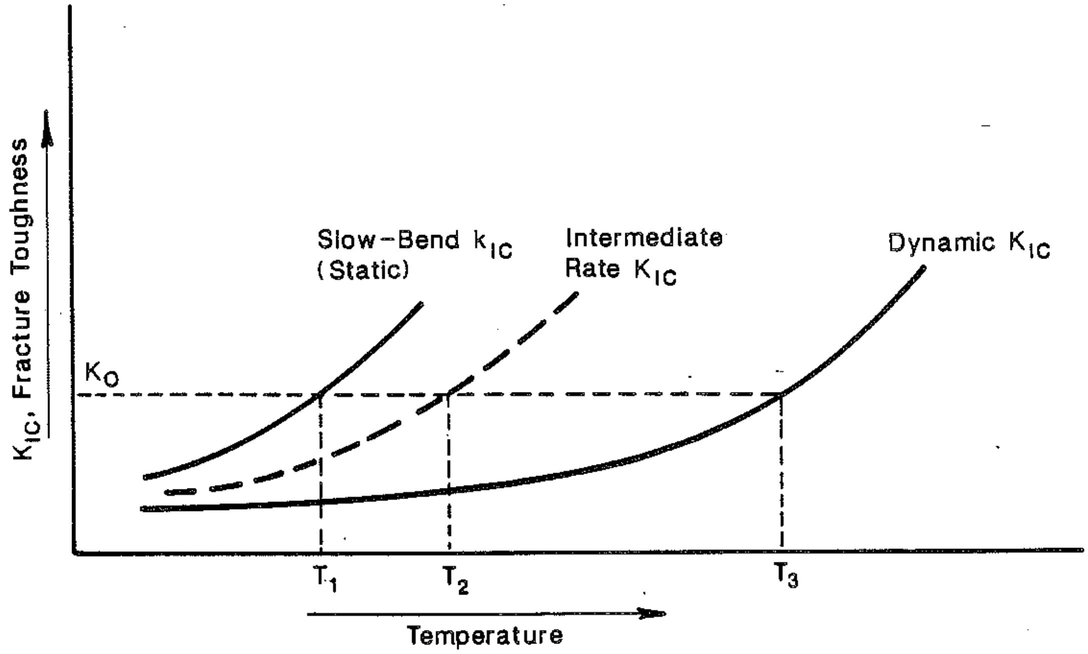

Figure 18. Schematic showing the effect of temperature and loading rate on K_{IC}, the material fracture toughness.

and T_3 for dynamic loading. This should illustrate clearly the need for conducting fracture toughness tests on a given steel at the lowest and anticipated service temperature (LAST) and at the maximum rate of loading that the steel member will experience.

The results of the K_{IC}, fracture toughness tests conducted on all the various submerged arc and electrosalg weldment types are reported in Tables 10 through 12. Similar tests conducted on some of the A36 and A588 base plates used in this study are reported in Table 13. Several features of these data should be pointed out before the results are discussed and compared.

1) The differences between the various types of weldments may be recalled by referring back to Tables 1, 4, and 5 where the procedures and welding variables are detailed.

2) The second column of the table notes what type of weld zone grain structure was involved in the crack propagation (fracture) region. Remember that each of these zones constitute radically different metallurgical structures in electroslag and electrogas weldments. The material property of fracture toughness is dependent on the steel microstructure so a noticable difference should appear as it did in the Charpy V-notch impact testing. The specimens are numbered in the order they were removed from the weldments, starting from the top of the weld in the case of the electroslag and electrogas welded joints.

TABLE 10
FRACTURE TOUGHNESS DATA, K_I ELECTROSLAG WELDMENTS, A588 STEEL

Weldment Type	Specimen Number/ Weld Zone	Specimen Thickness	K_Q Ksi·in.$^{1/2}$	K_{cmax} Ksi·in.$^{1/2}$	P_{max}/P_Q	K_{IC} Ksi·in.$^{1/2}$	Test Validity Conditions[1] (ASTM E399)
ESW588-A2	1/℄, Zones 1+2	3T	49.1	49.1	1.0	49.1	Valid
	2/℄, Zones 1+2	3T	85.2	85.2	1.0	—	Invalid (2,3,4,5)
(Bridge Shop A)	3/℄, Zones 1+2	3T	52.0	55.6	1.07	52.0	Valid
	4/ Zone 2	3T	60.9	63.3	1.04	—	Invalid (3,4,5)
	5/ Zone 2	3T	55.5	55.5	1.0	55.5	Valid
ESW588-A3	1/℄, Zones 1+2	3T	47.2	56.6	1.20	—	Invalid (1)
	2/ Zone 2	3T	65.7	76.2	1.16	—	Invalid (1,2)
(Bridge Shop A)	3/ Zone 2	3T	46.7	66.8	1.43	—	Invalid (1)
ESW588-A7	1/℄, Zone 2	2.25T	46.5	59.5	1.28	—	Invalid (1)
	2/℄, Zone 2	2.25T	52.1	52.6	1.01	—	Invalid (2,5)
(Bridge Shop A)	3/℄, Zone 2	2.25T	56.7	60.1	1.06	56.7	Essentially Valid[2] (2)
	4/℄, Zones 1+2	2.25T	53.0	60.9	1.15	53.0	Essentially Valid (1)
	5/℄, Zones 1+2	2.25T	44.2	54.8	1.24	—	Invalid (2,3,5)
ESW588-A8	1/℄, Zones 1+2	2.25T	57.9	62.0	1.07	57.9	Valid
	2/ Zone 2	2.25T	73.0	73.0	1.0	—	Invalid (2,5)
(Bridge Shop A)	3/℄, Zones 1+2	2.25T	46.9	54.4	1.16	46.9	Essentially Valid (1)
	4/ Zone 2	2.25T	60.7	68.6	1.13	—	Invalid (1,2)
	5/℄, Zones 1+2	2.25T	45.5	59.2	1.30	—	Invalid (1)
	6/ Zone2	2.25T	43.2	56.2	1.30	—	Invalid (1)
ESW588-A11	1/℄, Zones 1+2	3T	59.8	59.8	1.0	—	Invalid (2)
	2/℄, Zones 1+2	3T	62.9	62.9	1.0	—	Invalid (2)
(Bridge Shop A)							
ESW588-B2	1/℄, Zone 2	3T	57.5	68.4	1.19	—	Invalid (1,2)
	2/℄, Zone 2	3T	63.6	76.3	1.2	—	Invalid (1,2)
(Welding Lab B)	3/ Zones 1+2	3T	69.5	97.3	1.4	—	Invalid (1,2)
	4/ Zones 1+2	3T	60.5	60.5	1.0	—	Invalid (2)
	5/ Zone 2	3T	63.3	88.6	1.4	—	Invalid (1,2)
ESW588-B7	1/℄, Zone 2	3T	51.8	88.1	1.7	—	Invalid (1)
	2/℄, Zone 2	3T	59.7	101.5	1.7	—	Invalid (1)
(Welding Lab B)	3/ Zone 2	3T	48.6	92.3	1.9	—	Invalid (1)
	4/ Zone 2	3T	60.3	84.4	1.4	—	Invalid (1)
ESW588-C1	1/℄, Zones 1+2	3T	64.7	77.6	1.2	—	Invalid (1,2)
	2/℄, Zones 1+2	3T	60.5	96.8	1.6	-	Invalid (1,2,5)
(Bridge Shop C)	3/℄, Zones 1+2	3T	66.0	71.9	1.09	—	Invalid (2)
EGW588-D1	1/℄, Zones 1+2	3T	61.5	64.0	1.04	61.5	Valid
	2/℄, Zones 1+2	3T	65.9	65.9	1.0	65.9	Valid
(Welding Lab D)	3/℄, Zones 1+2	3T	74.7	74.7	1.0	—	Invalid (2)

[1] The numbers 1 through 6 indicate that the K_Q test result was not a valid K_{IC} result according to the requirements of ASTM E399 because one or more of the following conditions were violated:

1. $P_{max}/P_Q \leq 1.10$
2. a and/or B > $2.5 \left(\frac{K_Q}{\sigma_{y.s.}}\right)^2$
3. Test record slope > 0.70 and < 1.50
4. Fatigue precracking loading conditions
5. Fatigue crack front conditions -
   - a varies < 0.10 $a_{av.}$
   - Surface trace of crack > 0.90 $a_{av.}$
   - $0.45 < \frac{a}{w} < 0.55$
6. Crack plane at angle < 10° to the width and thickness directions

[2] "Essentially Valid" means that the above requirements were not met exactly but were nearly met by the conditions listed and thus deemed to be near valid results.

TABLE 11
FRACTURE TOUGHNESS DATA, K_I ELECTROSLAG WELDMENTS A36 STEEL

Weldment Type	Specimen Number/ Weld Zone	Specimen Thickness	K_Q Ksi·in.$^{\frac{1}{2}}$	K_{cmax} Ksi·in.$^{\frac{1}{2}}$	$\frac{P_{max}}{P_Q}$	K_{IC} Ksi·in.$^{\frac{1}{2}}$	Test Validity Conditions[1] (ASTM E399)
ESW36-A2	1/℄, Zones 1+2	3T	51.5	53.6	1.04	—	Invalid (2)
	2/℄, Zones 1+2	3T	59.3	60.5	1.02	—	Invalid (2)
(Bridge Shop A)	3/℄, Zones 1+2	3T	54.3	54.3	1.0	—	Invalid (2)
	4/ Zone 2	3T	60.6	60.6	1.0	—	Invalid (2)
	5/ Zone 2	3T	51.7	51.7	1.0	—	Invalid (2)
ESW36-A3	1/℄, Zones 1+2	3T	49.5	58.4	1.18	49.5	Essentially Valid[2] (1)
	2/ Zone 2	3T	49.0	49.0	1.0	49.0	Essentially Valid (5)
(Bridge Shop A)	3/℄, Zones 1+2	3T	47.0	47.5	1.01	47.0	Valid
	4/ Zone 2	3T	52.1	52.1	1.0	52.1	Essentially Valid (2)
ESW36-A6	1/℄, Zones 1+2	3T	61.8	74.8	1.21	—	Invalid (1,2)
	2/℄, Zones 1+2	3T	61.2	92.4	1.51	—	Invalid (1,2)
(Bridge Shop A)							
ESW36-B2	1/℄, Zones 1+2	3T	47.1	67.4	1.43	—	Invalid (1)
	2/℄, Zones 1+2	3T	60.1	81.7	1.36	—	Invalid (1,2)
(Welding Lab B)	3/ Zone 2	3T	67.0	93.8	1.4	—	Invalid (1,2,5)
	4/ Zone 2	3T	62.9	100.6	1.6	—	Invalid (1,2)
	5/℄, Zones 1+2	3T	88.5	104.4	1.18	—	Invalid (1,2)
ESW36-C1	1/℄, Zones 1+2	3T	67.2	67.2	1.0	—	Invalid (2,5)
	2/℄, Zones 1+2	3T	67.6	67.6	1.0	—	Invalid (2,5)
(Bridge Shop C)							

[1]The numbers 1 through 6 indicate that the K_Q test result was not a valid K_{IC} result according to the requirements of ASTM E399 because one or more of the following conditions were violated:

1. $P_{max}/P_Q \leq 1.10$
2. a and/or B > 2.5 $\left(\frac{K_Q}{\sigma_{y.s.}}\right)^2$
3. Test record slope >0.70 and <1.50
4. Fatigue precracking loading conditions
5. Fatigue crack front conditions -
   - a varies < 0.10 $a_{av.}$
   - Surface trace of crack > 0.90 $a_{av.}$
   - $0.45 < \frac{a}{W} < 0.55$
6. Crack plane at angle < 10° to the width and thickness directions

[2]"Essentially Valid" means that the above requirements were not met exactly but were nearly met by the conditions listed and thus deemed to be near valid results.

TABLE 12

FRACTURE TOUGHNESS DATA, K_I SUBMERGED ARC WELDMENTS, A588 STEEL AND A36

Weldment Type	Specimen Number[2]	Specimen Thickness	K_Q Ksi·in.$^{1/2}$	K_{cmax} Ksi·in.$^{1/2}$	$\frac{P_{max}}{P_Q}$	K_{IC} Ksi·in.$^{1/2}$	Test Validity Conditions[1] (ASTM E399)
SAW588-A2	1	3T	44.4	60.4	1.36	—	Invalid (1,5)
	2	3T	92.3	92.3	1.0	—	Invalid (2,3,5)
(Bridge Shop A)	3	3T	47.7	61.5	1.3	—	Invalid (1,5)
SAW588-A7	1	3T	65.6	66.9	1.02	—	Invalid (2,3,5)
	2	3T	84.9	119.7	1.41	—	Invalid (1,2,3,5)
(Bridge Shop A)	3	3T	52.6	58.4	1.30	—	Invalid (1,5)
SAW36-A2	1	3T	44.3	45.6	1.03	—	Invalid (5)
	2	3T	74.9	83.1	1.11	—	Invalid (1,3,5)
(Bridge Shop A)	3	3T	62.2	62.2	1.0	—	Invalid (3,5)

[1] The numbers 1 through 6 indicate that the K_Q test result was not a valid K_{IC} result according to the requirements of ASTM E399 because one or more of the following conditions were violated:

1. $P_{max}/P_Q \leq 1.10$
2. a and/or B > 2.5 $\left(\frac{K_Q}{\sigma_{y.s.}}\right)^2$
3. Test record slope >0.70 and <1.50
4. Fatigue precracking loading conditions
5. Fatigue crack front conditions -
   - a varies < 0.10 $a_{av.}$
   - Surface trace of crack > 0.90 $a_{av.}$
   - $0.45 < \frac{a}{w} < 0.55$
6. Crack plane at angle < 10° to the width and thickness directions

[2] All specimens were located on the weld ℄ and the fracture was propagated through the middle of the weld metal nugget.

3) The calculated values shown for K_Q, K_{cmax}, and K_{IC} have meaning as defined by ASTM E399 Standard Test Method for Plane-Strain Fracture Toughness of Metallic Materials and will be explained in the following section.

4) The connotation of the terms 'valid' or 'invalid' in the last column should be understood in view of the E399 test method. A 'valid' K_{IC} test is one which meets all the conditions specified in the E399 specification as noted in the tables. Thus, by definition of the test method the conditions of plane-strain were all met and the **fracture was brittle in nature.** The **K_{IC} value then represents a material property that is the lowest fracture toughness that can be exhibited by the material.** The term 'invalid' noted in the tables simply means that one or more of the conditions (1 through 6 in the table footnoote) specified by the E399 method were not satisfied. These conditions relate to the existence of true plane-strain existing at the tip of the fatigue precrack. When they are not satisfied the term 'invalid' does not mean that the test results are of no interest. What is indicated is that the fracture is a combination of elastic (brittle) and

TABLE 13
FRACTURE TOUGHNESS DATA, K_I BASE METAL, A588 AND A36

Test Material	Specimen Number	Specimen Thickness	K_Q Ksi·in.$^{1/2}$	K_{cmax} Ksi·in.$^{1/2}$	P_{max}/P_Q	K_{IC} Ksi·in.$^{1/2}$	Test Validity Conditions[1] (ASTM E399)
A588 Base Plates	1	3T	64.3	64.3	1.0	—	Invalid (2,3)
	2	3T	50.7	50.7	1.0	50.7	Valid
	3	3T	59.5	67.2	1.13	59.5	Essentially Valid[2] (1,2)
	4	3T	49.0	49.0	1.0	49.0	Valid
A588 Base Plates	1	2.25T	54.7	54.7	1.0	54.7	Valid
	2	2.25T	66.7	66.7	1.0	—	Invalid (2)
	3	2.25T	71.4	94.2	1.32	—	Invalid (1,2)
	4	2.25T	73.2	96.6	1.32	—	Invalid (1,2)
	5	2.25T	68.0	79.6	1.17	—	Invalid (1,2)
	6	2.25T	55.8	55.8	1.0	55.8	Valid
A36 Base Plates	1	3T	57.7	84.8	1.47	—	Invalid (1,2,3)
	2	3T	62.3	86.6	1.39	—	Invalid (1,2)
	3	3T	63.7	92.4	1.45	—	Invalid (1,2)
	4	3T	54.2	86.7	1.6	—	Invalid (1,2)
	5	3T	57.0	85.5	1.50	—	Invalid (1,2)
	6	3T	58.1	91.8	1.58	—	Invalid (1,2,3)
	7	3T	55.9	83.9	1.5	—	Invalid (1,2)
	8	3T	62.8	89.8	1.43	—	Invalid (1,2)
	9	3T	59.8	89.7	1.5	—	Invalid (1,2)

[1] The numbers 1 through 6 indicate that the K_Q test result was not a valid K_{IC} result according to the requirements of ASTM E399 because one or more of the following conditions were violated:

1. $P_{max}/P_Q \leq 1.10$
2. a and/or B > 2.5 $\left(\frac{K_Q}{\sigma_{y.s.}}\right)^2$
3. Test record slope >0.70 and <1.50
4. Fatigue precracking loading conditions
5. Fatigue crack front conditions -
   - a varies < 0.10 $a_{av.}$
   - Surface trace of crack > 0.90 $a_{av.}$
   - $0.45 < \frac{a}{W} < 0.55$
6. Crack plane at angle < 10° to the width and thickness directions

[2] "Essentially Valid" means that the above requirements were not met exactly but were nearly met by the conditions listed and thus deemed to be near valid results.

plastic (ductile) in behavior and does not represent the lower bound value of fracture toughness. The data are still of great engineering interest and may be used to estimate and compare the fracture behavior of the materials in question. The term 'essentially valid' means that one or two of the conditions were slightly violated and the results represent a test that was essentially plane-strain in nature. These values of K_{IC} have the same connotation as those listed as valid, depending on the judgement of the person evaluating the data.

Discussion of K_{IC} Test Results

The results of the K_{IC} type fracture toughness tests are discussed in the following observations and conclusions:

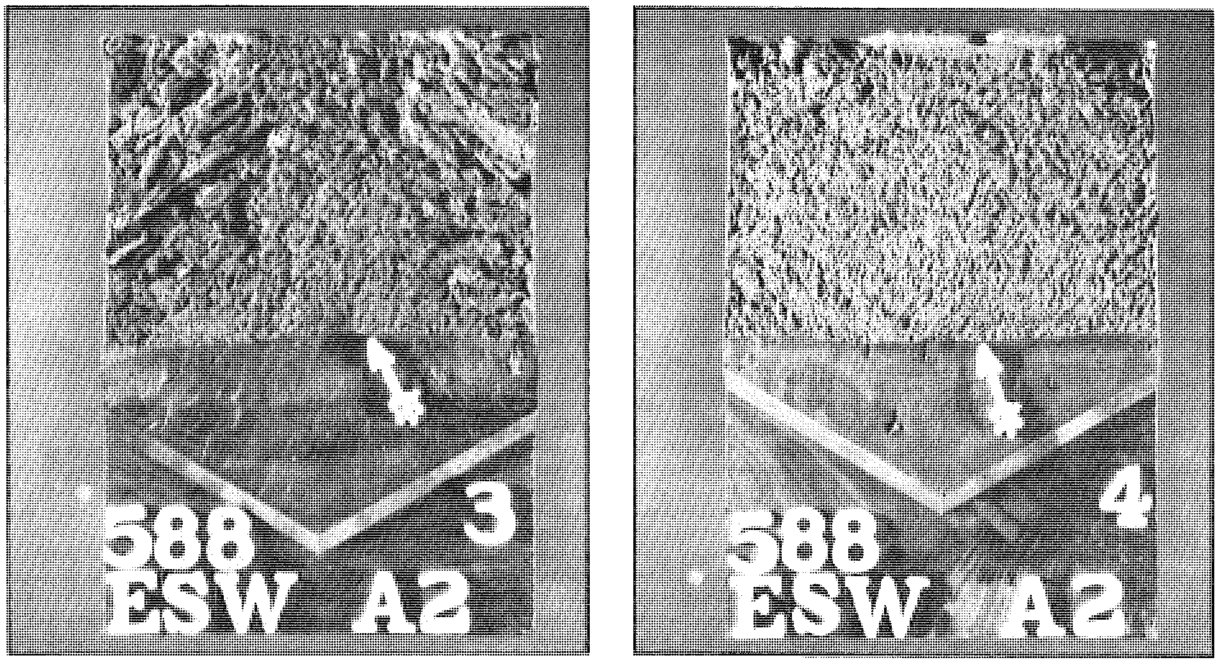

(a) Zones 1 and 2 on the centerline of the weld. Valid K_{IC} result.

(b) Zone 2 off the center of the weld. Invalid result (Conditions 3, 4, 5).

Figure 19. K_{IC} test specimens in 3-in. thick electroslag weldment produced in A588 steel. Fracture surfaces shown pass through the weld metal zones as noted.

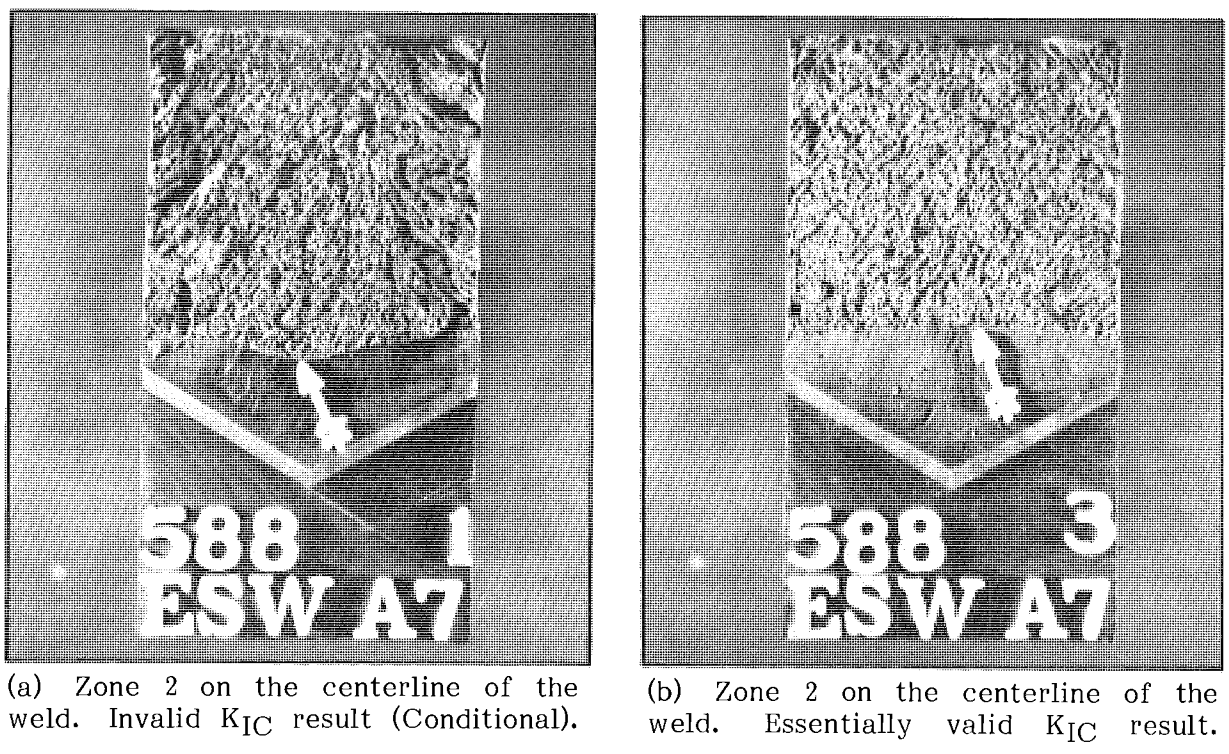

(a) Zone 2 on the centerline of the weld. Invalid K_{IC} result (Conditional).

(b) Zone 2 on the centerline of the weld. Essentially valid K_{IC} result.

Figure 20. K_{IC} test specimens in 2-5/16-in. thick electroslag weldment produced in A588 steel. Fracture surfaces shown pass through the weld metal zones as noted.

1) 'Valid' or 'essentially valid' plane-strain fracture results were achieved in three electroslag weldment types in A588 steel, the electrogas weldment in A588 steel and one electroslag weldment type in A36 steel. None of the submerged arc weldments exhibited valid plane-strain behavior. This is one of the most significant observations revealed by the K_{IC} test results. Rational establishment of an adequate toughness criterion is difficult and will be discussed later. However, it should be a general goal of any fracture control plan to avoid the use of any material or weldment that can exhibit a brittle fracture behavior at the lowest anticipated service temperature and loading rate that will exist for the structure (19). The minimum toughness criterion is usually established at a high enough level to ensure that all potential fractures will occur in the elastic-plastic mode, as is apparent in the other weldment types. Those weldments that can exhibit plane-strain behavior possess the potential for sudden brittle-fracture in bridge structures. This potential exists due to the high constraint conditions that exist at the tip of a crack in a thick girder flange plate splice and the relatively small critical crack size that can be tolerated before sudden fracture occurs. Based on this observation alone, the electroslag and electrogas welding processes should be viewed as unsuitable for bridge girder butt splices in thick plates that are subject to tension loading, such as occurs in girder flanges.

2) The majority of the valid K_{IC} tests occurred in the A588 alloy weldments (only one case in the A36 alloy). ASTM A588 steel is a high strength low alloy steel that was developed for use as a steel with a 50,000 psi minimum yield strength and claimed to have an enhanced resistance to atmospheric corrosion. Consequently it has a very complex alloy composition which yields a high potential for microstructural problems in a complex grain structure such as that present in electroslag and electrogas weldments. It was reported in the previous study (1) and in the Charpy V-notch data of this report that the A588 alloy weldments exhibit low notch toughness. It should also be observed that the higher yield point typical of the A588 alloy will also have the effect of lowering the apparent fracture toughness since the potential for plane-strain conditions increase with increasing yield point. It is probably a combination of these factors that make the A588 alloy weldments more prone to brittle fracture behavior.

3) The appearance of a fractured surface reveals a great deal of information about the nature of the fracture. Details can be discovered such as the extent and origin of the fatigue cracking phase, the direction of the crack propagation, and whether the fracture was brittle (elastic or plane-strain), ductile (plastic or plane-stress) or a combination (termed elastic-plastic), in nature. Figures 19 through 27 show typical fracture surfaces of the K_{IC} weldment and base metal tests reported in Tables 10 through 13. The following observations are important to note in the figures:

a) The fatigue precracking front is indicated in the figures by an arrow. This front is the location of the fatigue-induced precrack that was present at the moment of sudden fracture. The V-notch or chevron that is located

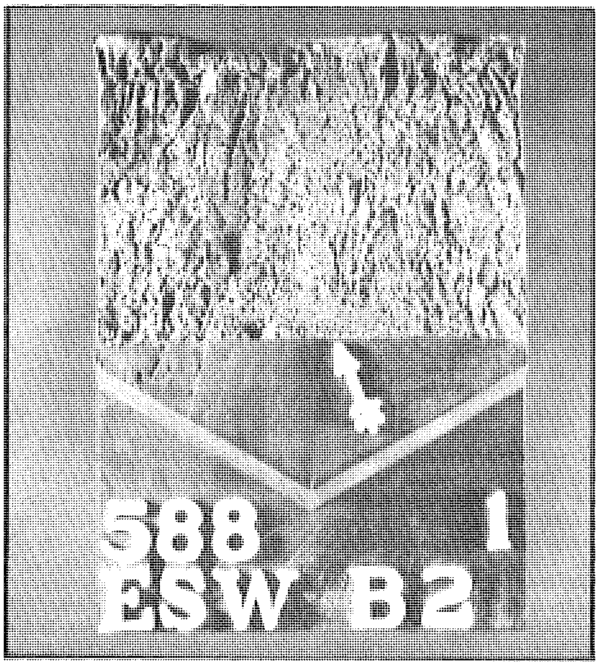

(a) Zone 2 on the centerline of the weld. Invalid K_{IC} result (Conditions 1, 2).

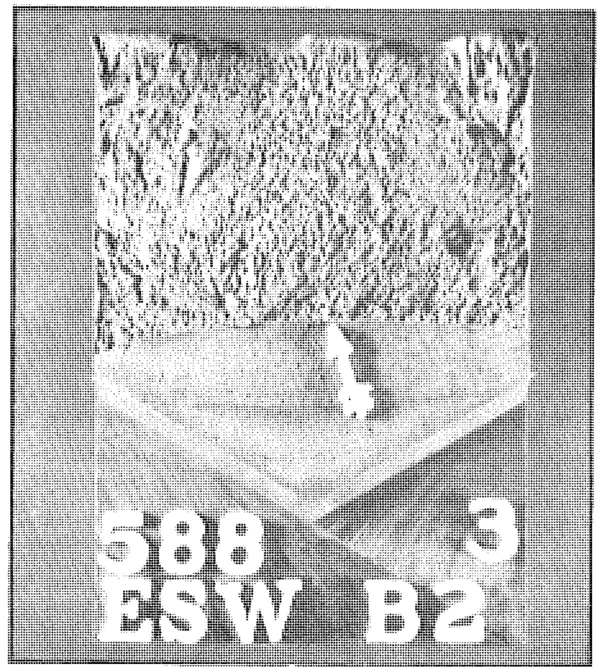

(b) Zones 1 and 2 offset from the centerline of the weld. Invalid K_{IC} result (Conditions 1, 2).

Figure 21. K_{IC} test specimens in 3-in. thick electroslag weldment produced in A588 steel. Fracture surfaces shown pass through the weld metal zones as noted.

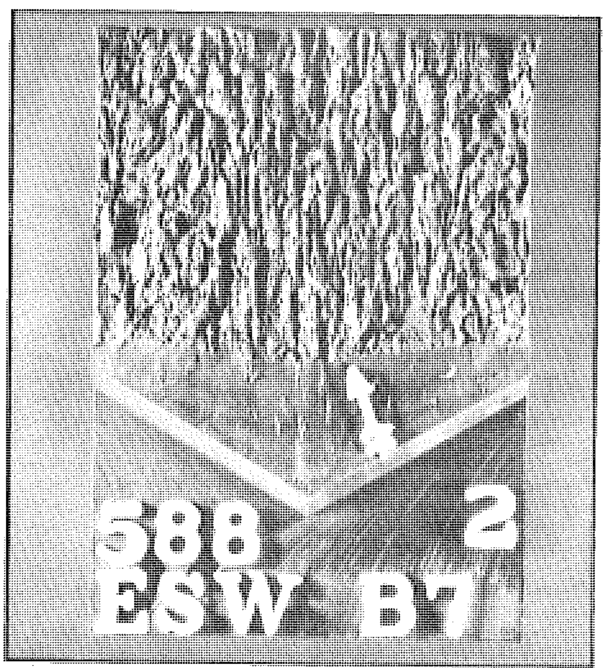

(a) Zone 2 on the centerline of the weld. Invalid K_{IC} result (Condition 1).

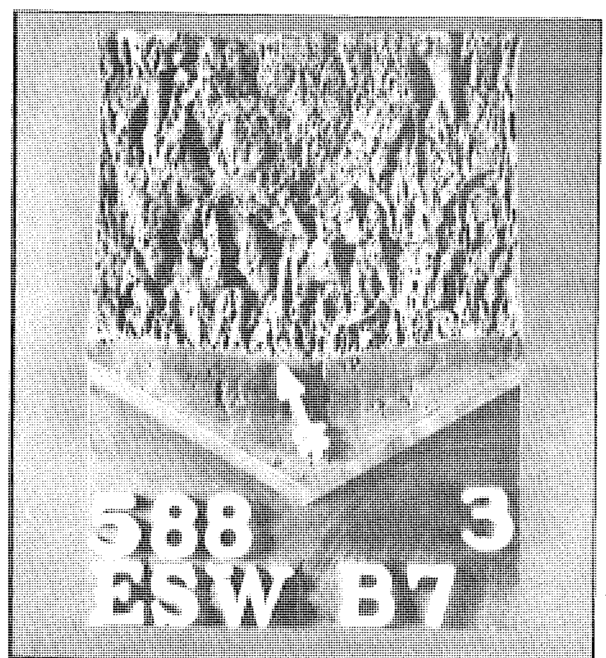

(b) Zone 2 off the center of the weld. Invalid K_{IC} result (Condition 1).

Figure 22. K_{IC} test specimens in 3-in. thick electroslag weldment produced in A588 steel. Fracture surfaces shown pass through the weld metal zones as noted.

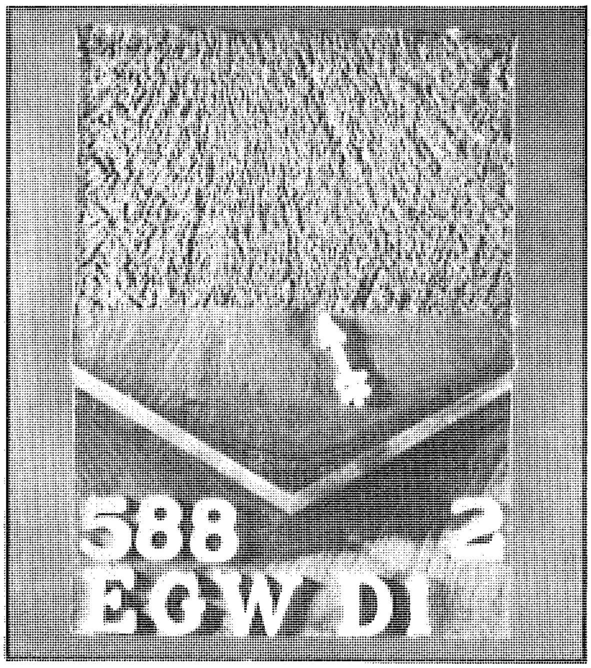

Figure 23. K_{IC} test specimen in 3-in. thick electrogas weldment produced in A588 steel. Fracture surface shown passes through Zones 1 and 2 weld metal on the centerline of the weld. Valid K_{IC} result.

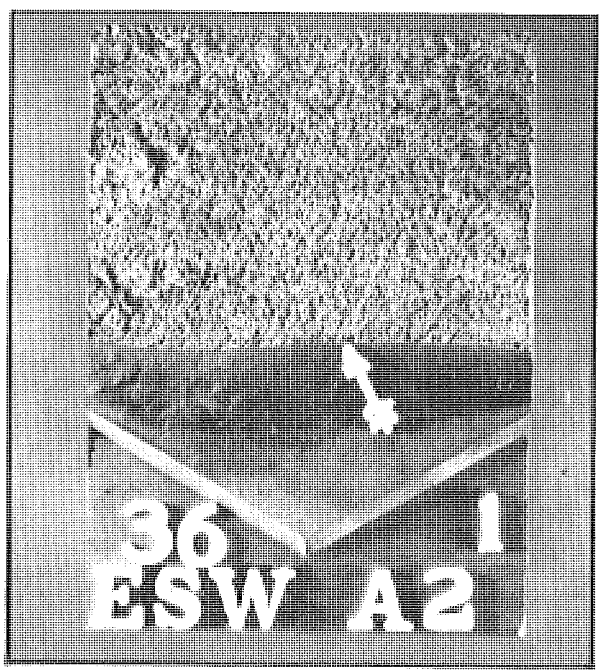

(a) Zones 1 and 2 on the centerline of the weld. Invalid K_{IC} result (Condition 2).

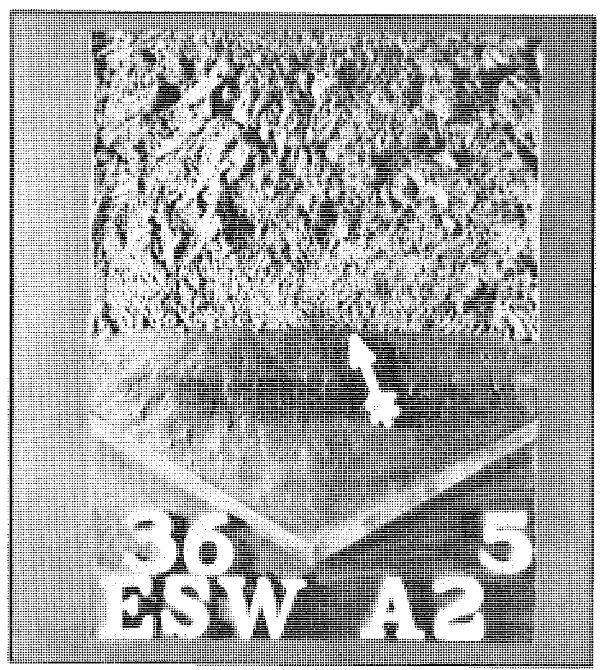

(b) Zone 2 off the center of the weld. Invalid result (Condition 2).

Figure 24. K_{IC} test specimens in 3-in. thick electroslag weldment produced in A36 steel. Fracture surfaces shown pass through the weld metal zones as noted.

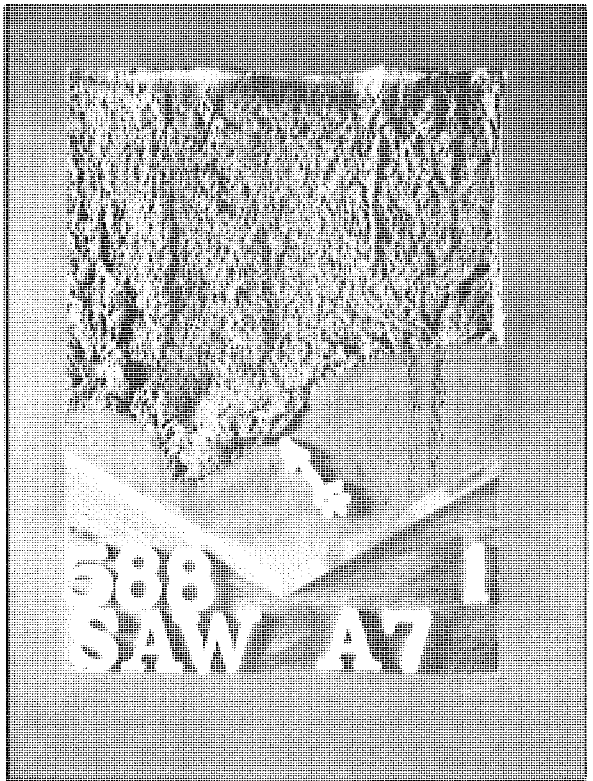

(a) A588 steel.

(b) A588 steel.

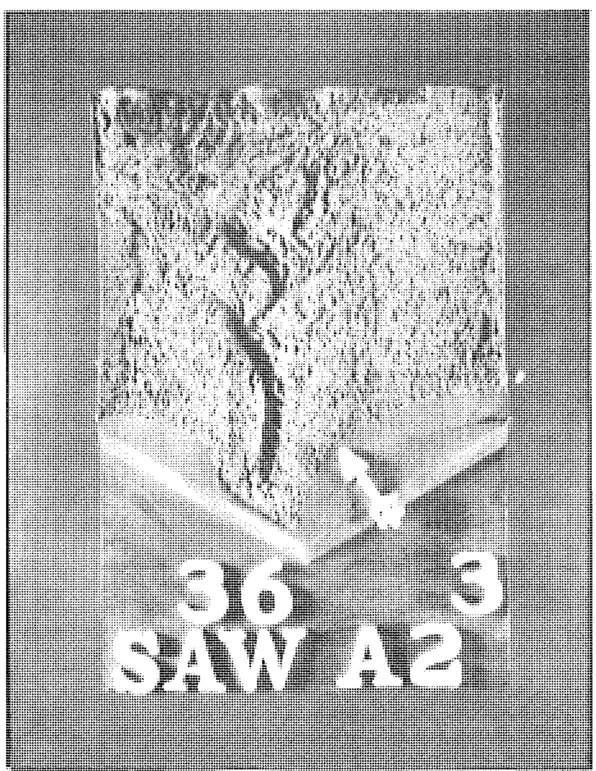

(c) A36 steel.

Figure 25. K_{IC} test specimens in 3-in. thick submerged arc weldments. Fracture surfaces shown pass through the weld metal on the centerline of the weld. Invalid K_{IC} results. Note uneven precrack front caused by residual stress pattern in weldment.

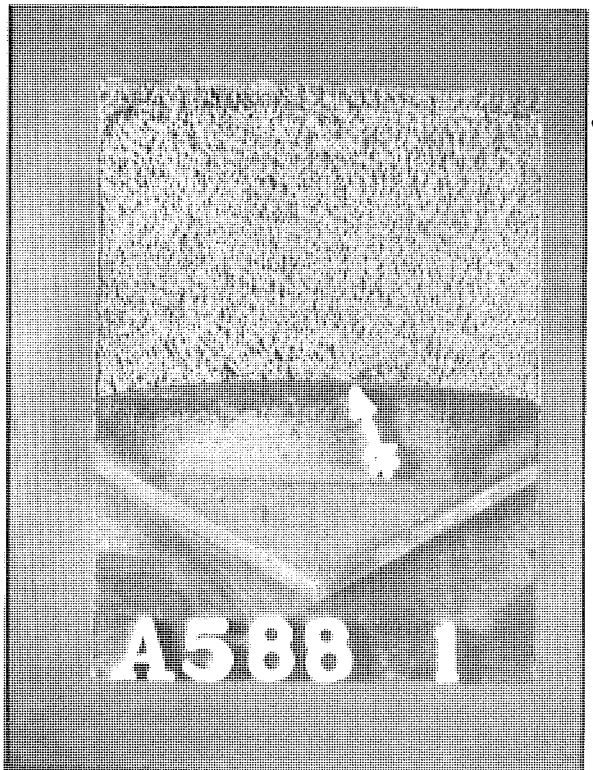

(a) 3-in. thickness. Invalid K_{IC} result (Conditions 2,3).

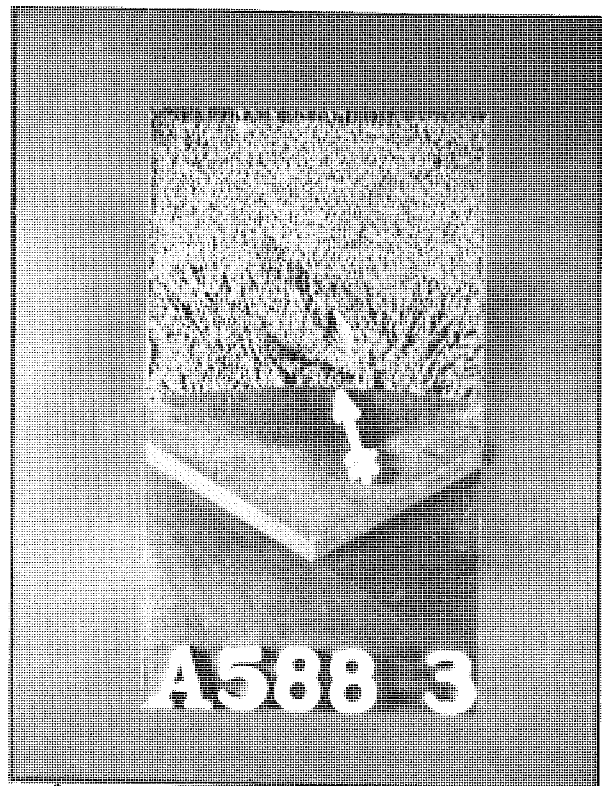

(b) 2-5/16-in. thickness. Invalid K_{IC} result (Conditions 2,3).

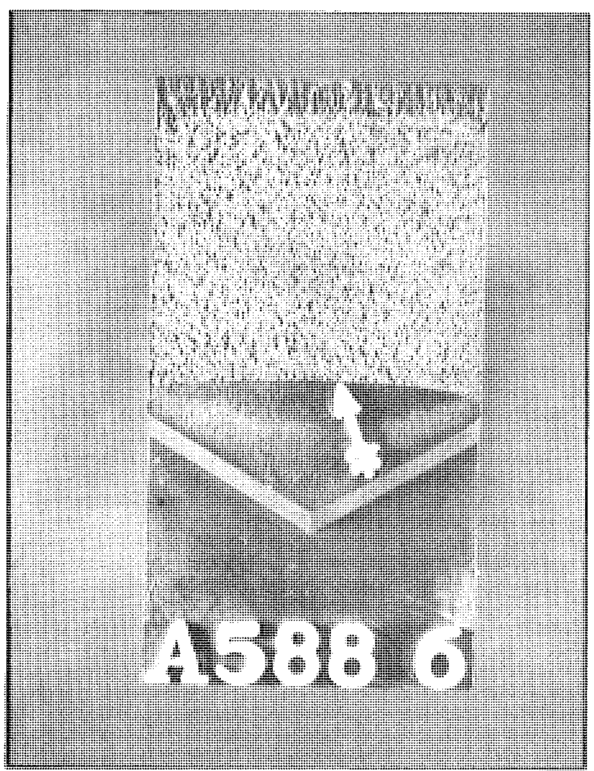

(c) 2-5/16-in. thickness. Valid K_{IC} result.

Figure 26. K_{IC} test specimens in A588 steel base plate. Fracture surfaces shown are from full-thickness specimens with the fracture running transverse to the direction of rolling.

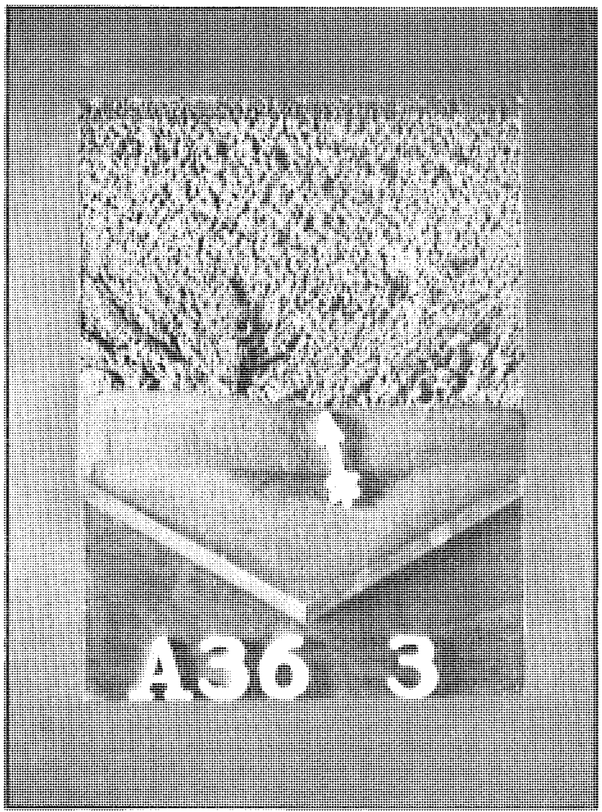

Figure 27. K_{IC} test specimen in 3-in. thick A36 steel. Fracture surface shown is from a full-thickness specimen with the fracture running transverse to the direction of rolling. Invalid K_{IC} result (Condition 1,2).

below the fatigue crack front is the machined notch that was used as a fatigue crack-starter mechanism. This forces the fatigue crack to initiate in the weldment zone that is to be tested. Note that many details of the electroslag weld metal structure are evident in the area where the fatigue crack has passed. For example, the coarse grain structure revealed in Figure 19a compared to the fine grained structure revealed in Figure 23. Note also that the fatigue crack fronts in the electroslag and electrogas weldments are quite straight and uniform generally meeting the ASTM E399 requirement for crack front straightness (condition 5 in Tables 10 through 12). The electroslag and electrogas weld metal exhibited very little resistance to this fatigue precracking. The crack lengths shown were generally reached within a few hundred thousand cycles at the ASTM prescribed load limitations. In comparison, the submerged arc weldments usually took one to two million cycles of load to initiate and propagate a fatigue crack. The electroslag weld specimens also cracked easier than the base metal specimens, which are shown in Figures 26 and 27.

A very interesting phenomenon occurs in the fatigue cracking of the submerged arc weldments as illustrated in Figure 25. Approximately 25 percent of the width, located on one side of the mid-thickness region, always exhibited an extreme resistance to fatigue cracking. The resulting irregular crack front, which occurred in all cases, immediately invalidates the K_{IC} toughness evaluation of the fractured specimens (condition 5).

The development of this unusual crack front can be expalined as follows: Figure 28 shows a schematic of the welding joint preparation used in producing the submerged arc weldments (also see Fig. 2). Side 1 was V-gouged to the mid-thickness and welded by depositing the appropriate number of weld passes to completely fill to the plate surfaces. The plates are then turned over and Side 2 is back-gouged and similarly welded.

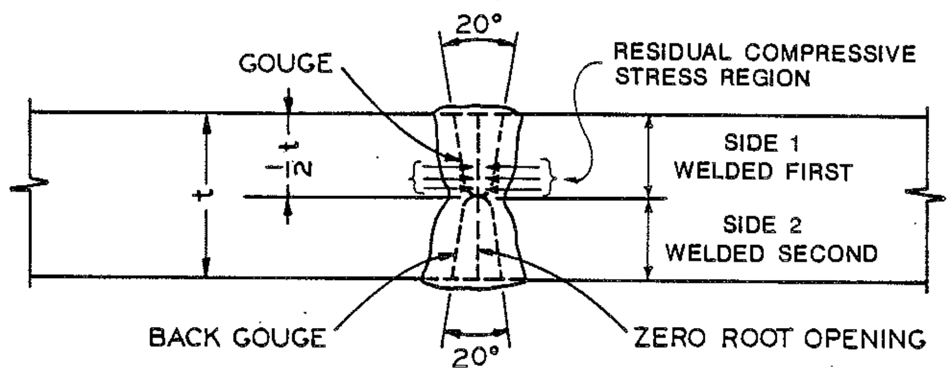

Figure 28. Submerged arc welding joint procedure used illustrating the residual compression zone created that resists fatigue cracking.

When the weld metal shrinkage occurs in the weld nugget on Side 2, it pulls in on the Side 2 V-gouge and thereby squeezes or compresses the adjacent region of the Side 1 weld nugget. This action creates a permanent compressive residual stress field in the central 1/4 thickness region of Side 1 as illustrated by arrows in Figure 28. When a K_{IC} specimen is subjected to a fatigue tensile stress cycle, the compression stresses shown are superimposed on the applied tensile stress, having the effect of greatly reducing the resultant tensile component in this region. Since it is only an applied tensile stress range that can drive a fatigue crack, it is easy to see why the crack growth is inhibited in this region. A modified K_I test is reported in the next section that attempts to circumvent this difficulty in growing a crack front in submerged arc weldments. It should be pointed out that in the actual use of this type of welded butt joint in a bridge girder flange, this compressive residual stress zone will have the same beneficial effect of retarding both fatigue crack growth and fracture. This is one of the advantages of evaluating weld joint toughness on a full-scale plate specimen. These effects are not noticed when subsize specimens, such as the Charpy V-notch test, are used to evaluate toughness.

b) The appearance of a brittle fracture is usually described as a flat, crystalline fracture surface that lacks evidence of shear or ductile tearing. A ductile fracture is described as one exhibiting tears and dimples, shear lips at the edges, and out-of-plane ridges or lumps across the surface. As can be seen, most of the electroslag and electrogas weldments exhibited flat, crystalline types of fractures **that indicate a mostly brittle mode of failure.** Some of the fractured surfaces look quite rough, such as in Figures 19a and 22a, but remember that in these weldments the primary grain structure or crystals are extremely large. Hence, a crystalline type fracture appears coarse. Indeed, careful analysis of these surfaces reveals that when the primary grain structure is oriented approximately in line with a propagating fracture, the crack will form by separating the coarse grains along their boundaries (termed intergranular cracking). This effect is well illustrated in Figure 22 where in photo **a**, the coarse grains aligned with the crack and in photo **b** the coarse grains were more transversely oriented to the crack. Hence, photo **b** shows a combination of transgranular and intergranular cracking along with some ductile tearing. Figure 22a shows mostly brittle fracturing of the primary grain structure.

The submerged arc specimens in Figure 25 illustrate typical ductile fracture appearance with shear lips, ridges, and irregular tears. Remembering that since the primary grain structure of the submerged arc weld metal is very fine, the coarse fracture appearance is attributed to ductile behavior. This will also be evident by the shape of the load vs. crack-opening-displacement graphs that will be shown in a later discussion.

The appearance of the base metal K_{IC} test specimens are shown in Figures 26 and 27. Figure 26b shows a ductile fracture in 2-5/16-in. thick A588 steel in contrast to a brittle fracture in the same steel in Figure 26c. Figure 27 shows the ductile type appearance that was typical of the lower yield strength A36 steel specimens.

c) Figure 23 shows the typical fracture appearance of the electrogas weld specimens. Note the long, slender crystalline structure of the weld metal as revealed on the fracture surface. Since these long, thin grains were oriented in line with the propagating crack, they offered very little resistance and the flat, brittle fracture appearance is evident. A very narrow shear lip along the specimen edges is the only evidence of ductility shown by the electrogas specimen.

d) Figures 26 and 27 show the straight fatigue crack front typical of the base metal speciments. Since no large, localized residual stress zones were present in the base plate, there was no problem in growing uniform fatigue crack fronts. However, the base metal specimens did demonstrate more resistance to the fatigue cracking and generally required more cycles to grow to the prescribed length than electroslag and electrogas weld metal specimens.

e) The effect of the weld metal grain structure orientation with respect to the direction of crack propagation is illustrated in Figure 19. The valid, brittle fracture in Figure 19a resulted from the crack propagating along the weld centerline plane and hence being essentially in line with the grain structure. This resulted in a predominately intergranular cracking where the large weld metal grains separated along their boundaries. Figure 19b illustrates the effect of shifting the propagating crack off the weld centerline plane and forcing it to propagate transgranularly or through the grains. A totally different fracture appearance is evident and the added ductility at this fracture position caused the K_{IC} test to demonstrate an elastic-plastic behavior. Thus, the most susceptable portion of an electroslag weldment to a brittle fracture is along a plane passing down the center of the weldment.

4) In the second column of the electroslag and electrogas K_{IC} data tables, the specimens that have "℄" noted were oriented with the fatigue precrack centered on the weld nugget. This position caused the fracture to propagate through the full thickness of the weldment and hence encounter both Zone 1 and Zone 2 types of microstructure when present. Recall that Zone 1 weld metal (when present) generally occurs in the central core of the weld nugget and is composed of long, thin, crystals that are oriented almost in line with the longitudinal weld axis. Zone 2 weld metal appears around the periphery of the weld nugget and is composed of coarse prior austinite grains formed at some acute angle to the weld ℄, with relatively fine secondary transformation products within the grains. The specimens that do not have the "℄" designation were located with the crack shifted off the weld centerline and the fracture was propagated through the coarse grained Zone 2 structure, with the crystals oriented at various acute angles to the crack. In the case of weldment ESW588-B7 in Table 10, only Zone 2 weld structure existed and the two test positions compare the ℄ region where the grains nearly align with the crack to the offset region where the grains are at an angle with the crack. **The result evident in the K_{IC} test data is that the Zone 2, offset weld metal position does not exhibit significantly higher fracture toughness than the ℄ position.** This is surprising because the small Charpy V-notch impact test predicted that the Zone 2 weld metal was significantly tougher off-center. This can be seen by referring back to Figures 12 through 15 on the Charpy tests. An explanation of this differing conclusion apparently lies in the discussion of the Charpy V-notch specimen size being too small to evaluate the Zone 2 weld metal toughness. Since the size of the primary grain structure of Zone 2 weld metal is the same order of magnitude as the Charpy specimen, a transgranular test yields unrealistic high results. It was also shown in the previous study (1) how sensitive the Charpy test results were to placement and orientation within this coarse grain structure. Fractographic studies on the fractured surfaces of the K_{IC} test specimens reveal that the coarse grained Zone 2 weld metal usually fails by the crack propagating along the ferrite-rich grain boundaries. This indeed represents the path of least resistance to fracture. Thus it can be concluded from the K_{IC} test, using a full plate thickness specimen, that the Charpy V-notch specimen can give an overestimate of the Zone 2 weld metal toughness

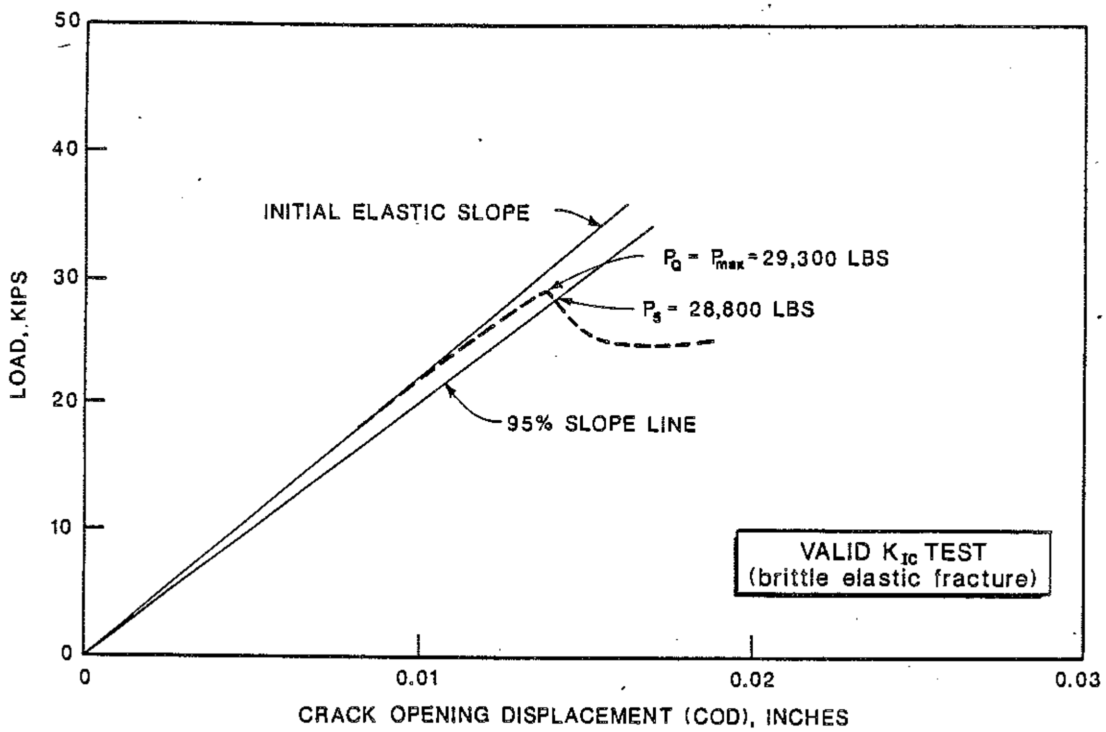

Figure 29. Load vs. COD plot for a valid K_{IC} test on electroslag weldment ESW588-A2, Specimen 5. Crack propagated through Zone 1 and Zone 2 weld metal along the weld centerline (see Figure 19a).

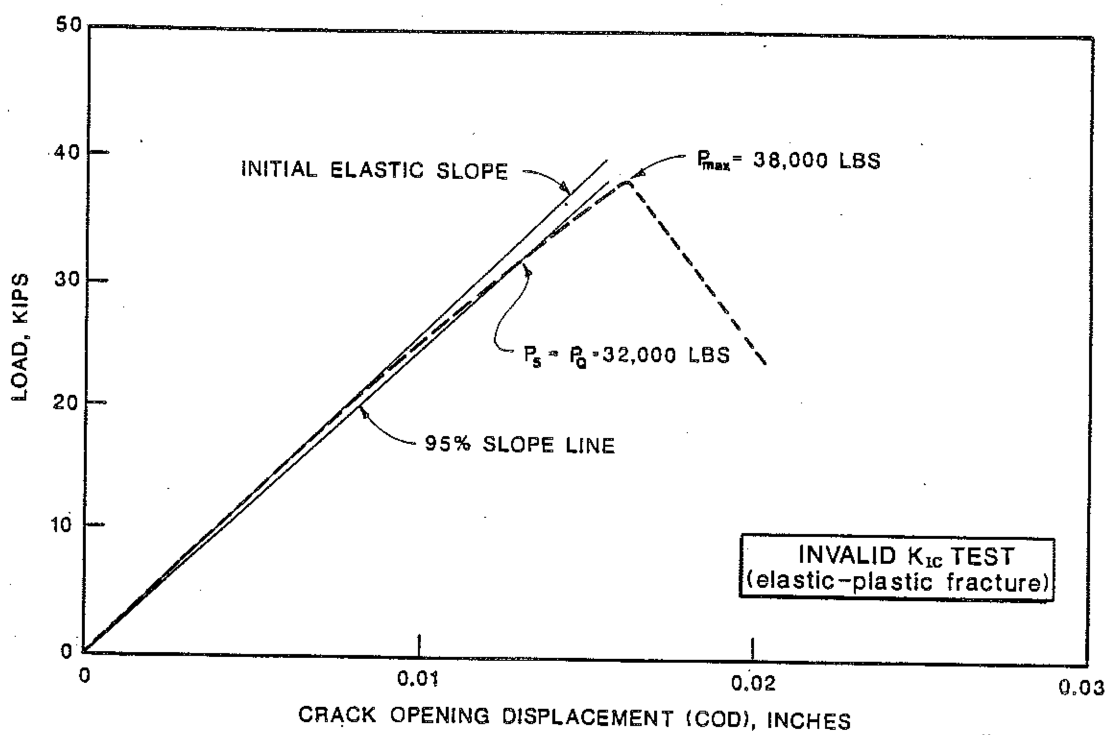

Figure 30. Load vs. COD plot for an invalid K_{IC} test on electroslag weldment ESW588-B2, Specimen 1. Crack propagated through Zone 2 weld metal along the weld centerline.

in electroslag and electrogas weldments when the orientation of the Charpy V-notch specimen relative to the grain is such that the crack is forced to cross the grain instead of follow the grain boundary.

5) Load vs. Crack Opening Displacement Plots - K_{IC} Tests

The ASTM E399 Standard Test Method for Plane-Strain Fracture Toughness of Metallic Materials (23) requires that an autographic plot be made during the K_{IC} fracture test. This plot records the load applied to the specimen against the 'crack opening displacement' (COD) as measured by a clip gage spanning the specimen crack (see Fig. 16). An analysis of the resulting plot reveals whether the fracture is elastic (brittle) or plastic (ductile) in nature. Several Load vs. COD traces are shown in Figures 29 through 35 which are representative of the fractured specimens shown in Figures 19 through 27. The following observations can be made from these load traces which further aid in understanding the results of the K_{IC} fracture toughness tests.

a) Figure 29 shows a plot typical of the fracture surface shown in Figure 19a. This fracture was a valid K_{IC} test, which means that all the conditions of a linear elastic crack propagation and limited crack tip plasticity in ASTM E399 were satisfied. The linear elastic nature of the fracture is evident by the straight line behavior of the load vs. COD curve, followed by a sudden drop in the load after the unstable crack growth occurs. The straight line portion of the curve corresponds to stable crack growth which is linearly related to the COD. The sudden drop in load occurring after P_{max} represents the onset of unstable crack growth or fracture. The top straight line represents the slope of the elastic portion of the load vs. COD curve. The bottom straight line represents a line drawn at 95 percent of the initial elastic slope, as required by the ASTM E399 test method. The point where the 95 percent slope intersects the load vs. COD curve is denoted as P_5 which is compared to the load P_{max} in accordance with the E399 test requirements. If the load on each point of the trace preceeding P_5 is lower than P_5, then P_5 is considered to be P_Q, the fracture load. However, if there is a maximum load, P_{max}, preceeding P_5, then the P_{max} is considered to be the fracture load (as is the case in Fig. 29).

b) The load vs. COD plots in Figures 30 and 31 correspond to the specimens shown in Figure 21a and b, respectively. Both of these tests failed to satisfy the conditions for linear elastic behavior in that the crack tip plastic zone was excessively large. However, a noticeable contrast exists between the plot for Specimen 1 (Fig. 30) and Specimen 3 (Fig. 31) in the amount of curvature of the trace up to the fracture point. The cause of this inelastic behavior is the additional resistance to the crack propagation exhibited in Specimen 3 where the crack was located off-center from the weld centerline. This caused the crack to propagate transversely to the grains of the weld metal, rather than separating them along their boundaries as occurred in Specimen 1. This fracture behavior was previously discussed as being evident in Figure 21 by the appearance of the fractured

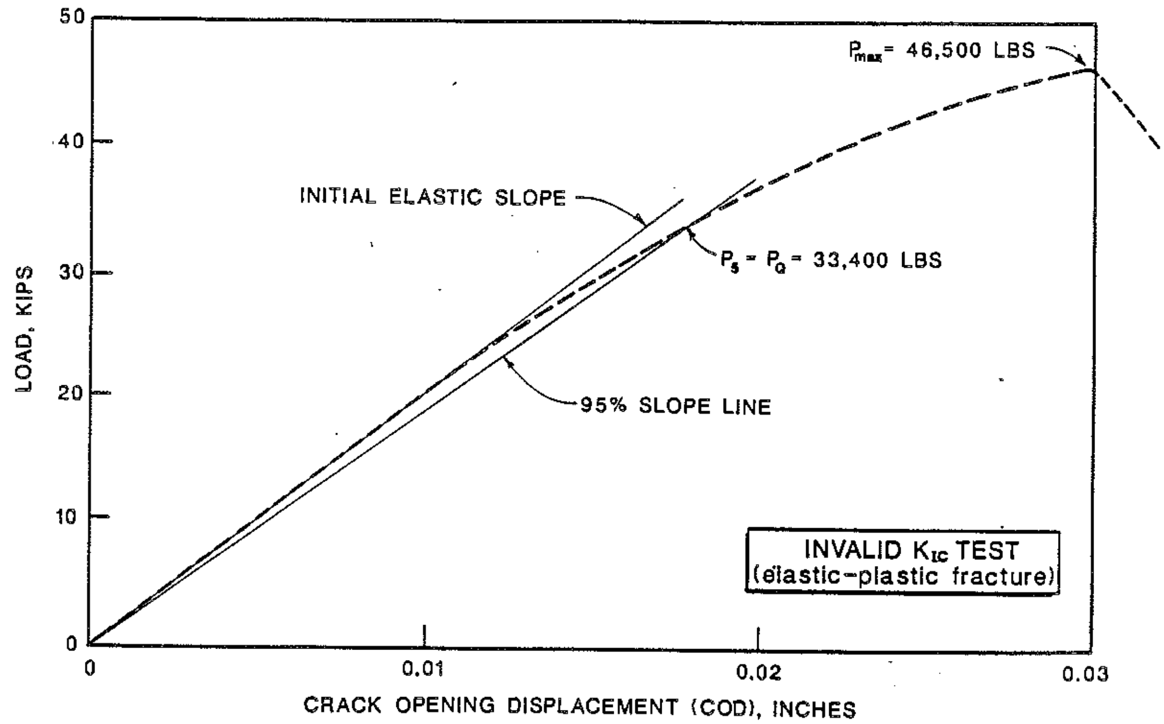

Figure 31. Load vs. COD plot for an invalid K_{IC} test on electroslag weldment ESW588-B2, Specimen 3. Crack propagated through Zone 1 and Zone 2 weld metal offset from the weld centerline.

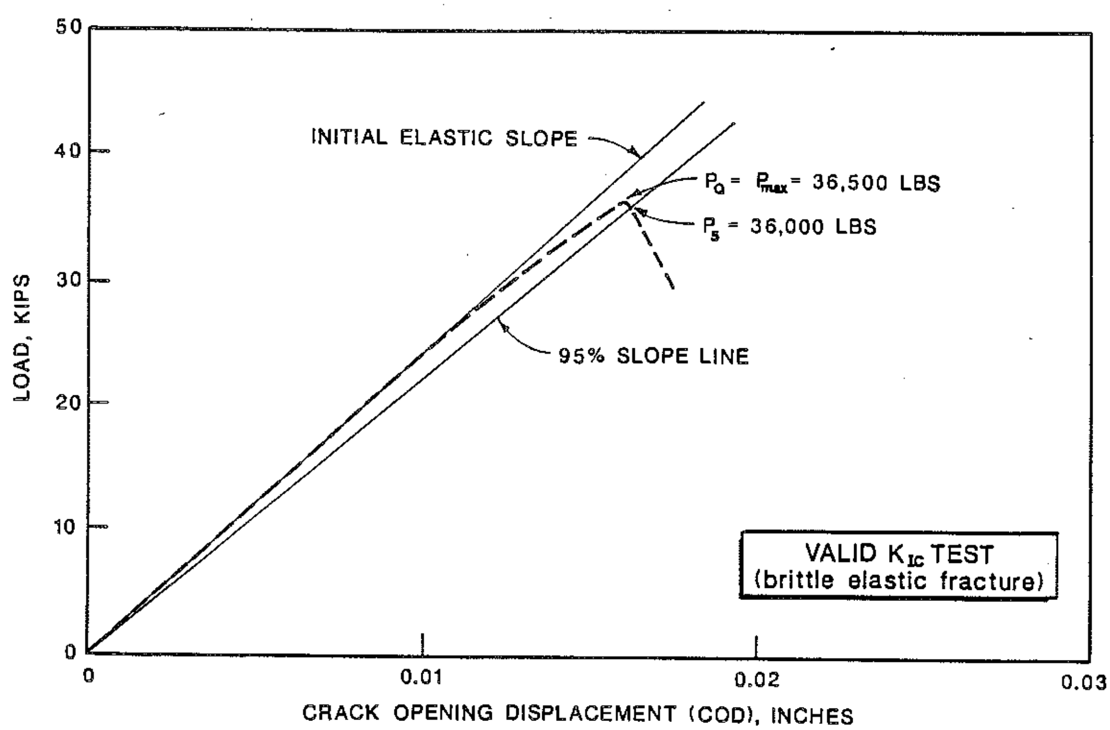

Figure 32. Load vs. COD plot for a valid K_{IC} test on electrogas weldment EGW588-D1, Specimen 2. Crack propagated through Zone 1 weld metal along the weld centerline.

surfaces. Thus we see that even though the fracture was not a valid K_{IC} test, it does illustrate that the weld centerline plane represents the position of lowest crack resistance in an electroslag weldment. This is an important fact as relates to both the testing of electroslag weldments and the analysis and evaluation of a cracked or flawed electroslag weldment in a bridge structure. Note also in Figures 30 and 31 that P_{max} is much larger than P_5. This is commonly the case in fracture tests that do not satisfy the conditions of linear elastic fracture as stated in the ASTM E399 test method. The rounding or curvature at the upper portions of the load vs. COD curves are the results of inelastic, stable crack growth.

c) The plot in Figure 32 is from the test specimen from the electrogas weldment shown in Figure 23. The linear elastic nature of the stable crack extension is clearly evident, followed by the sudden onset of fracture at the load P_{max}. This is a classic illustration of brittle elastic behavior and the corresponding specimen in Figure 23 is a good example of how a brittle fracture surface appears in this type of weldment. Note that this specimen had the crack propagating down the weld centerline, which is again the path of least crack resistance due to the alignment of the weld metal grains with the crack direction.

d) The plot in Figure 33 corresponds to the specimen shown in Figure 24b. This is a specimen from an electroslag weldment in 3-in. thick A36 steel where the crack was propagated off-center from the weld centerline. Note that in this case, even though the load vs. COD trace has a linear elastic appearance, the other conditions in ASTM E399 on crack tip plasticity were exceeded, thus the results did not yield a valid K_{IC} value. The fracture resistance calculated from P_{max} is, however, useful for comparing the relative toughness of the weldment to other weldments. In only one case did the lower yield strength A36 steel electroslag weldment exhibit a valid K_{IC} fracture behavior (Table 11).

e) The plot in Figure 34 corresponds to the submerged arc weldment specimen shown in Figure 25b. Note that the stable crack extension in this specimen is almost entirely inelastic in nature as evidenced by the curved or 'roundhouse' nature of the load vs. COD trace. As evidenced by the fracture surface appearance in Figure 25b, this fracture test was dominated by the plasticity effects present in the submerged arc weld metal. The obvious conclusion to be made is that this type of weldment has an immediate advantage over the electroslag and electrogas weldments since brittle fracture is not possible at the test temperature and loading rate that correspond to bridge structure service conditions. Hence, the potential for sudden, rapid fracture of a submerged arc bridge weldment is minimized in comparison with an electroslag or electrogas weldment. Also, there are no low-toughness grain boundary paths for the crack to follow through the submerged arc weld.

f) The final load vs. COD plot shown in Figure 35 corresponds to the ASTM A588 base metal test specimen shown in Figure 26c. Note the total elastic nature of the load trace and the sudden onset of fracture

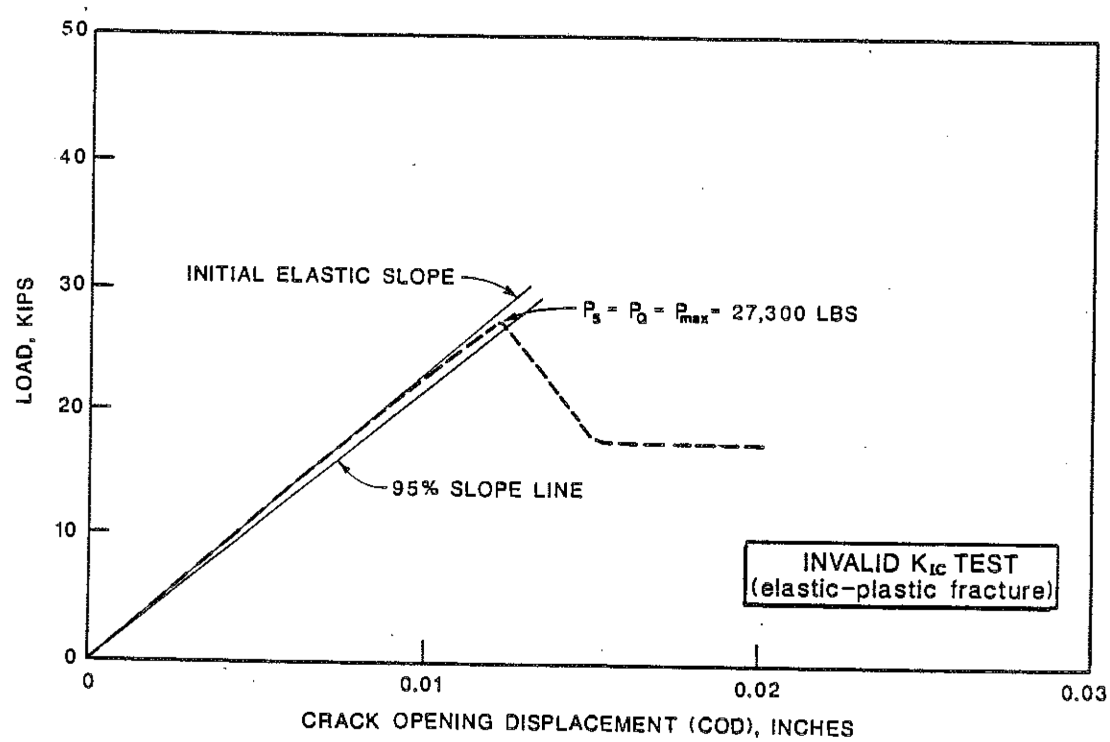

Figure 33. Load vs. COD plot for an invalid K_{IC} test on electroslag weldment ESW36-A2, Specimen 5. Crack propagated through Zone 2 weld metal offset from the weld centerline.

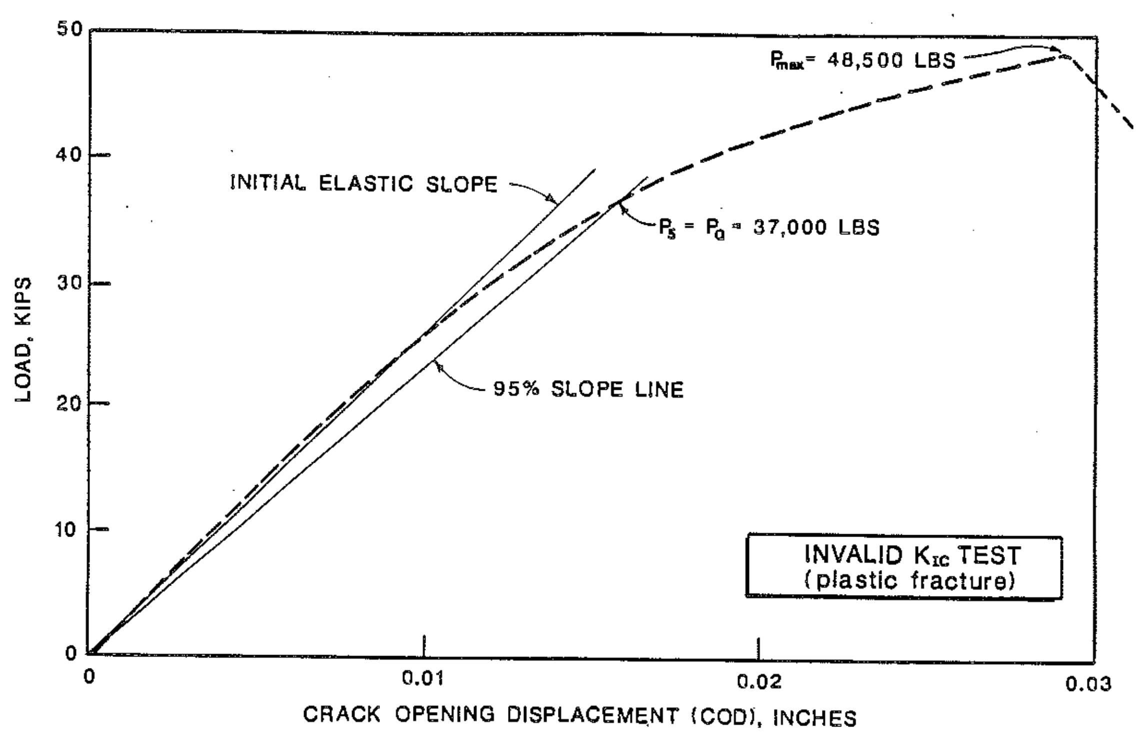

Figure 34. Load vs. COD plot for an invalid K_{IC} test on submerged arc weldment SA588-A7, Specimen 3. Crack propagated through weld metal along the weld centerline.

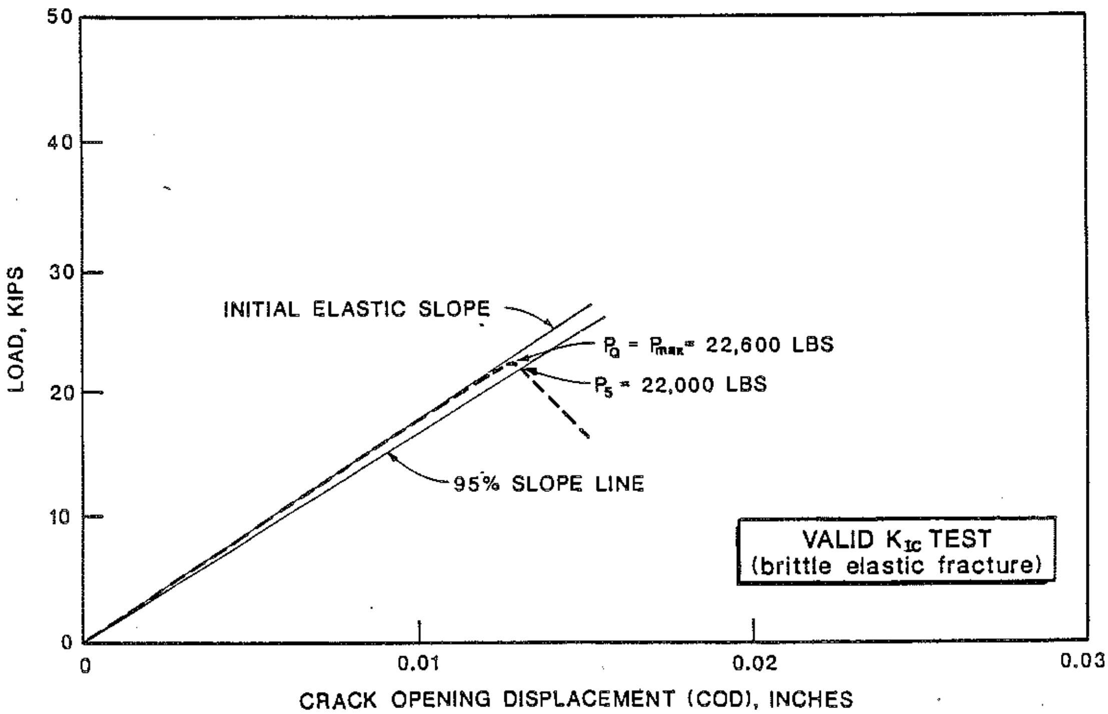

Figure 35. Load VS. COD plot for a valid K_{IC} test on ASTM A588 base metal specimen A588-6 (2.25T.)

at the load P_{max}. The fracture surface in Figure 26c shows a corresponding lack of ductility with a perfectly flat, brittle cleavage appearance. This brittle behavior was not experienced in the ASTM A36 base metal (Fig. 27) which has a lower yield point (36,000 min. psi vs. 50,000 min. psi for A588). As stated before, this illustrates the fact that increasing the yield strength of a steel has the effect of lowering its resistance to brittle fracture (or its fracture toughness). Therefore, bridge engineers need to be very cautious in their use of high strength steels (yield point in excess of 50,000 psi) since the resistance to fracture may control the safety or structural integrity of the bridge structure.

6) The fracture toughness values reported in Tables 10 through 13 are useful in comparing the resistance to fracture of the various base metals, types of weldments, and positions or orientation of the crack related to the grain boundaries within the weldments. Since the specimens tested represent a typical maximum service condition, i.e., 3-in. thick flange plate weldments tested at the Lowest Anticipated Service Temperature and bridge loading rate, the fracture resistance measured is relevant even though a valid K_{IC} test was not always achieved. Two values of the fracture resistance are listed in the tables, K_Q and $K_{c_{max}}$. K_Q is the value of the fracture toughness calculated from the load P_Q as defined in the ASTM E399 test method. (Note that when the conditions for plane-strain fracture are satisfied, the value $K_Q = K_{IC}$). $K_{c_{max}}$ was similarly calculated using the load P_{max} from the load vs. COD trace. Even though

the formula given in E399 for calculating K on the three-point bend specimen is not strictly accurate when a large plastic crack tip zone is present, the value $K_{c_{max}}$ (or P_{max}) is very useful as a comparison of the total maximum load sustained by the specimen before the onset of unstable crack propagation (or fracture). Comparisons of the K_I data in these tables thus yield the following observations:

a) The submerged arc weldments exhibit higher total fracture resistance than the electroslag and electrogas weldments.

b) The Zone 2 electroslag weld metal, when tested by orienting a specimen off-center from the weld centerline, **does not always exhibit a significant increase** in fracture resistance compared to the central Zone 1 weld metal. As noted in discussions on the fracture appearance and load vs. COD traces, there is often more plastic or inelastic fracture behavior present, but the total resistance to fracture is not always improved. This is an important observation that is contrary to the toughness predictions of the small size Charpy V-notch test results. The Charpy test would predict a significantly higher fracture toughness through the off-center Zone 2 weld metal. This again underscores the danger involved in evaluating weldment toughness of a specimen that is significantly smaller than the size of the weldment plate or the weldment grain structure.

c) Table 13 reveals that the ASTM A36 steel tested exhibits higher total fracture resistance than the ASTM A588 steel tested. This is a commonly understood result in that as the yield point of a steel increases (50,000 psi min. for A588, 36,000 psi min. for A36), the fracture toughness decreases. This emphasizes the importance of the design engineer's awareness that when a high strength steel is used, one must be cautious to guard against details that may induce growing fatigue cracks, or three-dimensional stresses, and to specify a minimum toughness requirement that is compatable with the inspection reliability. The history of engineering failure analysis is replete with case studies where a stronger steel led to a failure due to a lower resistance to fracture.

d) Note that in the valid K_{IC} tests, the values calculated for K_{IC} range from 47.0 to 65.9 ksi in. These values correspond to data reported on similar tests by others (11, 26). The lower values correspond to K_{IC} results that are typically obtained on steel or weld metal specimens that have less than 10 ft-lb of energy as measured by the Charpy V-notch impact test. Very little published data or information exists relating to what minimum K_{IC} values should be required for steel bridge girder applications. Hence, there exist no standards with which to compare the results. In an actual bridge girder weldment, the K_{IC} toughness values can be used to estimate the critical crack size that could be sustained by the girder, at a given temperature and under a given maximum loading condition, without the onset of rapid, brittle fracture. This is one of the main uses of such fracture toughness data, to evaluate the danger or safety of a flawed bridge weldment. These data should be very useful in future cases where flawed electroslag weldments must be so analysed. There is very little data published on the types of weldments evaluated in this project. The base metal toughness requirements established by the AASHTO Specifications (7, 15, 21), are expressed in terms of a minimum required Charpy V-notch impact toughness at various testing temperatures, dependent upon the region of the United States where the bridge will be located. These values were arrived at empirically by correlation tests done between the Charpy V-notch test and the fracture toughness K_{IC} test (19). The critical flaw size criteria built into the AASHTO specifications allow for a girder flange transverse crack to grow to a size equivalent to through-the-thickness (T) by 2T in length without triggering brittle fracture. The low values of K_{IC} recorded for the electroslag and electrogas weldments and the brittle fracture behavior exhibited by these tests, indicate that the critical crack size will be significantly smaller in these cases. The increased susceptibility to fatigue crack initiation and propagation in electroslag and electrogas weldments make the risk of such fractures a reality.

The AASHTO Charpy toughness requirements were also designed to preclude the occurrence of brittle fracture in bridge steels and weldments. In other words, when fracture does occur in an AASHTO specification steel type, it should be an elastic-plastic or ductile failure behavior and not an elastic or brittle failure. This is why the Charpy V-notch impact value of 15 ft-lb frequently appears in specifications. The 15 ft-lb transition temperature is normally assumed to be the temperature at which the mode of fracture changes from ductile (or plastic) to brittle (or elastic) (19). Thus, by requiring 15 ft-lb of Charpy impact energy at an appropriate temperature, related to the lowest anticipated service temperature, the brittle fracture mode is eliminated from the service application. As can be seen from the results of these tests this condition is not true for the electroslag and electrogas weldments and for some of the ASTM A588 steel plates.

It is not, then, currently possible to state a minimum K_{IC} type fracture toughness that would ensure the safety and reliability of a weld spliced girder flange. Even if it were possible, the test is too complex and expensive to run to be useful as a standard quality control test. It is very useful, however, in evaluating the brittle verses ductile behavior of full size weldment specimens and in estimating the fracture toughness material property that allows an evaluation of the significance of cracks in in-service bridge girders. It is useful as well in providing additional insights into the possible modes of failure, and reasons for variations in toughness values that occur within a weldment.

Modified Fracture Toughness Test - K_I

A modified fracture toughness test was attempted to circumvent the problems encountered in the standard K_{IC} test in the submerged arc weldments. As illustrated in the previous section, the residual compressive stress field that exists in a multipass submerged arc weldment prevents the proper growth of a fatigue crack front (Fig. 25). This irregular crack

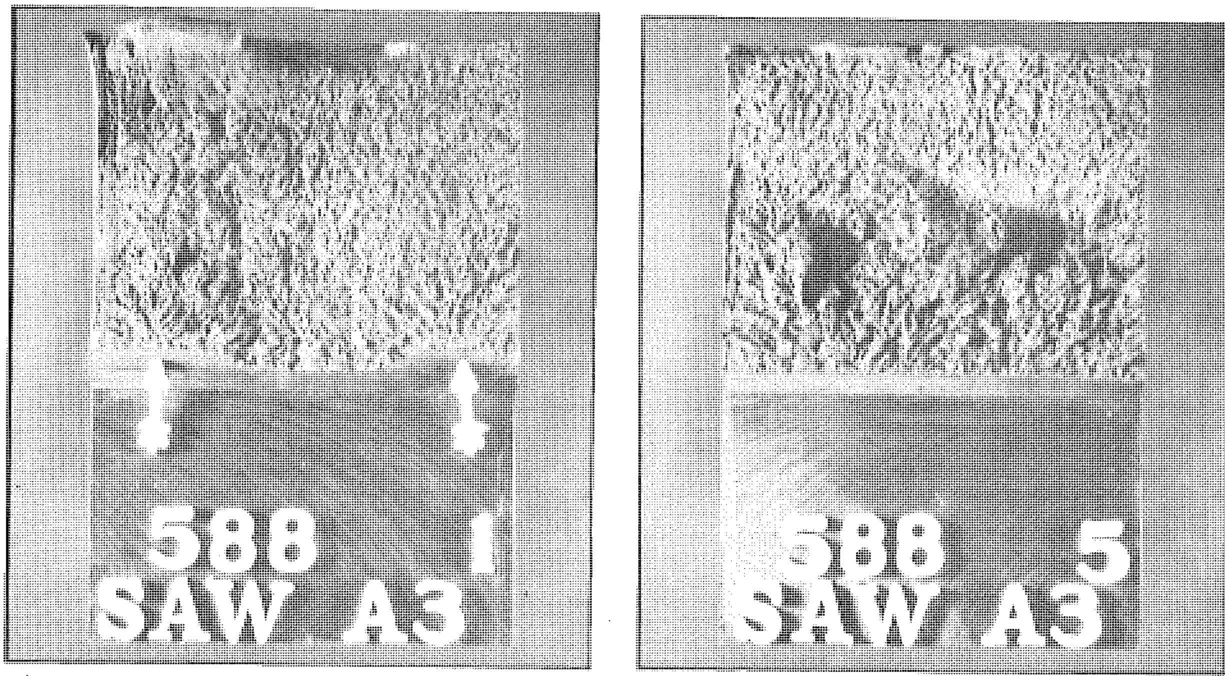

a) Fatigue precracking in regions noted by arrows.

b) No fatigue precracking.

Figure 36. Modified K_I test specimens in 3-in. thick A588 steel submerged arc weldments.

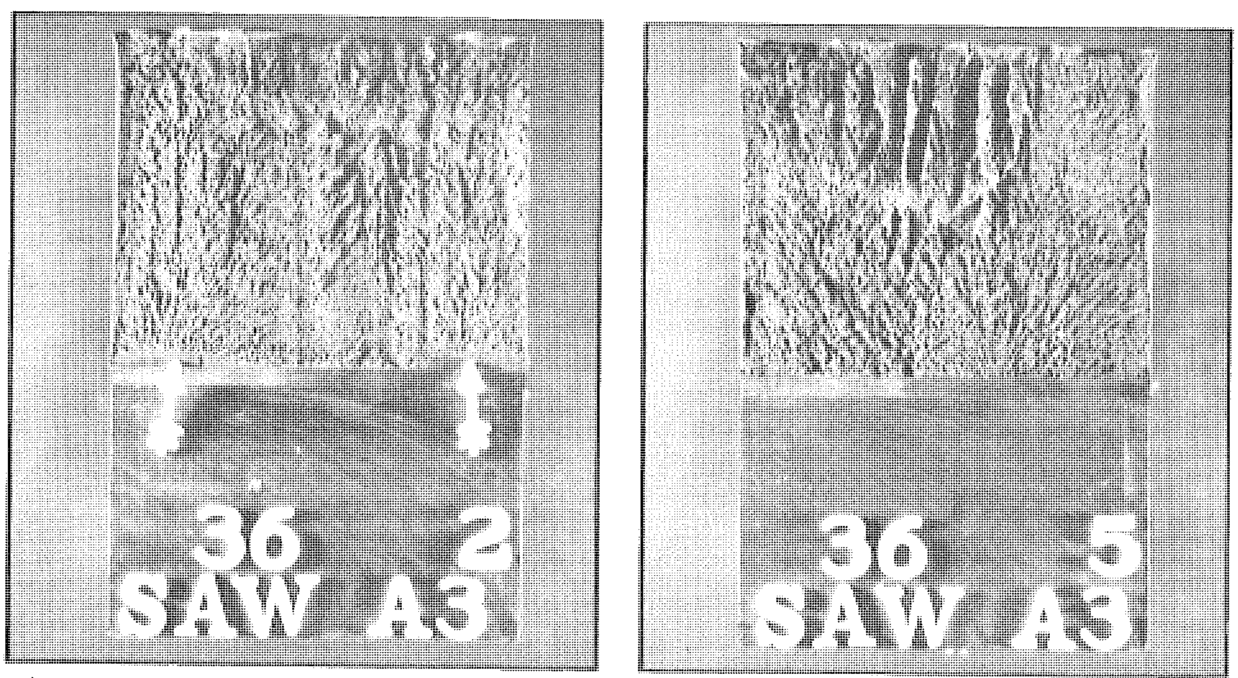

a) Fatigue precracking in regions noted by arrows.

b) No fatigue precracking.

Figure 37. Modified K_I test specimens in 3-in. thick A36 steel submerged arc weldments.

front invalidates the calculation of the fracture toughness, K_{IC}, as defined in the ASTM E399 test method. Two different modifications of the E399 test were conducted to achieve a straight crack front in the submerged arc weldments and hence a more meaningful fracture test result.

Modification 1 - The first modification was to grow a fatigue precrack from a straight machined V-notch that had a sharp tip radius of 0.003 in. The fatigue crack traces on the surfaces of the submerged arc specimen were monitored and the fatigue cracking stopped when a small crack growth distance was detected on both sides. (A point of interest is that a light film of oil brushed on the specimen surfaces proved to be a good fatigue crack detection device. When a crack appeared, the cyclic opening and closing was sufficient to blow small bubbles in the oil film making it easily visible to the naked eye.) By stopping the fatigue cracking after a short distance from a straight machine starter notch, a relatively straight crack front was achieved as shown in Figures 36a and 37a. The resulting test specimens did not satisfy the conditions of the ASTM E399 test requirements for minimum fatigue crack extension, but they did satisfy the conditions for crack front straightness. These specimens had a sharp tipped, fatigue crack over approximately 2/3 of the width and a machined-notch with a 0.003-in. tip radius over the central 1/3. The machined-notch region lies in the zone with the residual compressive stress field. This straight crack front at least is consistent with the assumptions of the analytical model of the fracture specimen, even though the residual stress fields are not accounted for. The specimens were then loaded to failure in the same manner as the standard three-point bend specimens in the previous section, using one-second loading and a test temperature of -30 F.

Modification 2 - The second modification test was run on all the weldment types, submerged arc and electroslag. These three-point bend specimens were fractured in exactly the same manner as the standard K_{IC} test specimens, but without any fatigue precracking. The machined-notch was made straight across the specimens with a notch tip radius of 0.003 in. Fractured specimens are shown in Figures 38 for electroslag weldments and 36b and 37b for submerged arc weldments. This modified test does not satisfy the requirements in ASTM E399 for the growth of a fatigue precrack front. However, the machined-notch does represent a constant fracture starter mechanism and the resistance of the specimens to fracture should be in relation to their fracture toughness. This specimen could be viewed as a giant size slow-bend Charpy V-notch test. The specimens were fractured using one-second loading and a test temperature of -30 F.

In both of these modified fracture toughness tests the objective was to keep a straight fracture crack front and stay as close to the other conditions of the ASTM E399 test method as possible. Note that in both cases the beneficial effects of the compressive residual zone in the central portion of submerged arc weldment are measured by the test. Although the results of these tests are somewhat empirical, they should give an interesting comparison between the weldment types as tested full size from an identical initial condition.

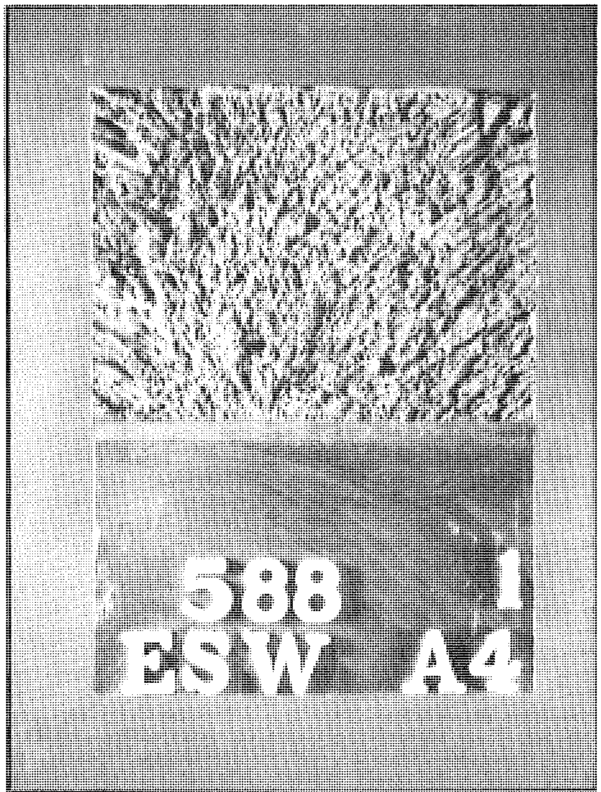

a) A588 steel. Zones 1 and 2 weld metal on the centerline of the weld.

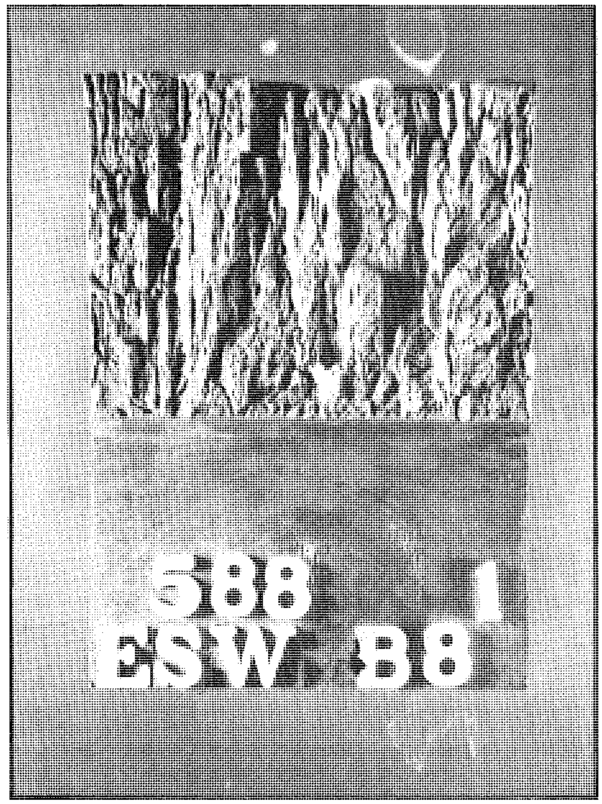

b) A588 steel. Zones 1 and 2 weld metal on the centerline of the weld.

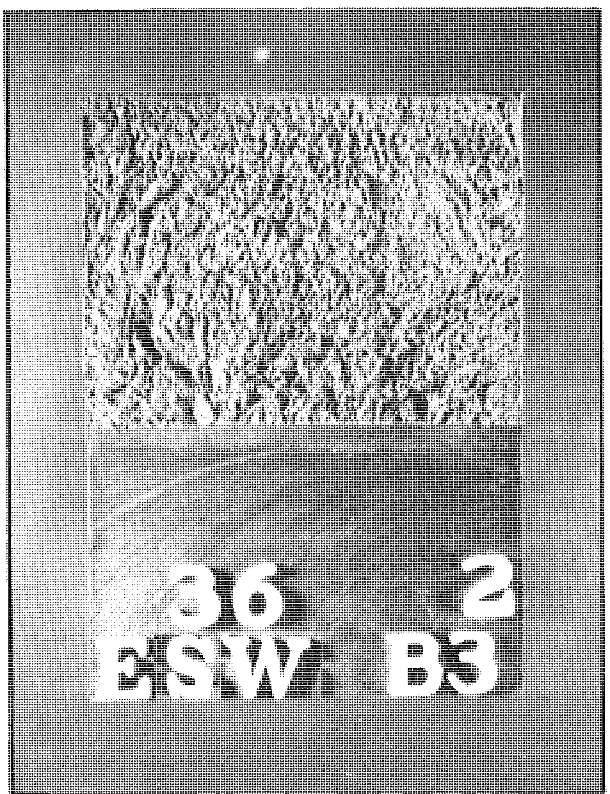

c) A36 steel. Zones 1 and 2 weld metal on the centerline of the weld.

Figure 38. Modified K_I test specimens in 3-in. thick electroslag weldments using a machined notch condition with no fatigue precrack.

Discussion of Results - Modified K_I' Test

The results of the modified K_I' tests are shown in Tables 14 and 15. Table 14 presents the results of the first modification, where the fatigue crack front was grown for a short distance. These test results were analyzed in accordance with the ASTM E399 test method. Even though the fatigue precracking conditions were not met, the test represents as close a condition as possible to these conditions. It is interesting to note that even though the remaining plane-strain fracture conditions of E399 are not satisfied, several of the specimens came close. These data, then, may represent a best possible estimate of an E399 fracture toughness evaluation for these type of weldments. Note that both the values of K_Q, defined as the 95 percent slope intercept in E399, and $K_{c_{max}}$, based on the maximum load sustained at fracture are very high. It is the opinion of the author that these values represent a high resistance to fracture (or toughness) in the submerged arc weldments. It is interesting to note that the toughness values are somewhat higher than those previously presented in Table 12. This is most likely due to the elimination of the large crack front disparity present in the previous tests (illustrated in Fig. 25) which would tend to concentrate the initial test loading on the central or trailing portion of the fatigue crack front. In the modified test the fracture loading is distributed nearly evenly across the specimen, thus giving a higher and more representative toughness measurement. The load vs. COD traces in Figures 39 and 40 illustrate the nature of the submerged arc weldment fracture specimen behavior. These traces are on two adjacent specimens removed from the same submerged arc weldment. Note that in Figure 39, the nature of the load trace is nearly linear elastic and the test conditions were closely approaching a valid K_{IC} result ($P_{max}/P_Q < 1.10$ requirement). The specimen corresponding to this load trace is shown in Figure 37a. The load trace in Figure 40, however, again reveals that large plastic crack extension has dominated the tests. A portion of this behavior is undoubtedly due to the presence of the compressive residual stress zone which can vary from specimen to specimen. A low toughness or brittle submerged arc weldment should be reliably revealed by this modified K_I' test and the results should satisfy all the conditions of the ASTM E399 test method, except for the fatigue crack extension requirement and the presence of the compressive residual stress field. Again, it is the opinion of the author that these tests represent a best approximation to the E399 fracture toughness evaluation of the submerged arc weldments. This modified test should, therefore, prove useful in circumventing the testing problems encountered with variable residual stress zones, but still give a realistic estimate of the fracture toughness or resistance to brittle crack propagation under service loading conditions.

Table 15 tabulates the results of the fracture tests conducted with the second modification, i.e., no fatigue crack present in the specimens. In this case the data present values for $K_{c_{max}}$ as calculated from the formula presented in ASTM E399 for the three-point bend specimen.

TABLE 14
FRACTURE TOUGHNESS DATA FROM THE MODIFIED K_I TEST - SHORT FATIGUE CRACK SUBMERGED ARC WELDMENTS, A588 AND A36 STEEL

Weldment Type	Specimen Number	Specimen Thickness	K_Q Ksi·in.$^{1/2}$	K_{cmax} Ksi·in.$^{1/2}$	P_{max}/P_Q	K_{IC} Ksi·in.$^{1/2}$	Test Validity Conditions[1] (ASTM E399)
SAW588-A3	1	3T	67.9	81.5	1.2	—	Invalid (1,5)
	2	3T	62.3	121.5	1.95		Invalid (1,5)
	3	3T	69.4	104.8	1.51	—	Invalid (1,5)
SAW588-A8	1	3T	75.3	128.8	1.71	—	Invalid (1,2,5)
	2	3T	70.8	119.7	1.69	—	Invalid (1,5)
	3	3T	61.1	124.0	2.03	—	Invalid (1,5)
SAW36-A3	1	3T	63.8	88.7	1.39	—	Invalid (1,5)
	2	3T	64.8	77.1	1.19	—	Invalid (1,5)
	3	3T	63.4	71.8	1.13	—	Invalid (1,5)

[1]The numbers 1 through 6 indicate that the K_Q test result was not a valid K_{IC} result according to the requirements of ASTM E399 because one or more of the following conditions were violated:

1. $P_{max}/P_Q \leq 1.10$
2. a and/or B > 2.5 $\left(\frac{K_Q}{\sigma_{y.s.}}\right)$
3. Test record slope >0.70 and <1.50
4. Fatigue precracking loading conditions
5. Fatigue crack front conditions -
   - a varies < 0.10 $a_{av.}$
   - Surface trace of crack > 0.90 $a_{av.}$
   - $0.45 < \frac{a}{W} < 0.55$ (violated by the short fatigue crack condition of the modified test)
6. Crack plane at angle < 10° to the width and thickness directions

TABLE 15
FRACTURE TOUGHNESS DATA, K_I MODIFIED K_I TEST - NO FATIGUE PRECRACKING SUBMERGED ARC AND ELECTROSLAG WELDMENTS, A588 AND A36 STEEL

Weldment Type	Specimen Number	Specimen Thickness	K_{cmax} Ksi·in.$^{1/2}$	P_{max}/P_Q
SAW588-A3	1	3T	143.3	2.54
	2	3T	145.0	2.06
SAW588-A8	1	3T	146.6	1.97
	2	3T	130.8	2.05
SAW36-A3	1	3T	141.2	2.27
	2	3T	139.5	2.07
ESW588-A4	1	3T	126.8	
	2	3T	126.8	
ESW588-A9	1	2.25T	122.6	1.90
	2	2.25T	123.0	2.03
ESW588-B3	1	3T	105.1	1.58
	2	3T	123.5	1.86
ESW588-B8	1	3T	138.9	2.48
	2	3T	126.6	2.31
ESW36-A4	1	3T	83.7	1.84
	2	3T	90.1	2.49
ESW36-B3	1	3T	110.3	1.7
	2	3T	106.9	2.04

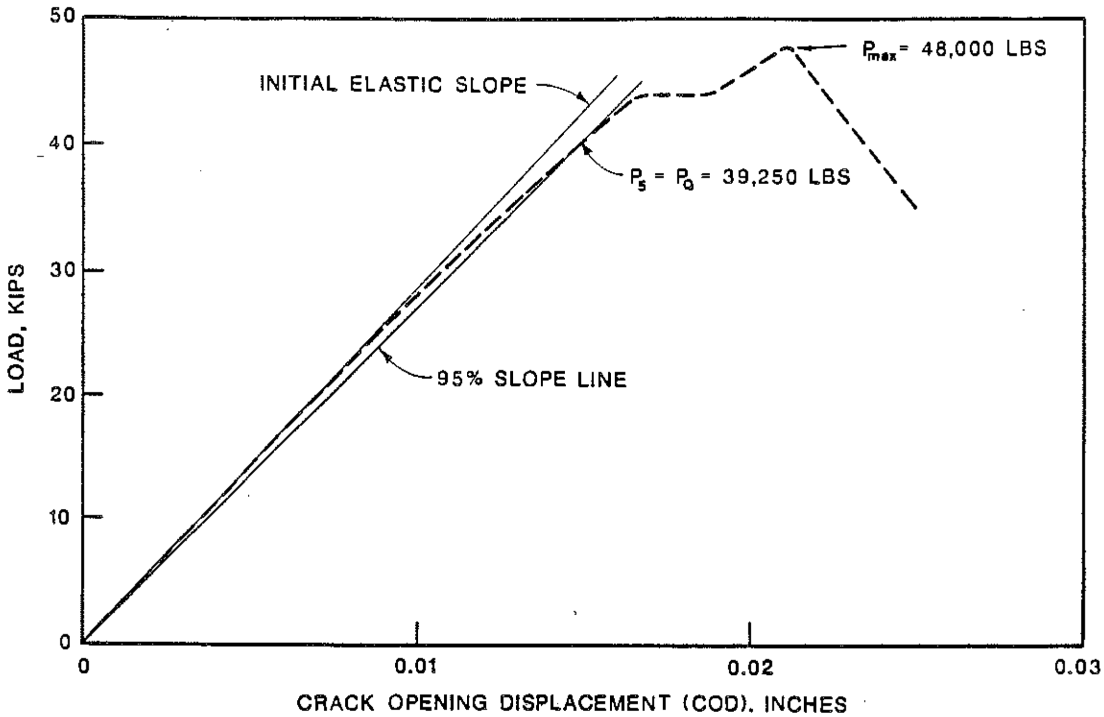

Figure 39. Load vs. COD plot for modified K_I test on submerged arc weldment SAW588-A3, Specimen 1 (see Figure 36a). (Shortened fatigue crack modification.)

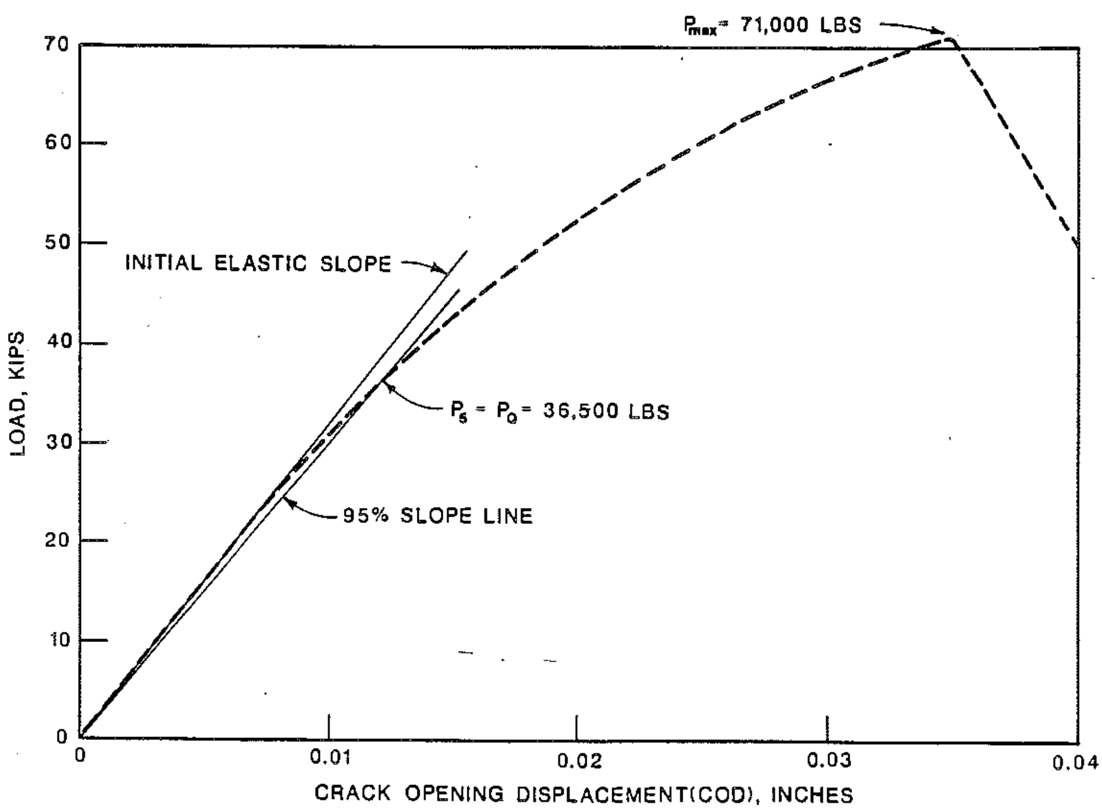

Figure 40. Load vs. COD plot for modified K_I test on submerged arc weldment SAW588-A3, Specimen 2. (Shortened fatigue crack modification.)

Although the values have no analytical significance, it is interesting to note that the $K_{c_{max}}$ values for the submerged arc weldments are consistently higher than those of the electroslag weldments. This is as expected since all other fracture tests have also rated the submerged arc weldments as having more fracture toughness than the electroslag weldments. It is interesting to note in Figure 36 that the large grained nature of the electroslag weldment is evident on the fracture surfaces, as seen in previous tests. It is also interesting to observe the plastic fracture effects in this test that result from the relatively blunt machined-notch that was used as a fracture initiation condition. This is particularly evident in Figures 37 and 38 where the **b** figures, which have no fatigue precrack, show much more ductility in the fractured surface than the **a** figures. Indeed, as evident in the large P_{max}/P_Q ratios in Table 15 and the 'roundhouse' shape of the load vs. COD traces, this second modified test was dominated by crack tip plasticity effects. In conclusion, it has no real relevance other than to nicely illustrate the importance of crack-tip acuity in a fracture toughness test and to give a direct comparison of fracture for the two types of welding processes subjected to the same loading conditions.

IMPLEMENTATION OF RESEARCH

The Michigan Department of Transportation has not allowed the use of electroslag or electrogas butt welding on tension bridge components since June 1974. This has effectively eliminated the use of these welding processes from our segment of the fabricating industry. Based on the results of this study we cannot envision its use being acceptable in the future. Thus, implementation of these research results relate to the inspection and maintenance of the 126 bridges within the state's highway system that contain electroslag weldments. The following recommendations are made concerning these bridges:

1) All fracture critical bridge components that contain electroslag or electrogas weldments should be immediately inspected for weldment defects and retrofitted by bolt splice repair to preclude any chance of failure. (This has not been done on Michigan bridges with the exception of one pedestrian bridge.)

2) All other multi-stringer, redundant bridges that are known to contain electroslag or electrogas weldments should be closely monitored to detect the onset of either fatigue cracking or girder fracture at the locations of the weldments. Several case studies have arisen around the country where such fractures have occurred. In redundant structures, the fractures can be repaired before they become a serious threat to the structural integrity of the bridge.

3) Special bridge maintenance inspection and repair guidelines should be prepared for bridges containing electroslag or electrogas weldments. These guidelines should be adopted as part of the yearly maintenance

inspection program required by the Federal Highway Administration. They should include recommended methods for nondestructive testing of the weldments, criteria for identifying which weldments are most likely to develop cracks, and recommended repair methods.

Further implementation of the results of these research findings relate to the following points noted on the submerged arc weldments and base metal tests:

1) The modified K_I' fracture toughness test run on the submerged arc weldments may represent the best approximation of its true fracture behavior. This should be further explored and may be a useful method for evaluating submerged arc butt weldments to be placed in fracture critical applications.

2) The valid K_{IC} fracture toughness results achieved on the ASTM A588 base plates illustrates the need for caution in the use of high-strength, low alloy steels. In thick plates the specifying of a minimum Charpy V-notch impact test toughness does not preclude the possibility of brittle fracture in a bridge member. To guard against this the designer should strive to keep his maximum plate thickness as low as possible (preferably 2-1/2 in. maximum) and avoid details known to have low fatigue resistance or result in high tritensile restraint in the plate.

REFERENCES

1. Culp, J. D., "Fracture Toughness and Fatigue Properties of Steel Plate Butt Joints Welded by Submerged Arc and Electroslag Welding Procedures," Research Report No. R-1011, Testing and Research Division, Michigan Department of State Highways and Transportation, May 1976.

2. Albrect, P., "Fatigue Design Stresses for Weathering Steel Structures," Corrosion Fatigue: Mechanics, Metallurgy, Electrochemistry, and Engineering, ASTM STP 801, T. W. Crooker and B. N. Leis, Eds., American Society for Testing and Materials, 1983, pp. 445-471.

3. "Welding Terms and Definitions," AWS A3.0-80, American Welding Society, 1980.

4. Fisher, J. W., et. al., "Effect of Weldments on the Fatigue Strength of Steel Beams," NCHRP Report No. 102, National Cooperative Highway Research Program, Washington, D.C., 1970.

5. Pense, A. W., et. al., "Examination and Repair of Bridge Structures," Welding Journal, Vol. 63, No. 4, pp. 19-25, 1984.

6. "Structural Welding Code, Steel," AWS D1.1-83, American Welding Society, 1983.

7. "Standard Specifications for Welding of Structural Steel Highway Bridges," 3rd Edition, American Association of State Highway and Transportation Officials, 1981.

8. "Supplemental Specification for Fabricating Structural Steel and Aluminum," 5.04(1f), Michigan Department of Transportation, 1984.

9. "Welding Handbook," 7th Edition, Chapter 7 - Electroslag and Electrogas Welding, Vol. 2: 225-247, American Welding Society, Miami, 1978.

10. Cambell, H. C., "Electroslag, Electrogas, and Related Welding Processes," Welding Research Council, Bulletin No. 154, p. 14, Sept. 1970.

11. Benter, W. P., and Schilling, C. G., "Acceptance Criteria for Electroslag Weldments in Bridges," NCHRP Report 201, National Research Council, Washington, D, C., 1979.

12. Pense, A. W. , Wood, J. D., and Fisher, J. W., "Recent Experiences with Electroslag Welded Bridges," Welding Journal, Vol. 60, No. 12, Dec. 1981, pp. 33-42.

13. Davenport, J. A., Qian, B. N., Pense, A. W., and Stout, R. D., "Ferrite Vein Cracking in Electroslag Welds," Welding Journal, Vol. 60 No. 12, pp. 2375-2435.

14. "Structural Welding Code, Steel," AWS D1.1-79, American Welding Society, 1979.

15. "Standard Specifications for Welding of Structural Steel Highway Bridges," 2nd Edition, American Association of State Highway and Transportation Officials, 1977.

16. "Supplemental Specification for Welding Structural Steel," 5.04 (1d), Michigan Department of Transportation, 1980.

17. Paton, B. E., "Electroslag Welding," American Welding Society, 2nd Edition, New York, 1962.

18. Fisher, John, "Fatigue and Fracture in Steel Bridges," John Wiley and Sons, Inc., Somerset, New Jersey, 1984.

19. Rolfe, S. T., and Barsom, J. M., "Fracture and Fatigue Control in Structures," Prentice-Hall, Inc., Englewood Cliffs, New Jersey, 1977.

20. Hartbower, Carl E., "A Proposed Fracture Control Plan for New Bridges with Fracture Critical Members," Vol. 1-3, Structural Engineering Series No. 5, Federal Highway Administration, Washington, D. C., 1978.

21. "Guide Specifications for Fracture Critical Non-Redundant Steel Bridge Members" and "1981 Interim Revisions," American Association of State Highway and Transportation Officials, 1978.

22. "Manual for Railway Engineering," Chapter 15 - Steel Structures, pp. 15-1-38 to 15-1-48, American Railway Engineering Association, 1984.

23. "Metals - Mechanical Testing; Elevated and Low-Temperature Tests," Vol. 3.01, American Society for Testing and Materials, Philadelphia, PA.

24. "Standard Specifications for Highway Bridges," 13th Edition, The American Association of State Highway and Transportation Officials, 1984.

25. Barsom, J. M., "Development of the AASHTO Fracture-Toughness Requirements for Bridge Steels," Journal of Engineering Fracture Mechanics, 7, 1975, p. 605-618.

26. Sovak, J. F., "Fracture Resistance of 4-in. Thick A36 and A588 Grade A Electroslag Weldments," Welding Journal, Vol. 60, No. 12, Dec. 1981, pp. 2695-2725.